Development and Calibration of a Virtual Model of a University Building

Danielle Monfet

A Thesis

in

The Department

of

Building, Civil & Environmental Engineering

Presented in Partial Fulfillment of the Requirements
for the Degree of Master of Applied Science (Building Engineering) at
Concordia University
Montreal, Quebec, Canada

December 2006

Your file Votre référence
ISBN: 978-0-494-28888-7
Our file Notre référence
ISBN: 978-0-494-28888-7

ABSTRACT

Development and Calibration of a Virtual Model of a University Building

Danielle Monfet

Several simulation tools are available to evaluate the energy performance of buildings. EnergyPlus, a state-of-the-art building energy analysis program that features the best capabilities of DOE and BLAST programs, was first released in 2001. Several researchers have compared and evaluated particular features of the program in specific context. However, only a limited amount of information, related to the simulation of large buildings, has been published so far.

This thesis presents the development of a virtual model of an academic building using the EnergyPlus program. The Concordia Sciences building, located in Montréal, has a total floor area of 32,000 m^2. The building consists mainly of research and academic labs. The size and the complexity of the heating, ventilation and air conditioning (HVAC) and heat recovery systems make the modeling process a challenge and an excellent way to evaluate the capabilities and features of EnergyPlus.

This thesis presents the approach taken to develop the computer model, the analysis of measured data, the approach taken to calibrate the model, the results of calibration as well as comments about problems encountered throughout the process. Information about the as-built and as operated thermal performance of the Sciences building is obtained from the Monitoring and Data Acquisition System through the

collaboration of the Physical Plant of Concordia University. The model is calibrated over the spring season, from March 20th to June 20th. The comparison is performed between measured and simulated supply airflow rates and supply and return set point temperatures.

A sensitivity analysis of the computer model is presented to assess the impact of some selected parameters on the calibrated model. The annual demand and consumption are also evaluated using the calibrated model.

ACKNOWLEDGMENTS

I would first like to thank my supervisor, Dr. Radu Zmeureanu, for his great advice and support throughout this research. He made the research process enjoyable and undoubtedly interesting. Special thanks to Nicolas Lemire and Roland Charneux from the firm Pageau, Morel et Associés for providing design information about the building used for the case study, answering questions and encouraging me. Thank you to Yves Gilbert, Stéphane Drolet and Martin Dicaire from the Physical Plant, to Éric Ambroise from Environmental Health & Safety and Sylvain Bélanger from AITS of Concordia University. Thank you to Francis Chartier, from Siemens, for taking the time to explain the functions and capabilities of the software used for the monitoring and data acquisition system.

Special thanks to my friends and cousins for keeping my mind off things whenever it was necessary. Finally, my deepest appreciation goes to my parents and to Andrée, François-Pierre, Raphaël and Anne-Marie for always encouraging me and supporting all my career choices.

TABLE OF CONTENTS

List of Figures x

List of Tables xviii

Nomenclature xx

1. Introduction 1

1.1 Problem Statement 1

1.2 Scope and Methodology 2

2. Literature Review 5

2.1 Computer Simulation of Existing and New Buildings 5

2.2 Development of a Computer Model 8

2.2.1 Simulation Approach 8

2.2.1.1 Overall Modeling Approaches 9

2.2.1.2 Space Load Calculation 10

2.2.1.3 Secondary Equipment Load Calculation 16

2.2.1.4 Primary Equipment Load Calculation 19

2.2.2 Ventilation of Laboratories 23

2.3 Validation and Calibration 24

2.3.1 Validation of the Model 24

2.3.2 Calibration 25

2.4 Objective of the Thesis 28

2.5 Methodology 29

3. Energyplus 31

3.1 General Characteristics of the Program 31
3.2 Modeling Options 32
3.2.1 Zone Options 33
3.2.2 System Options 35
3.2.3 Plant Options 39
3.3 Verification and Use 42
4. Development of the Computer Model 45
4.1 Methodology 45
4.2 Short Description of the Sciences Building 46
4.2.1 Building Exterior Envelope 47
4.2.2 Heating and Cooling Space Loads 48
4.2.3 HVAC Systems 48
4.2.4 Primary Systems 49
4.3 Modeling Approach 51
4.3.1 Architectural Systems 52
4.3.2 HVAC Systems 58
4.3.3 Primary Systems 61
4.3.4 Computing Time 63
4.4 Summary 63
5. As-Operated Performance of the Sciences Building 65
5.1 Average Monitored Data at the Sciences Building 65
5.2 Analysis 70
5.2.1 Airflow Rates 71

5.2.1.1 Sectors B and C 71
5.2.1.2 Sector A 72
5.2.2 Supply and Return Air Temperatures 75
5.2.3 Air-Side Thermal Load 77
5.2.4 Water Systems 79
5.3 Detailed Analysis of Monitored Data for Selected Weeks 87
5.3.1 March 20th to March 26th 2006 88
5.3.2 April 24th to April 30th 2006 90
5.3.3 May 15th to May 21st 2006 92
5.3.4 June 12th to June 18th 2006 94
5.4 Summary 95
6. Computer Model Calibration 98
6.1 Comparison with Monitored Data 98
6.1.1 Analysis of Period A 99
6.1.1.1 Sectors B & C 99
6.1.1.2 Sector A 107
6.1.2 Analysis of Period B 113
6.1.2.1 Sectors B and C 113
6.1.2.2 Sector A 121
6.2 Sensitivity Analysis 126
6.2.1 Air Infiltration 129
6.2.2 Internal Gains 131
6.2.2.1 Lighting 131

6.2.2.2 Occupants 133
6.2.3 Economizer Settings 135
6.2.4 Fan Efficiency 137
6.3 Annual Energy Performance 141
6.4 Summary 142
7. Conclusions 144
7.1 Discussion of Results 144
7.2 Recommendations for Future Work 147
References 149

LIST OF FIGURES

Figure 2.1: Overall Modeling Strategy [2] 10

Figure 2.2: Diagram of Chiller [11] 22

Figure 3.1: Overall Structure of EnergyPlus [23] 32

Figure 3.2: Solution Manager for the Heat Balance Method in EnergyPlus [28] 34

Figure 3.3: Example of Air Loop Schematic [30] 36

Figure 3.4: Example of Plan Loop Schematic [30] 39

Figure 3.5: Plant Supply-Side Solution Scheme [29] 40

Figure 3.6: Loops Interaction for EnergyPlus Sizing [28] 40

Figure 3.7: Diagram of Vapour Compression Chiller: Electric with Heat Recovery [29] 41

Figure 4.1: General Building Layout 46

Figure 4.2: Simplified Schematic of HVAC Systems and Central Plant 50

Figure 4.3: Definition of the Partition Wall between two Adjacent Zones 53

Figure 4.4: Plenum and Zone Temperature Variation during the Summer Design Day .. 55

Figure 4.5: Plenum and Zone Temperature Variation during the Winter Design Day 55

Figure 4.6: Direct Exhaust Plenum and Zone Temperature Variation during the Summer Design Day 56

Figure 4.7: Direct Exhaust Plenum and Zone Temperature Variation during the Winter Design Day 56

Figure 4.8: Compact Zone System Inputs 58

Figure 4.9: Zone Sizing Inputs 59

Figure 4.10: Water-Side Zone Equipment Inputs 59

Figure 4.11: Air-Side Zone Equipment Inputs 60

Figure 4.12: Heating Water Loop Schematic 61

Figure 4.13: Cooling and Reheat Simulation Schematic 62

Figure 5.1: Outdoor Air Temperature for the month of May 66

Figure 5.2: Capture of Display Software for Sectors B & C Air Handling Unit 67

Figure 5.3: Airflow Variation for the Month of May; Sectors B & C 69

Figure 5.4: Air Temperature Variation for the Month of May; Sectors B & C 69

Figure 5.5: Variation of the Supply Airflow Rate with Outdoor Air Temperature for the Spring Season 75

Figure 5.6: Hourly Values of Supply Air Temperature versus Outdoor Air Temperature for the Spring Season; Sectors B & C 76

Figure 5.7: Hourly Values of Supply Air Temperature versus Outdoor Air Temperature for the Spring Season; Sector A 76

Figure 5.8: Sector Cooling Load versus Outdoor Air Temperature for the Spring Season; Sectors B and C 78

Figure 5.9: Sector Cooling Load versus Outdoor Air Temperature for the Spring Season; Sector A 78

Figure 5.10: Water Temperatures at Chiller CH-3 over the Spring Season 80

Figure 5.11: Water Temperatures at Chiller CH-4 over the Spring Season 80

Figure 5.12: Variation of Chiller Load from March 20th to May 4th. 82

Figure 5.13: Air Temperature Variation for March 30th and 31st, 2006 82

Figure 5.14: Chiller Load versus Building Load; March 20th to May 4th, 2006 83

Figure 5.15: Chiller Load versus Outdoor Air Temperature; March 20th to May 4th, 2006 83

Figure 5.16: Water Temperature of CNDS and HWS over the Spring Season 84

Figure 5.17: Heating Water Temperature versus Outdoor Air Temperature over the Spring Season..... 85

Figure 5.18: Condenser Water Temperature versus Outdoor Air Temperature over the Spring Season..... 85

Figure 5.19: Glycol Water Temperature Variation for the Spring Season; Sectors B & C 86

Figure 5.20: Glycol Water Temperature Variation for the Spring Season; Sector A 86

Figure 5.21: Glycol Temperature Difference versus Outdoor Air Temperature over the Spring Season; Sectors B and C..... 87

Figure 5.22: Glycol Temperature Difference versus Outdoor Air Temperature over the Spring Season; Sector A 87

Figure 5.23: Airflow Variation for the Week of March 20th to March 26th..... 88

Figure 5.24: Air Temperature Variation for the Week of March 20th to March 26th..... 88

Figure 5.25: HW and CND Water Temperature Variation for the Week of March 20th to March 26th 89

Figure 5.26: Chilled Water Temperature Variation for the Week of March 20th to March 26th 89

Figure 5.27: Glycol Temperature Variation for the Week of March 20th to March 26th .. 90

Figure 5.28: Airflow Variation for the Week of April 24th to April 30th..... 90

Figure 5.29: Air Temperature Variation for the Week of April 24th to April 30th..... 90

Figure 5.30: HW and CND Water Temperature Variation for the Week of April 24th to April 30th 91

Figure 5.31: Chilled Water Temperature Variation for the Week of April 24th to April 30th 91

Figure 5.32: Glycol Temperature Variation for the Week of April 24th to April 30th 92

Figure 5.33: Airflow Variation for the Week of May 15th to May 21st 92

Figure 5.34: Air Temperature Variation for the Week of May 15th to May 21st 93

Figure 5.35: Water Temperature Variation for the Week of May 15th to May 21st 93

Figure 5.36: Glycol Temperature Variation for the Week of May 15th to May 21st 93

Figure 5.37: Airflow Variation for the Week of June 12th to June 18th 94

Figure 5.38: Air Temperature Variation for the Week of June 12th to June 18th 94

Figure 5.39: Water Temperature Variation for the Week of June 12th to June 18th 95

Figure 6.1: Revised Outdoor Air Temperature for the Month of May 99

Figure 6.2: Airflow Rate Variation from May 4th to June 20th; Sectors B & C 100

Figure 6.3: Air Temperature Variation from May 4th to June 20th; Sectors B & C 101

Figure 6.4: Revised Air Temperature Variation from May 4th to June 20th; Sectors B & C 101

Figure 6.5: Revised Airflow Rate Variation from May 4th to June 20th; Sectors B & C 102

Figure 6.6: Supply Airflow Rate including Laboratories Requirements from May 4th to June 20th; Sectors B & C 103

Figure 6.7: Sector Load from May 4th to June 20th; Sectors B & C 105

Figure 6.8: Estimated Sector Air-Side Thermal Load versus Outdoor Air Temperature from May 4th to June 20th; Sectors B & C 106

Figure 6.9: Estimated Zone Thermal Load of all Zones versus Outdoor Air Temperature from May 4th to June 20th; Sectors B & C 106

Figure 6.10: Estimated Cooling Coil Load versus Outdoor Air Temperature from May 4th to June 20th; Sectors B & C 106
Figure 6.11: Airflow Rate Variation from May 4th to June 20th; Sector A 107
Figure 6.12: Air Temperature Variation from May 4th to June 20th; Sector A 108
Figure 6.13: Revised Air Temperature Variation from May 4th to June 20th; Sector A . 109
Figure 6.14: Revised Airflow Rate Variation from May 4th to June 20th; Sector A 109
Figure 6.15: Airflow Rate including Laboratories Requirements from May 4th to June 20th; Sector A 110
Figure 6.16: Sector Load from May 4th to June 20th; Sector A 111
Figure 6.17: Estimated Sector Air-Side Thermal Load versus Outdoor Air Temperature from May 4th to June 20th; Sector A 112
Figure 6.18: Estimated Thermal Load of all Zones versus Outdoor Air Temperature from May 4th to June 20th; Sector A 112
Figure 6.19: Estimated Cooling Coil Load versus Outdoor Air Temperature from May 4th to June 20th; Sector A 113
Figure 6.20: Airflow Rate Variation from March 20th to May 3rd; Sectors B & C 114
Figure 6.21: Predicted Airflow Rate versus Outdoor Air Temperature from March 20th to May 3rd; Sectors B & C 115
Figure 6.22: Air Temperature Variation from March 20th to May 3rd; Sectors B & C ... 116
Figure 6.23: Predicted Supply Air Temperature versus Outdoor Air Temperature from March 20th to May 3rd; Sectors B & C 116
Figure 6.24: Revised Airflow Rate Variation from March 20th to May 3rd; Sectors B & C 117

Figure 6.25: Revised Air Temperature Variation from March 20th to May 3rd; Sectors B & C 117
Figure 6.26: Revised Predicted Airflow Rate versus Outdoor Air Temperature from March 20th to May 3rd; Sectors B & C 118
Figure 6.27: Revised Predicted Air Temperature versus Outdoor Air Temperature from March 20th to May 3rd; Sectors B & C 119
Figure 6.28: Sector Air-Side Thermal Load from March 20th to May 3rd; Sectors B & C 119
Figure 6.29: Estimated Sector Air-Side Thermal Load versus Outdoor Air Temperature from March 20th to May 3rd; Sectors B & C 120
Figure 6.30: Estimated Re-heat and Heating Coils Load versus Outdoor Air Temperature from March 20th to May 3rd; Sectors B & C 120
Figure 6.31: Airflow Rate Variation from March 20th to May 3rd; Sector A 121
Figure 6.32: Air Temperature Variation from March 20th to May 3rd; Sector A 122
Figure 6.33: Supply Air Temperature versus Outdoor Air Temperature from March 20th to May 3rd; Sector A 122
Figure 6.34: Sector Air-Side Thermal Load from March 20th to May 3rd; Sector A 123
Figure 6.35: Estimated Sector Air-Side Thermal Load versus Outdoor Air Temperature from March 20th to May 3rd; Sector A 124
Figure 6.36: Estimated Re-heat and Heating Coils Load versus Outdoor Air Temperature from March 20th to May 3rd; Sector A 124
Figure 6.37: Outdoor Air Temperature Variation from March 20th to March 26th; Without Mechanical Cooling 127

Figure 6.38: Outdoor Air Temperature Variation from June 12th to June 18th; With Mechanical Cooling 127

Figure 6.39: Variation of the Supply Airflow Rate without and with Air Infiltration; Sectors B & C 130

Figure 6.40: Variation of the Return Air Temperature without and with Air Infiltration; Sectors B & C 130

Figure 6.41: Variation of the Supply Airflow Rate with Lighting Load; Sectors B & C132

Figure 6.42: Variation of the Cooling Air-Side Thermal Load with Lighting Load; Sectors B & C 132

Figure 6.43: Variation of the Return Air Temperature with Lighting Load; Sectors B & C 133

Figure 6.44: Variation of the Supply Airflow Rate with Occupancy Level; Sectors B & C 134

Figure 6.45: Variation of the Return Air Temperature with Occupancy Level; Sectors B & C 134

Figure 6.46: Variation of the Cooling Air-Side Thermal Load with Occupancy Level; Sectors B & C 135

Figure 6.47: Variation of the Supply Airflow Rate with Economizer Cut-Off Temperature; Sectors B & C 136

Figure 6.48: Variation of the Cooling Coil Load with Economizer Cut-Off Temperature; Sectors B & C 136

Figure 6.49: Variation of the Supply Fan Electricity Consumption with Fan Efficiency; Sectors B & C 137

Figure 6.50: Variation of the Return Fan Electricity Consumption with Fan Efficiency; Sectors B & C 138

LIST OF TABLES

Table 2.1: Regression Coefficients for the Fan Model [10] 18

Table 2.2: Different Forms of Sensitivity Coefficients [20] 27

Table 2.3: Sensitivity Coefficients for Office Buildings [20] 28

Table 4.1: Zone Distribution by Sector 52

Table 4.2: Definition of Partition Vertices 53

Table 4.3: Computing Time 63

Table 5.1: Description of Monitored Data 65

Table 5.2: Monthly Average of the Outdoor Air Temperature 66

Table 5.3: Daily Average Measurements on the Air-Side Loop for the Month of May; Sectors B & C 68

Table 5.4: Daily Average Water Temperature [°C] for the Month of May; Sectors B & C 70

Table 5.5: Design Assumptions for Exhaust Hoods [39] 72

Table 5.6: Summary of Airflow Rates 74

Table 5.7: Overview of Air Systems Data 79

Table 6.1: Overview of Period A 113

Table 6.2: Overview of Period B 124

Table 6.3: Overview of Spring Season 125

Table 6.4: Sensitivity Coefficients for Office Buildings [20] 138

Table 6.5: Overview of Average Influence Coefficients for Internal Gains; Sectors B & C 139

Table 6.6: Overview of Average Influence Coefficients for Fan Electricity Consumption; Sectors B & C 139

Table 6.7: Overview of Influence Coefficients for Economizer Cut-Off Temperature; Sectors B & C 140

Table 6.8: Cooling Coil Loads; Simulated versus Design 141

Table 6.9: Annual Electricity Consumption Estimated by the EnergyPlus Program 142

Table 6.10: Annual Electricity Consumption per Floor Area Estimated by EnergyPlus Program 142

NOMENCLATURE

Symbol		Units
Roman		
a, b	Air system coefficients for a certain range of zone air temperatures	
g_i	Air temperature weighting factor	
$h_{c,i}$	Surface convection coefficient	$W/m^2 \cdot °C$
$h_{in,\,air}$	Coil entering enthalpy	kJ/kg
$h_{out,\,air}$	Coil leaving enthalpy	kJ/kg
m	Mass flow rate	kg/s
q	Instantaneous heat gains	W
q_{conv}	Convective heat transfer from surfaces	W
$q_{conv,int}$	Sum of the convective portions of all internal heat gains	W
q_{CE}	Convective parts of the internal loads	W
q_{IV}	Sensible load due to infiltration and ventilation air	W
q_{sys}	Heat flow removed or supplied by the HVAC system	W
$q''_{\alpha sol}$	Absorbed direct and diffuse solar radiation flux	W/m^2
$q''_{conv,z}$	Convective heat flux to zone air	W/m^2
$q''_{conv,o}$	Convective exchange flux with outside air	W/m^2
q''_{ki}	Conductive heat flux on inside surface	W/m^2
q''_{ko}	Conductive heat flux on outside face	W/m^2
q''_{LWR}	Net long-wave radiation flux exchange with air and surroundings	W/m^2
q''_{LWS}	Long-wave radiation flux from equipment in zone	W/m^2
q''_{LWX}	Net long-wave radiant flux exchange between zone surfaces	W/m^2

q''_{sol}	Transmitted solar radiative flux absorbed at surface	W/m^2
q''_{SW}	Net short-wave radiation flux to surface from lights	W/m^2
t	Time	h
t_{sys}	System time step	h
v_i	Instantaneous heat gain factors	
w_i	Cooling/heating load factors	
A_i	Surface area	m^2
C	Capacity flow rate	$J/K \cdot s$
C_p	Specific heat	$kJ/kg \cdot K$
C_i	Equation coefficients	
ER	Extraction rate	W
FFLP	Fraction full load power	
HRE	Efficiency of the heat recovery system installed on the exhaust stream	
IC	Influence coefficient	
IP	Input parameter value	
M	Mass of water in the loop	kg
OP	Output parameter value	
P_i	Extraction rate weighting factor	
PLR	Part load ratio	W
Q	Load	W or kW
Q_{cd}	Heat rejected at the condenser	W
Q_{ev}	Heat absorbed at the evaporator	W
T_a	Zone air temperature	°C

$T_{di\text{-}new}$	Current demand side inlet temperature	°C
$T_{di\text{-}old}$	Previous time step demand inlet temperature	°C
T_o	Outdoor air temperature	°C
$T_{R/A}$	Weighted average return air temperature	°C
$T_{S/A}$	Weighted average supply air temperature	°C
T_{si}	Inside surface temperature	°C
T_{ssi}	Supply side inlet temperature	°C
T_{so}	Outside surface temperature	°C
T_{sso}	Supply side outlet temperature	°C
T_{su1}	Supply temperature of fluid 1	°C
T_{su2}	Supply temperature of fluid 2	°C
T_v	Ventilation air temperature	°C
$T_{w,ex}$	Exhaust water temperature	K
$T_{w,su}$	Supply water temperature	K
V	Volumetric flow rate	m^3/s
W	Power	W or kW
X_j	Outside Conductance CTF coefficient for j = 0,1,…nz	
Y_j	Cross CTF coefficient for j = 0,1,…nz	
Z_j	Inside CTF coefficient for j = 0,1,…nz	
Greek		
δ	Time step	h
ε	Semi-isothermal effectiveness	
ρ	Density	kg/m^3

ΔIP	Input difference	
ΔOP	Output difference	
ΔT	Temperature difference	°C
Φ_j	Flux CTF coefficient for j = 1,2,…nq	

Subscripts

a	Air
des	Design
f	Fluid
i	Counter
max	Maximum
min	Minimum
r	Rated
w	Water
B	Boiler
BC	Base Case
C	Compressor
F	Fan
HX	Heat exchanger
P	Pump
S	Shaft

1. INTRODUCTION

1.1 Problem Statement

In Canada, between 1990 and 2003, the energy demand has increased by 22%. Over the same period, in the commercial and institutional building sectors, the energy consumption has increased by 36% [1]. Understanding and properly evaluating the performance of buildings is essential to reduce the energy consumption of buildings. Different approaches are available to evaluate building energy performance. In most cases, a detailed modeling of systems allows the building manager to estimate the potential impact of retrofits or renovations on the overall energy performance of the building.

Since the mid-seventies, the complexity and accuracy of energy analysis tools have considerably evolved. Different approaches have been used to evaluate the energy consumption in buildings and, with increased demand, computer simulation programs, such as DOE-2, BLAST and TRNSYS, were developed in the mid 1970's [2]. Later, more complex simulation programs, such as ESP-r and EnergyPlus, were developed. These new modular programs increase modeling capabilities by allowing designer to include their own subroutines for new and innovative heating, ventilation and air conditioning (HVAC) systems.

EnergyPlus, a state-of-the-art building energy analysis program that features the best capabilities of DOE and BLAST programs, was first released in 2001. Several researchers have compared and evaluated particular features of the program in specific

context. Window types and configurations, natural ventilation of an office building with open atrium using the COMIS module, and ground source heat pump systems are just a few features that have been simulated using EnergyPlus. However, only a limited amount of information, related to the simulation of large buildings, has been published so far.

The EnergyPlus simulation program is becoming more popular and used by consulting firms in the United States and, more recently, in Canada. Only a few detailed evaluations of the program for large buildings with complex electro-mechanical systems have been performed so far. The new Concordia Sciences building, located in Montréal, has a total floor area of 32,000 m^2. The building consists mainly of research and academic labs. The size and the complexity of the HVAC and heat recovery systems make the modeling process a challenge and an excellent way to evaluate the capabilities and features of EnergyPlus.

1.2 Scope and Methodology

The main objective of the thesis is to develop a virtual model of the Concordia Sciences building using the EnergyPlus program. The virtual model could eventually be used by the building operators to evaluate the impact of future modifications made to the HVAC and architectural systems on the overall energy performance of the building.

To achieve this objective, a review of the literature on computer simulation programs, modeling techniques and model validation and calibration techniques is first presented (Chapter 2). Characteristics and solving techniques used in the EnergyPlus

program are reviewed to have a better comprehension of its features and capabilities (Chapter 3). This section is essential to understand and properly integrate all the architectural, electrical and mechanical features in the virtual model.

Characteristics of the Concordia Sciences building are presented in Chapter 4. A short description of the architectural and electrical features is included as well as a detailed descriptions of the HVAC systems, and of the heat recovery systems present in the building. The accurate modeling of the components/subsystems of the building and mechanical systems have a significant impact on the simulation of building energy use. The approach undertaken to develop the virtual model is presented as well as major assumptions and simplifications used to obtain a practical model of the building.

Information about the as-built and as-operated thermal performance of the Sciences building is obtained from the Monitoring and Data Acquisition System through the collaboration of the Physical Plant of Concordia University. Data used in this study were collected from March 13th to June 30th 2006 and were analyzed for a better understanding of how the air and water systems interact together (Chapter 5). Conclusions drawn from the analysis are included in the computer model for calibration purposes.

The model used for the case study is tuned up using monitored data collected at the building (Chapter 6). The model is calibrated over the spring season, from March 20th to June 20th. Since the annual or daily electrical and gas consumption information

are not available, comparison is performed in terms of supply airflow rates, and supply and return air temperatures. A sensitivity analysis is also performed on the calibrated model for selected input parameters to increase the level of confidence in the developed model. The analysis evaluates the impact of the assumptions made in the building simulation. The calibrated model is finally used to estimate annual indices such as energy demand and consumption.

General conclusions and recommendations related to the use of EnergyPlus for simulating large and complex buildings are presented in Chapter 7 as well as recommended future work.

2. LITERATURE REVIEW

2.1 Computer Simulation of Existing and New Buildings

Building simulation is a systemic, dynamic, non-linear and complex process. Simulation programs are based either on response function methods or on numerical methods using finite differences or, equivalently, finite volumes [3]. Computer models are developed by first creating mathematical models that describe the physical process to be simulated such as heat transfer through walls. Then a step-by-step approach for solving the mathematical model is built: that is the algorithm. The computer model is the implementation of the algorithm in a code. To create a virtual model, the building is defined based on the architectural drawings, site visits, the development of the components of the heating, ventilation and air conditioning (HVAC) systems according to the installed equipment and specifications, and the calibration of the model using monitored data and utility bills. The calibrated model can further be used to evaluate the impact of changes in equipment or operational strategies on the energy performance of the whole building or sub-systems.

Since the mid-seventies, the complexity and accuracy of energy analysis tools have considerably evolved. Initially, CPU capacity was a major concern when developing an energy simulation tool. Field measurements, theoretical developments, design analysis and case studies have expanded the knowledge on the subject leading to advancement in simulation tools [4]. Dynamic models have been developed since the late 1960's. Response factors, thermal network and Fourier analysis methods are just a few methods to mention. Different options have then been used to evaluate energy

consumption in buildings and with increased demand, computer simulation program such as DOE-2, BLAST and TRNSYS were developed in the mid 1970's [2]. Later, more complex simulation programs, such as ESP-r and EnergyPlus, were developed. These new modular programs increase modeling possibility and capabilities by allowing designer to include their own subroutines.

A total of twenty major building energy performance simulation programs have recently been indexed by the United States Department of Energy (DOE), the University of Strathclyde, and the University of Wisconsin [4]. These simulation programs have different capabilities and have been evaluated based on their general modeling features, such as zone loads, building envelope and daylighting, air infiltration, ventilation and multizone airflow, renewable energy systems, electrical systems and equipments, HVAC systems and equipments, just to name a few. Not all the listed programs have every features available. The key in the selection of a program is to determine the level of detail required for simulation purposes. At an early stage, the use of a simpler program might be sufficient to determine the initial design criteria, while more complex programs, such as DOE-2, TRNSYS, ESP-r and EnergyPlus, are more appropriate to obtain a detailed building performance analysis [4].

The energy performance of a building depends on its architectural, mechanical and electrical features. Different approaches are available to evaluate building energy performance. Life cycle cost, life emissions cost and life energy cost, including both operating energy and embodied energy costs, are just a few of the criteria used to asses

building performance. In most cases, detailed modeling of the systems allows the building manager to determine the overall energy consumption of the building. Monitoring and commissioning usually assist in the comprehension of the building operations. In Canada, the minimum requirements influencing the energy consumption are suggested in the Model National Energy Code for Buildings (MNECB). Two different approaches are proposed: the prescriptive and the performance path. The prescriptive path recommends minimum standards of construction for building components and features that affect a building's energy efficiency [5]. However, designers usually choose the building energy performance approach. Energy efficient buildings are at least 25% more efficient than what is proposed in the MNECB. Also, to encourage the building owners and investors to achieve 25% reduction in energy consumption, the commercial building incentive program (CBIP) has been put into place by the government of Canada. To receive the incentive, the designer must model the building using EE4. EE4 is a simulation program based on the DOE-2 energy analysis program that is used to demonstrate the impact of energy conservation measures and to prove that the design leads to annual energy consumption lower than that of the building designed in compliance with MNECB. Similarly, for existing buildings, the objective is to determine the overall energy consumption of the building compared with similar buildings and to simulate diverse scenarios to study the variation in energy consumption. For low-rise residential buildings, the HOT2000 program uses the bin method to evaluate energy consumption and impact of design building options [6]. The ultimate purpose of these programs is to raise the energy performance of the building.

2.2 Development of a Computer Model

Two subjects are considered when developing a simulation model used to predict the energy consumption of a building: 1) the modeling of components and subsystems, and (2) the overall modeling strategy. Most building energy programs compute the heating and cooling loads of every space for every hour of the simulation period, the system response, and then evaluate the overall energy consumption [2]. Generally, simulation programs are developed based on one of the following two approaches: 1) the forward or classical approach, and 2) the inverse or data-driven approach.

2.2.1 Simulation Approach

Most computer models have been developed using either the forward or the inverse approaches. The inverse approach is not commonly embraced by the professional community due to its lack of flexibility and the amount of information required to build the algorithm [2]. Therefore, only a brief description of its characteristics is presented. Emphasis is put on the forward approach, which is used in most cases.

The inverse or data-driven approach mathematically describes the systems parameters with the support of known and measured input and output variables. Two different set of data can be used to achieve this goal: intrusive and non-intrusive. Intrusive data are collected by operating the systems for predetermined or planned conditions for a broad range of normal system operation [2]. By setting some restrictions on the system parameters, the inputs and outputs acquired allow more accurate model developments and identifications. Non-intrusive data are collected under normal system operations and are used to develop the mathematical model. This approach is quite

useful to predict future system behaviours, but is not as flexible as the forward approach. PRISM, the Princeton Scorekeeping Method, is an example of data-driven approach. The method uses information from past utility bills and weather data to evaluate energy savings due to renovations, for instance the replacement of a boiler. The normalized annual consumption (NAC) index, which is determined based on the design conditions of the house, is calculated for the pre- and post-retrofit periods to evaluate the energy savings. The information collected is then used to evaluate savings on future houses retrofit [7]. Claridge and Haberl [8] have also developed a system to evaluate energy consumption of institutional and commercial buildings. The program is developed based on the Principal Component Analysis (PCA) of intercorrelated parameters to predict electricity consumption. Most inverse model programs used a combination of measured data to evaluate anticipated energy savings for building retrofits.

2.2.1.1 Overall Modeling Approaches

The following sections introduce the concepts used for the forward/direct approach. The heating and cooling load calculations are essential to develop the virtual model of a building. However, it is also necessary to develop an overall solving approach to interconnect all building components. Building and mechanical systems are simulated in sequence in most computer programs [9]. The space loads are first determined, followed by the secondary and primary system calculations for every hour. This approach leads to computational problems related to the limited interaction between each component and the utilization of data obtained from the previous time step in the process. Today's energy-efficient designs required the simulation of building and mechanical systems to be done simultaneously (Figure 2.1) [9]. This procedure gives

superior results since the interaction between different modules is instantaneous. However, this solving technique depends primarily on computer capacities and solving time is quite high. A compromise between the two approaches is usually sufficient to obtain satisfying modeling results.

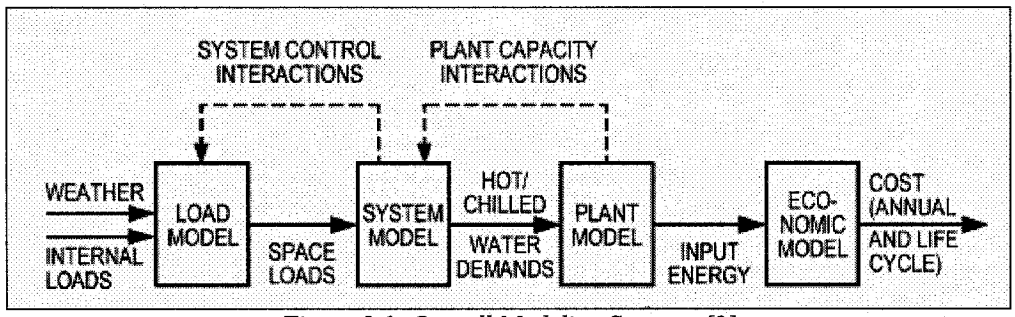

Figure 2.1: Overall Modeling Strategy [2]

2.2.1.2 Space Load Calculation

The forward approach is based on the calculation of three main components: the space load, the secondary equipment load, and the primary equipment energy requirements. The load for each component can be estimated using different techniques. Major distinctions are made between steady-state methods and dynamic methods. Steady-state models do not consider thermal mass or capacitance effects causing short-term temperature transients. Dynamic models, however, capture the effect of building warm-up or cool-down as well as peak loads. They are mainly used in situation where building load control, fault detection and diagnosis (FDD), and equipment control are of significant importance [2].

When using the forward approach, space loads are calculated using the general heat balance method, which evaluates heat fluxes using Conduction Transfer Functions (CTFs), or the weighting factor method or numerical methods. Emphasis is put on the

heat balance using CTFs and the weighting factor methods. Both approaches are based on the rate of heat flow into the space air mass. This is considered as the instantaneous space load and takes into consideration convective and radiative heat transfers. The air is assumed to have no thermal mass and equilibrium is achieved when the instantaneous load corresponds to the heat removed by the conditioning equipment. The two methods are briefly described.

Heat Balance Method

The heat balance method is based on the energy conservation principle, and the system of equations is usually solved using matrix algebra. Heat balance equations are developed for each surface and for the room air. Conductance Transfer Function (CTF) coefficients are used for the development of the outside and inside heat flux, as used in modeling tools such as BLAST and EnergyPlus. In order to develop the model, the following assumptions are made about room surfaces: uniform surface temperatures, uniform long-wave and short-wave irradiation, diffuse radiating surfaces and one-dimensional heat conduction through each building element. A set of equations is thus developed for the outside surface heat balance, the wall conduction, the inside face heat balance and the room air heat balance [2]. For the outside surface, the heat balance is given as follows:

$$q''_{\alpha sol} + q''_{LWR} + q''_{conv,o} - q''_{ko} = 0 \qquad (2.1)$$

where

$q''_{\alpha sol}$ is the absorbed direct and diffuse solar radiation flux [W/m^2];

q''_{LWR} is the net long-wave radiation flux exchange with air and surroundings [W/m^2];

$q''_{conv,o}$ is the convective exchange flux with outside air [W/m^2];

q''_{ko} is the conductive heat flux on outside face [W/m^2].

Similarly, the heat balance for the inside surface is given as follows:

$$q''_{LWX} + q''_{SW} + q''_{LWS} + q''_{ki} + q''_{sol} + q''_{conv,z} = 0 \qquad (2.2)$$

where

q''_{LWX} is the net long-wave radiant flux exchange between zone surfaces [W/m^2];

q''_{SW} is the net short-wave radiation flux to surface from lights [W/m^2];

q''_{LWS} is the long-wave radiation flux from equipment in zone [W/m^2];

q''_{ki} is the conductive heat flux on inside surface [W/m^2];

q''_{sol} is the transmitted solar radiative flux absorbed at surface [W/m^2];

$q''_{conv,z}$ is the convective heat flux to zone air [W/m^2].

The outside and inside conductive fluxes are, respectively, given as follows:

$$q''_{ko}(t) = -Y_o T_{si,t} - \Sigma\, Y_j\, T_{si,t-j\delta} + X_o T_{so,t} + \Sigma\, X_j\, T_{so,t-j\delta} + \Sigma\, \Phi_j\, q''_{ko,t-j\delta} \qquad (2.3)$$

$$q''_{ki}(t) = -Z_o T_{si,t} - \Sigma\, Z_j\, T_{si,t-j\delta} + Y_o T_{so,t} + \Sigma\, Y_j\, T_{so,t-j\delta} + \Sigma\, \Phi_j\, q''_{ki,t-j\delta} \qquad (2.4)$$

where

X_j is the outside CTF coefficient for j = 0,1,…nz;

Y_j is the cross CTF coefficient for j = 0,1,…nz;

Z_j is the inside CTF coefficient for j = 0,1,…nz;

Φ_j is the flux CTF coefficient for j = 1,2,…nq;

t is the time [h];

δ is the time step [h];

T_{si} is the inside surface temperature [°C];

T_{so} is the outside surface temperature [°C];

q''_{ki} is the conductive heat flux on inside surface [W/m^2];

q''_{ko} is the conductive heat flux on outside face [W/m^2].

Conduction transfer functions are response factors that relate conductive heat fluxes to the current and past surface temperatures and the past heat fluxes.

The room air heat balance is defined as follows:

$$q_{conv} + q_{CE} + q_{IV} \pm q_{sys} = 0 \qquad (2.5)$$

where

q_{conv} is the convective heat transfer from surfaces [W];

q_{CE} is the convective parts of the internal loads [W];

q_{IV} is the sensible load due to infiltration and ventilation air [W];

q_{sys} is the heat flow removed or supplied by the HVAC system [W].

Equation (2.5) can be re-written as follows:

$$q_{sys} = \Sigma A_i h_{c,i} (T_{si} - T_a) + q_{CE} + q_{IV} \quad (2.6)$$

The set of equations form by equations (2.1) and (2.2) can be rearranged to solve for the heat extraction rate. Generally, the heat extraction rate is expressed linearly and is defined as follows: $q_{sys} = a + b \cdot T_a$ (2.7)

where

q_{sys} is the heat flow removed or supplied by the HVAC system [W];

a, b are coefficients that apply over a certain range of zone air temperatures;

T_a is the zone air temperature [°C].

Equation (2.7) is solved using simultaneously the zone temperature equation, the outside surface temperature and the inside surface temperature. The zone temperature equation is given as follows:

$$T_a = \frac{a + \Sigma A_i h_{c,i} T_{si} + \rho_a C_{p,a} V_{infil} T_o + \rho_a C_{p,a} V_{vent} T_v + q_{conv,int}}{-b + \Sigma A_i h_{c,i} + \rho_a C_{p,a} V_{infil} + \rho_a C_{p,a} V_{vent}} \quad (2.8)$$

where

T_a is the zone air temperature [°C];

A_i is the area of i^{th} surface [m^2];

$h_{c,i}$ is the convection coefficient for i^{th} surface [$W/m^2 \cdot °C$];

$T_{si,i}$ is the surface temperature for i^{th} surface [°C];

ρ_a is the air density [kg/m^3];

$C_{p,a}$ is the specific heat of air [$J/kg \cdot K$];

V_a is the volumetric airflow rate [m^3/s];

T_o the outdoor air temperature [°C];

T_v is the ventilation air temperature [°C];

$q_{conv,int}$ is the sum of the convective portions of all internal heat gains [W].

The inside and outside surface air temperatures are defined in terms of response factors based on heat flux and face temperatures as describe in equations (2.9) and (2.10).

$$T_{s,o} = \frac{Y_o T_{si,t} + \Sigma Y_j T_{si,t-j\delta} - \Sigma X_j T_{so,t-j\delta} - \Sigma \Phi_j q''_{ko,t-j\delta} + \alpha G + h_{c,o} T_o}{X_0 + h_{c,o}} \quad (2.9)$$

$$T_{s,i} = \frac{Y_o T_{so,t} + \Sigma Y_j T_{so,t-j\delta} - \Sigma Z_j T_{si,t-j\delta} + \Sigma \Phi_j q''_{ki,t-j\delta} + T_{aj} h_{ci,j} + q''_{LWS} + q''_{LWX} + q''_{SW} + q''_{sol}{}^{e}}{Z_0 + h_{c,i}} \quad (2.10)$$

The CFT coefficients are evaluated based on the appropriate temperature range. The heat balance solution is iterative and based on hourly weather data and indoor design conditions. The solutions are first initialized, and then incident and transmitted solar flux for all surfaces are calculated, followed by the wavelength and convective energy from internal loads. The necessary calculations to determine the heat balance are completed with infiltration and ventilation loads calculations. Based on data obtained for all hours, iterations are performed until convergence is achieved. Convergence is necessary to obtain realistic and accurate simulation results. The method is also extended to heat transfer between zones [2].

Weighting Factor Method

The weighting factor method, used in the DOE-2 program, is a simplified form of the heat balance method. This method determines the space heat gains based on building geometry, ambient weather conditions, and internal load profiles [2]. The procedure includes the determination of (1) the instantaneous heat gains (q), (2) the cooling/heating load (Q), and (3) the extraction rate (ER) and indoor air temperature. The weighting

factors used in this method represent transfer functions for both the heat gain and air temperature. The heat gain factors are represented by *v* and *w*. The load at hour *t* for each type of heat gain (*q*) under consideration is given as follows:

$$Q_t = v_0 q_t + v_1 q_{t-1} + \ldots - w_1 Q_{t-1} - w_2 Q_{t-2} - \ldots \quad (2.11)$$

The heat gain weighting factors determine quantitatively the amount of energy entering a room that is stored and at what rate it is released afterwards [2]. Subsequently, the total cooling load is used, along with HVAC systems information for each zone and air temperature weighting factors, to calculate the heat extraction rates. The temperature at hour *t* is defined as follows:

$$T_t = 1/g_0 + [(Q_t - ER_t) + P_1 (Q_{t-1} - ER_{t-1}) + P_2 (Q_{t-2} - ER_{t-2}) + \ldots - g_1 t_{t-1} - g_2 t_{t-2} - \ldots] \quad (2.12)$$

where ER_t is the energy removal rate of the HVAC system at specified hour, and g_0, g_1, g_2, …, P_1, P_2, … are the air temperature weighting factors [2]. Two main assumptions characterize the weighting factor method: the processes modeled are linear, and the weighting factors are invariable with respect to time.

2.2.1.3 Secondary Equipment Load Calculation

The secondary equipment consists of all components located between the central plant and the building thermal zones. It consists of air-handling equipment, such as packaged air conditioners, air distribution systems including ductwork, dampers, fans, and heating, cooling, and humidity conditioning equipment. Liquid distribution systems (piping, valves and pumps) are also considered part of the secondary systems [2]. Two main categories are used to describe equipment: distribution components and heat transfer components. A combination of components from both categories forms the secondary system. Two different approaches are possible when simulating the secondary

equipment: (1) system-based approach (BLAST, DOE) and (2) component-based approach (TRNSYS, ESP-r, and EnergyPlus). When using the system-approach, complexity related to interconnecting all distribution and heat transfer components is eliminated. Variable air volume (VAV), constant air volume (CAV), or multi-zone systems are just a few examples of the standard systems available. Selecting one of the above options generates standard components linked with the specific system, thus simplifying the modeler's task. Component-based systems can be more detailed and flexible. Information about all components present in the system must be entered individually and connected to one another. This can considerably increase modeling time, but it has the advantages of proposing an endless amount of system configurations. In both cases, calculations of the energy consumption of the system are based on operating conditions and effectiveness. Each piece of equipment is considered separately to estimate the total energy requirement of the system. The type of equipment used determines the appropriate formula to be employed.

Energy calculations for secondary systems are based on variables such as dry-bulb temperature, humidity ratio and pressure. Enthalpy relationships are used to determined energy consumption. Fluid thermophysical properties play an important role in determining the characteristics of the systems.

Example of a Component-Based Model for a Simple Fan

Fan performance is determined for a given flow rate and is characterized by constant pressure rise across the fan. Negligible change in air density across the fan is

also assumed. The actual shaft power (W_s) is calculated from the rated fan power ($W_{s,rat}$) and the fraction full load power ($FFLP_F$) as follows [10]:

$$W_s = FFLP_F \, W_{s,rat} \tag{2.13}$$

The fraction of the rated power formula is given as follows:

$$FFLP_F = C_0 + C_1 \, PLR_F + C_2 \, PLR_F^2 + C_3 \, PLR_F^3 \tag{2.14}$$

Values for C_0, C_1, C_2 and C_3 are determined by the type of control used on the fan. Table 2.1 shows values for discharge dampers, inlet vanes and variable speed drive (VSD) control.

Table 2.1: Regression Coefficients for the Fan Model [10]

	C_0	C_1	C_2	C_3
Discharge Dampers	0.3507123	0.3085	-0.54137	0.871988
Inlet Vanes	0.3707	0.9725	-0.3424	0.0
VSD	0.00153	0.005208	1.1086	-0.11635563

The part load ratio (PLR_F) is given by equation (2.15).

$$PLR_F = \frac{m_a}{\rho_a \cdot V_{rat,F}} \tag{2.15}$$

where,

m_a is the air mass flow rate [kg/s];

ρ_a is the air density [kg/m^3];

$V_{rat,F}$ is the fan rated volumetric airflow rate [m^3/s].

Temperature increase due to the motor and transmission is also calculated if the motor is located inside the air stream. This approach is especially well-suited for system with fixed supply duct static pressure [10].

Example of a Component-Based Model for a Simple Pump

Calculations for pressure independent pump systems are similar to fan calculations. The required power is determined using regression analysis based on empirical relationships [10]. The fraction full load power ($FFLP_P$) is defined as follows:

$$FFLP_P = C_0 + C_1\, PLR_P + C_2\, PLR_P^2 + C_3\, PLR_P^3 \qquad (2.16)$$

Values for C_0, C_1, C_2 and C_3 are evaluated for the particular pump performance and system configuration. The part load ratio (PLR_P) is given by equation (2.17).

$$PLR_P = \frac{m_f}{\rho_f \cdot V_{rat,P}} \qquad (2.17)$$

where,

m_f is the fluid mass flow rate [kg/s];

ρ_f is the fluid density [kg/m^3];

$V_{rat,P}$ is the pump rated volumetric fluid flow rate [m^3/s].

In secondary systems, fans and pumps are the pieces of equipment with the highest contribution to the energy use. Components related to the air and water distribution systems must be included to determine the appropriate level of energy required to have the systems functioning properly. By using the appropriate combination of algorithms, the energy used by the secondary systems can be evaluated.

2.2.1.4 Primary Equipment Load Calculation

Primary HVAC systems deliver heating and cooling to a building through secondary systems. The primary components of the HVAC systems are the energy-consuming equipments. The load varies depending on the building characteristics, the design, the environmental conditions, and the control strategies. Primary system

components are modeled using either regression methods or first–principle methods. Functional form of the regression analysis is developed using exponential forms, Fourier series, and second- or third-degree polynomials. Manufacturer data combined with one of the above mentioned functional forms allow the designer to estimate the equipment energy consumption at total and partial load.

The first-principle methods are developed based on fundamental engineering analysis. These methods have the advantage of diminishing the number of unknown parameters and allow flexibility outside the range of available data. The first-principle approaches are more theoretical and give more accurate predictions of the equipment performances than results obtained by regression analysis. However, this approach is usually not practical because components sometimes need to be defined using empirical data obtained from experimentation [11]. The solving approach consists of describing each unit using a conceptual approach. The conceptual schema combines assembly of simple ideal components to reproduce the behaviour of the equipment. In general, a first set of parameters is determined based on the information available from the manufacturer. The identified parameters are then used to determine the behaviour of the component.

Example of a Component-Based Model for a Boiler

The development of models for primary systems is based on incompressible fluid. This assumption simplifies the computation process. Based on this assumption, empirical formulas are developed for each primary component. For boilers, the objective is to

determine the exhaust water temperature under steady-state conditions, both at maximum capacity and under partial loading [11]. The power is determined as follows:

$$W_B = C_w (T_{w,ex} - T_{w,su}) \quad (2.18)$$

where

W_B is the boiler power output [W];

$C_w = C_{p,w}\, m_w$, which is the capacity flow rate of water given by the specific heat [J/kg K] of water multiplied by the water mass flow rate [kg/s];

$T_{w,ex}$ and $T_{w,su}$ are the exhaust and supply water temperature [K].

In order to determine all parameters used to calculate the power output, the adiabatic temperature, the fuel/air ratio, the enthalpy and composition of the products as well as the gas mass flow rate is determined based on manufacturer information. Then, the gas enthalpy at the exhaust of the heat exchanger, the gas mean specific heat and the exhaust gas temperature are calculated until convergence is achieved. When the values are converging, the program determines the power output of the boiler.

Example of a Component-Based Model for a Chiller

For chillers, the overall model is based on the assumptions that the refrigerant is leaving the condenser as a saturated liquid and the evaporator at the saturated vapour state [11]. Identification of variables, based on manufacturer information, is first performed followed by the component simulation. It is also assumed that no heat exchange occurs with the environment. Chillers are modeled using four components: a condenser, a compressor, an evaporator and an expansion valve (Figure 2.2).

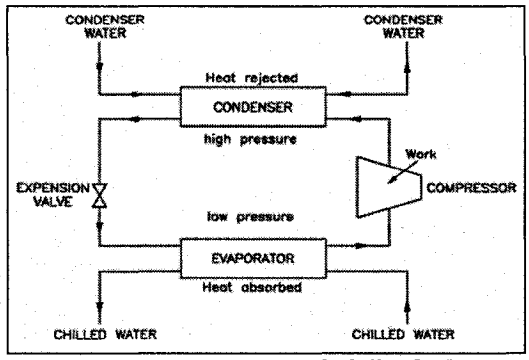

Figure 2.2: Diagram of Chiller [11]

For the stated assumptions, the following is applicable.

$$Q_{cd} = W + Q_{ev} \tag{2.19}$$

where

Q_{cd} is the heat rejected at the condenser [W];

W_C is the power required by the compressor [W];

Q_{ev} is the heat absorbed at the evaporator [W].

The condenser and evaporator are modeled as classical heat exchangers. The heat exchanger output is given by the following.

$$W_{HX} = \varepsilon C_{min} (T_{su1} - T_{su2}) \tag{2.20}$$

where

W_{HX} is the power output [W];

ε is the semi-isothermal effectiveness;

C_{min} is the minimum of the two capacity flow rates, which is given by the specific heat [J/kg · K] of water multiplied by the water mass flow rate [kg/s];

m_w is the water mass flow rate [kg/m^3];

$C_{p,w}$ is the water specific heat [J/kg · K];

T_{su1} is the supply temperature of fluid 1 [°C];

T_{su2} is the supply temperature of fluid 2 [°C].

The models for the condenser and evaporator are combined with the one for the compressor to model the chiller as a whole. Different types of chillers are available on the market. Majority of chillers are of the following three types: reciprocating, screw or centrifugal chillers. Since the project under discussion uses centrifugal chillers, emphasis is put on this type. To model a centrifugal chiller, the compressor is represented by only one stage. Also, isentropic behaviour is assumed so that all loses are occurring in the motor/transmission module. By combining the condenser, the evaporator and the compressor, the chiller operation can be modeled.

2.2.2 Ventilation of Laboratories

Ventilation of laboratories is essential for the safety of personal, and many factors must be taken into consideration throughout the design process. Most laboratories use 100% outside air, thus the system must be able to respond to a broaden range of conditions [12]. The amount of air ventilation required is determined based on either the total amount of exhaust from containment and exhaust devices, the cooling required for offsetting internal heat gains, or the minimum ventilation rate required [12]. For most lab applications, duct reheat is also available to ensure occupant comfort and temperature requirements for specific processes. The supply air systems provide thermal comfort for occupants, replace air exhausted through fume hoods, control space pressurization and the overall laboratories environment.

The presence of laboratories in institutional buildings has an enormous influence on its energy performance, since a significant part of the energy used is for heating, cooling and distribution of air ventilation to laboratories. Evaluating the ventilation

requirements and including energy efficient measures improve the overall performance of the building. Integrating all of the above in a model is challenging and careful attention must be given to each parameter to adequately represent the installed systems.

2.3 Validation and Calibration

The use of computer models as design tools is constantly rising. The challenge however is to determine the accuracy and to perform the validation of the model. This has led to the development of guidelines to validate and calibrate computer models.

2.3.1 Validation of the Model

Model validation can be achieved using different techniques. It can either be done using analytical models, experimental data or through comparison between outputs from different computer models. The analytical approach compared results obtained using the computer program with data obtained analytically for the same set of conditions. Analytical model are based on mathematical formulation of building behaviour. For empirical validation, information obtained from experimental or existing buildings is used to compare with data generated by modeling with the computer program [13]. The International Energy Agency has developed HVAC BESTEST, a series of steady-state tests used to evaluate the ability of whole-building simulation programs [14]. The tests consist of analytical verifications of a specified mechanical system applied to a simplified near-adiabatic building envelope [13]. Results for eight different commonly used simulation programs are also included as a comparison tool for new software [15]. HVAC BESTEST assists in identifying bugs, algorithm, physics and documentation

errors. This testing procedure ensures program credibility when new simulation programs are being developed.

2.3.2 Calibration

Calibration can be labour intensive and requires experience from the modeler. It requires a throughout understanding of the architectural layout and of mechanical systems. To adequately calibrate the model, the sources of errors need to be identified. The initial assumptions such as air infiltration and air ventilation need to be revisited. Also, the operating conditions must be verified. This includes schedule information and controls. Divergence between simulation and real life occupancy schedules influences the ventilation load throughout the day, and affects cooling and heating patterns. Inadequate modeling of the sequence of controls affects the overall functioning of a building. Comparison between designed and installed controls is necessary to reduce uncertainties in the model. Human factors also need monitoring. Modifications to the original design in response to comfort problems result in changes in energy consumption and building performances. When calibrating a computer model, revisions to the systems and initial assumptions are required to develop an accurate model.

Generally, when creating a virtual building model, utility bills are used as a comparison tool, when they are available. The model is modified to reach an acceptable degree of convergence between both set of data (utility bills and computer data). For example, the evaluation for the energy consumption for interior loads such as lighting, receptacles or domestic hot water is satisfactory when it is within 5% of the utility bills on a monthly basis, and 15% on a daily basis [16]. However, these percentages may be

increased to 15-25% and 25-35%, respectively, for HVAC systems [16]. It is recommended to be within 10% of monthly data and 15% for the daily data for the overall building. For annual consumption, the difference between simulated and monitored is recommended to be within 10% on an annual basis and 25% on a seasonal basis [17]. The weaknesses of a model are usually related to poor analysis of electrical demand, modeling of morning warm-up process, thermal mass simulation, control sequences simulation and simulation of actual operations [16]. Judgement should be used to improve the model and obtain results within the above mentioned calibration ranges.

Sensitivity analysis is often used to increase the level of confidence in the developed virtual model. The method tries to develop a mathematical foundation to calibrate simulation results with monitored data [18]. The complete analysis process includes 1) sensitivity analysis, 2) identification analysis, 3) numerical optimization, and 4) uncertainty analysis [19]. Most approaches are based on an objective function that attempts to minimize the month-by-month, or hour-by-hour if possible, mean square errors between measured and simulated data. The sensitivity analysis is used to reduce the number of parameters to be optimized. The least-squares method assumes that the best estimated parameters are those parameters that result in minimal sum of the deviations squared between the simulated outputs and the actual measured data [19]. It allows the identification of the input parameters with strong influence while keeping constant or as defaults the weak variables. The first step is to determine the strong variables. The use of correlation coefficients is usually used to investigate parameters

interdependence. The most commonly used sensitivity coefficients quantitatively compare changes in output with changes in input (Table 2.2).

Table 2.2: Different Forms of Sensitivity Coefficients [20]

Symbol	Formulae	Dimensions	Common name(s)
IC_1	$\Delta OP/\Delta IP$	with dimension	Sensitivity coefficient, influence coefficient
IC_2	$\frac{\Delta OP/OP_{BC}}{\Delta IP/IP_{BC}}$	$\frac{\%\text{ OP change}}{\%\text{ IP change}}$	Influence coefficient, point elasticity
IC_3	$\frac{\Delta OP/OP_{BC}}{\Delta IP}$	with dimension	Influence coefficient
IC_4	$\frac{\Delta OP \div [(OP_1+OP_2)/2]}{\Delta IP \div [(IP_1+IP_2)/2]}$	$\frac{\%\text{ OP change}}{\%\text{ IP change}}$	Arc mid-point elasticity
IC_5	$\frac{(\Delta OP/\Delta IP)}{(OP_{mean}/IP_{mean})}$	$\frac{\%\text{ OP change}}{\%\text{ IP change}}$	Slope of the linear regression line divided by the ratio of the mean output and mean input values are taken to determine the sensitivity coefficient

where,

ΔOP, ΔIP are changes in output and input, respectively;

OP_{BC}, IP_{BC} are base case values of output and input, respectively;

IP_1, IP_2 are two values of input;

OP_1, OP_2 are two values of the corresponding output;

OP_{mean}, IP_{mean} are mean values of output and input, respectively.

Parameters influencing simulation results are grouped in three main categories: 1) building load, 2) HVAC systems, and 3) HVAC refrigeration plant [20]. For each category, different input parameters can be identified for sensitivity analysis. Lam and Hui [20] have performed a sensitivity analysis of energy performance of office buildings. Changes in percent output over percent input for important parameters are presented for both annual electricity and peak electricity (Table 2.3). Results presented are a good indication of the input parameters having an influence on the building performance. For instance, the internal gains (lights and people) have the highest impact on the peak

electric demand: 0.289 and 0.328 %OP per %IP, respectively. Carroll and Hitchcock [21] presented methods and implementation techniques to calibrate simulated building. The guidelines presented are for the implementation of a mathematical model within a simulation program that assists in the tuning of certain simulation parameters. Results presented for the case study are useful for calibrating the building under study. Pasqualetto et al. [22] used sensitivity analysis to validate the MICRO-DOE2.1E program. Their results give good indications of the influential parameters in building simulation programs such as envelope thermal resistance, internal gains (equipment and lighting) and secondary systems settings, just to name a few. Overall, sensitivity analysis is mainly use as a tool to evaluate the accuracy of the model and demonstrate the validity of simulation assumptions.

Table 2.3: Sensitivity Coefficients for Office Buildings [20]

Category	Input Parameter	Annual Electricity (IC_2) [% OP per % IP]	Peak Electricity (IC_2) [% OP per % IP]
Building Load	Shading coefficient of windows	0.083	0.112
	Window-to-wall ratio	0.060	0.082
	Space air temperature [°C]	-0.140	-0.190
	Equipment load [W/m^2]	0.252	0.220
	Lighting load [W/m^2]	0.418	0.289
	Occupancy density [occ./m^2]	0.210	0.328
HVAC System	Outdoor airflow rate [l/s/person]	0.114	0.236
	Fan efficiency	0.145	0.154
	Fan static pressure (Pa)	0.148	0.155
HVAC Refrigeration Plant	Chilled water supply temp. [°C]	-0.136	-0.029
	COP	0.363	0.503

2.4 Objective of the Thesis

The main objectives of the thesis are (1) to develop a virtual model of the Concordia Sciences building using the EnergyPlus program, a state-of-the-art building energy analysis program; (2) to calibrate the computer model using monitored data; (3) to

test capabilities offered by the EnergyPlus program to develop a virtual model of a complex buildings for cold climate.

2.5 Methodology

The new Concordia Sciences building, located in Montréal, has a total building area of 32,000 m^2. The building has been in operation since September 2003 and consists mainly of research and academic labs. One section of the building is exclusively devoted to laboratory animals, and the remaining of the building area is mainly divided between academic laboratories with fume hoods and offices. The size and the complexity of the HVAC and heat recovery systems make the modeling process a challenge and an excellent way to evaluate the capabilities and features of EnergyPlus.

The building under study was submitted for Commercial Building Incentive Program (CBIP) application, which uses the DOE-2 program as the engine for EE4/CBIP program and encourages the reduction of energy consumption in commercial building. The files provided by the mechanical consultant, Pageau, Morel et Associés (PMA), were helpful to create the initial input file in this study and reduce the time needed for collecting the architectural data. Many energy recovery systems have been installed to reduce the building's energy requirements. Interconnecting and properly integrating all the systems in EnergyPlus is a challenge. The approach employed and the issues related to the development of the input file are presented.

Information about the as-built and as-operated thermal performance of the Sciences building is obtained from the Monitoring and Data Acquisition System through

the collaboration of the Physical Plant of Concordia University. The information collected, from March 13th to June 30th 2006, is analyzed to better understand the installed systems performance and the overall building behaviour. The EnergyPlus model is then modified to reflect the conclusions drawn from the analysis of monitored data.

The model is calibrated over the spring season, from March 20th to June 20th. Since the annual, monthly or daily electrical and gas consumption data are not available, comparison is performed with respect to monitored supply airflow rates and supply and return air temperatures. In addition, a sensitivity analysis is performed to assess the impact of some selected parameters and the validity of certain assumptions on the calibrated model. Finally, the annual demand and consumption is also evaluated using the calibrated model.

The final result is a model that the building operators could use to evaluate the impact of certain modifications made to the HVAC and architectural systems on the overall energy performance of the building. The thesis also present recommendations and conclusions related to the used of the EnergyPlus program to simulate large buildings in cold climate.

3. ENERGYPLUS

3.1 General Characteristics of the Program

EnergyPlus is a completely new, modular, structured code developed on the most popular features and capabilities of the BLAST and DOE-2 programs [23]. It also includes new features such as realistic system controls, moisture adsorption and desorption in building elements, radiant heating and cooling systems and inter-zone airflow just to name a few [24]. Fortran 90 has been selected as the programming language for its flexibility and modular approach. The program utilizes the heat balance approach to solve for the room temperatures and loads. To reduce the computation time, the program developers have assumed that the room surfaces have uniform temperatures, uniform long-wave and short-wave irradiation, diffuse radiating surfaces and one-dimensional heat conduction [24]. The ability for the end users to integrate additional simulation sequences to the program increased the overall flexibility of EnergyPlus.

The modular methodology gives endless possibilities to the designers to include new simulation sequences for specific applications. The overall program structure is presented in Figure 3.1.

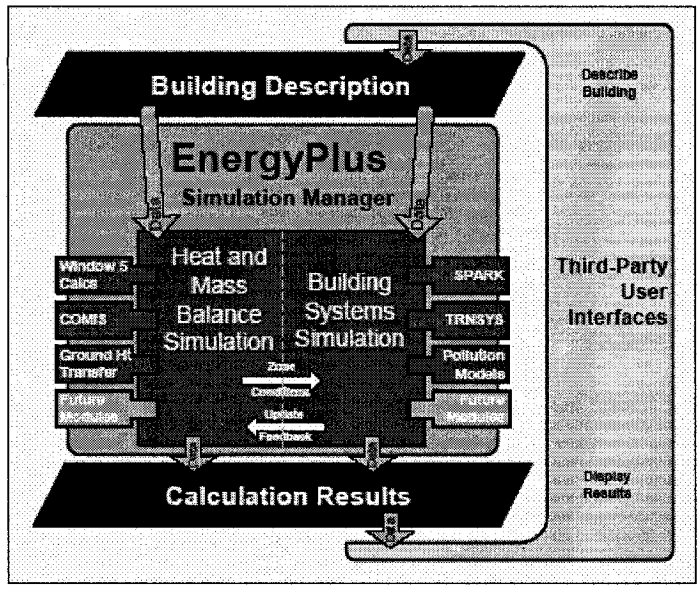

Figure 3.1: Overall Structure of EnergyPlus [23]

Three basic components describe the structure of EnergyPlus: the simulation manager, the heat and mass balance simulation module and the building systems module [25]. The structure allows the program to take into account feedback from sequential loads, system and plant calculations for the prediction of the space temperatures and loads, thus increasing the accuracy in the results obtained by simulation. EnergyPlus has also the ability to import HVAC data created from other common programs such as DOE and TRNSYS. Interfaces have been developed to convert data from one program to another, thus reducing the effort related to the data entry process [26]. The program also offers daylighting illumination, WINDOW 5-based fenestration and anisotropic sky capabilities.

3.2 Modeling Options

EnergyPlus is a simulation tool that determines the space thermal loads, the systems and plant loads as well as the energy consumption and related operating costs. The program allows users to utilize the auto sizing options or to enter detailed

information about each component present in the building. EnergyPlus is a flexible platform to simulate different scenarios and assists the designer throughout the design process.

3.2.1 Zone Options

The EnergyPlus program uses the heat balance method to solve for the zone loads. The program is modular in nature and set up energy balance equations using control volumes at the inside and outside surfaces of each wall/floor/ceiling in a particular zone as well as a control volume around the zone air [27]. The transient conduction heat transfer through walls and roofs, present in the heat balance method, has a direct impact on how the heat balance equations for the inside and outside surface are interacting with each other [28]. Equations (2.1), (2.2) and (2.5), presented in Chapter 2, are used to solve the heat balance equations at the outside and inside surfaces of each wall within a room and the heat balance for the room air. The program solves for the transient response through building elements using Conduction Transfer Functions (CTFs) and equations (2.3) and (2.4). Additional modules are also integrated to the EnergyPlus program to simulate windows, daylighting, and natural ventilation just to name a few. Figure 3.2 shows the integrated heat balance modules included and interacting in EnergyPlus.

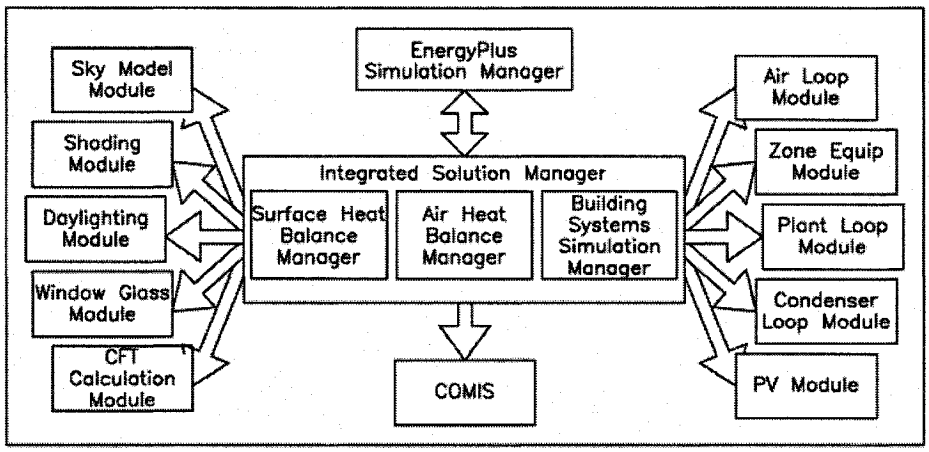

Figure 3.2: Solution Manager for the Heat Balance Method in EnergyPlus [28]

The basic mass balance equations are solved in two different ways, one with a predicted time step and one with a corrected time step. Also, zone air capacity is introduced into the heat balance equations to allow for a larger time step while preserving stability. An adaptive time step, shorter than an hour, is used to initially update the system conditions. The initial calculations estimate the input data to compute the zone thermal loads (internal gains, envelope gains, infiltration gains, etc.), while the second set of calculations is used to update the system response and the zone mean air temperature. The load calculations are linked to the system simulation through the zone air heat balance, thus the zone air temperature is the main interface variable in EnergyPlus program [29].

The EnergyPlus program requires the origin of each zone to be defined in reference to the origin of the building/floor, using x, y, z-coordinates. In order to obtain more accurate results, it is recommended to include every surface within a zone. In the case of one interior partition that separates two zones, the vertices of this partition must be defined in both zones. This condition helps in obtaining the same surface area on both

sides of the partition. This way, the conservation of energy principle applied to the partition is respected. In terms of internal gains, EnergyPlus requires the information to be entered as the total installed lighting power (W) or total equipment power (W) for each zone. For recessed fluorescent lighting, the default fraction of radiant (long-wave/thermal radiation) is 0.37 and the visible/short-wave fraction is 0.18 [29]. For the equipment load, the fraction radiant is estimated at 0.3. Similarly, the infiltration rate must be entered as a lump sum (m^3/s). The air infiltration model used in EnergyPlus takes into account the zone temperature, the outdoor dry-bulb temperature and the wind speed [29]. The number of occupants is defined as the maximum number of people for a specified zone. Data input at peak design conditions for internal gains (e.g. lights, people, appliances) are corrected by schedule of operation. For the envelope components, each layer and window component are entered separately and then combined for each construction type. Entering all the required information at the zone level is labour intensive, but necessary to ensure that the programmed heat balance equations properly interact together.

3.2.2 System Options

The predicted zone temperature is used to evaluate the required system output response. Based on that response, and taking into account the cooling/heating capacity of the secondary system, the change in zone temperature is re-calculated. This iterative process is performed until the zone design requirements are meet. The zone air heat balance links the load calculations to the system simulation. To limit the complexity of the simulation algorithm, the system energy balance method is calculated as a function of the zone temperature. The EnergyPlus program simulates systems using fluid loop

principles. For the air loop, two components are present: the primary air system, which represents the supply side of the loop, and the zone equipment, which represents the demand side of the loop (Figure 3.3). The primary air system consists of components included in the central air conditioning equipment (air handling units), such as cooling and heating coils, humidifiers, and fans. The zone equipment includes air terminal units (VAV boxes with re-heat, for example) or any other piece of equipment installed at the zone level (e.g..: fan coils, baseboards) as well as supply or return plenums. The system requirements are determined using algebraic energy and mass balance equations. The component models in EnergyPlus are algorithmic and forward models, i.e. the component inputs correspond to the inlet conditions and the outputs to the outlet conditions [29].

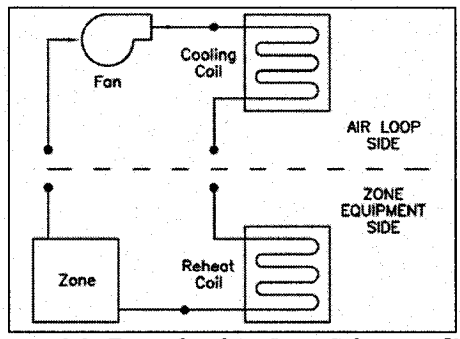

Figure 3.3: Example of Air Loop Schematic [30]

Few component models are presented to show the calculation process implemented in EnergyPlus. For central air system variable fan, the *SizeFan* subroutine calculates the maximum and minimum airflow rates (V_F) using equations (3.1) and (3.2).

$$V_{F,\,max} = DesMainVolFlow_{sys} \tag{3.1}$$

$$V_{F,\,min} = DesMainVolFlow_{sys} \cdot MinFlowRat_{sys} \tag{3.2}$$

where,

$DesMainVolFlow_{sys}$ is the design main supply duct volume flow [m^3/s];

$MinFlowRat_{sys}$ is the minimum main supply duct volume flow ratio.

For simple system water cooling coil, the *SizeWaterCoil* subroutine is used. The design mass flow rate ($m_{a,\,des}$) is first determined by multiplying the air density (kg/m^3) by the design main supply duct volume flow (m^3/s).

$$m_{a,\,des} = \rho_a \cdot DesMainVolFlow_{sys} \tag{3.3}$$

The coil load is then calculated using the system design mixed and supply air conditions:

$$Q_{coil,des} = m_{a,des} \cdot (h_{in,\,air} - h_{out,\,air}) \tag{3.4}$$

where,

$m_{a,des}$ is the design mass flow rate [kg/s];

$h_{in,\,air}$ is the $PsyHFnT_{dbW}(T_{coil,in}, W_{coil,in})$, the coil entering enthalpy [kJ/kg];

$h_{out,\,air}$ is the $PsyHFnT_{dbW}(T_{coil,out}, W_{coil,out})$, the coil leaving enthalpy [kJ/kg].

The maximum chilled water flow rate is then calculated using the user specified design chilled water temperature rise and the cooling coil load:

$$V_{coil,w,max} = Q_{coil,des} / (C_{p,w} \cdot \rho_w \cdot \Delta T_{plt,cw,des}) \tag{3.5}$$

where,

$Q_{coil,des}$ is the design cooling coil load [kW];

$C_{p,w}$ is the specific heat of water [kJ/kg · K];

ρ_w is the density of water [kg/m^3];

$\Delta T_{plt,cw,des}$ is the user -specified design chilled water temperature rise [K].

Calculations are performed for each component and outputs are inputted at the next level of analysis and used for the next iterations.

The HVAC simulation is based on a manager-interface protocol, high level component connectivity and a high degree of data encapsulation. Thermodynamic fluid properties are tracked around for each fluid loop by using loop nodes. The manager-interface module determines the flow direction, establishes the loop convergence criteria, and updates the set point information, for each node. For instance, at each node the fluid type, the mass flow rate and standard thermodynamic properties are defined. Each component present in the systems - fans, dampers, coils, boilers and chillers – is assigned an inlet and outlet node and added to the loop to complete the system description [30]. This high level of component connectivity allows the supply and demand sides to be coupled as well as the possibility of having different system layouts, thus giving the designer all the required flexibility to simulate new system configurations.

In EnergyPlus, compact HVAC systems are available to ease the data entry process for HVAC systems. Compact HVAC objects provide a shorthand way of describing standard HVAC system configurations. Those models include built-in default data and user input data entry for basic system options. EnergyPlus automatically sets up loops, branches, and node names for the specified objects. Each object can be expanded in future runs and each component can be further detailed by the user (refer to Chapter 4 for an example). This approach abbreviates and simplifies the initial modeling. The system configuration can then be completed by incorporating any additional components to the fluid loops.

3.2.3 Plant Options

The central plant interacts with the system components via a fluid loop that connects the plant components (e.g.: boilers, chillers) and the heat exchanger components/coils. The properties corresponding to the plant output nodes must match the component inlet node properties (Figure 3.4).

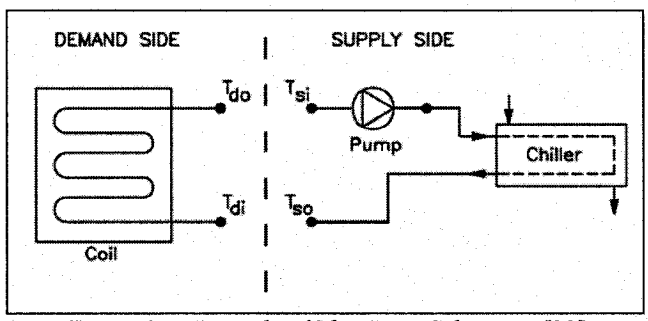

Figure 3.4: Example of Plan Loop Schematic [30]

The demand inlet temperature (T_{di}) is calculated at the end of each iteration, and the supply side outlet (T_{sso}) and the supply side inlet temperature (T_{ssi}) are calculated from results obtained at the previous time step (equation 3.6)

$$T_{di\text{-}new} = T_{di\text{-}old} + \left[\frac{(m_{max} \cdot t_{sys} \cdot 3600)}{M} \cdot (T_{sso} - T_{ssi})\right] \qquad (3.6)$$

where,

$T_{di\text{-}new}$ is the current demand side inlet temperature [°C];

$T_{di\text{-}old}$ is the previous time step demand inlet temperature [°C];

T_{sso} is the supply side outlet temperature [°C];

T_{ssi} is the supply side inlet temperature [°C];

m_{max} is the maximum expected supply side mass flow rate [kg/s];

t_{sys} is the system time step [h];

M is the mass of water in the loop [kg].

The plant models available in EnergyPlus can support both semi-deterministic models and demand-based models. The loop manager is thus set up to use the mass flow rate as the main input data. To simulate the plant and avoid the use of a pressure based flow network a simple predictor-corrector algorithm enforces mass continuity across the plant loop (Figure 3.5). The predictor algorithm establishes the flow rate for each branch and then the loop managers "corrects" the branch flow rate to enforce continuity on the loop [29].

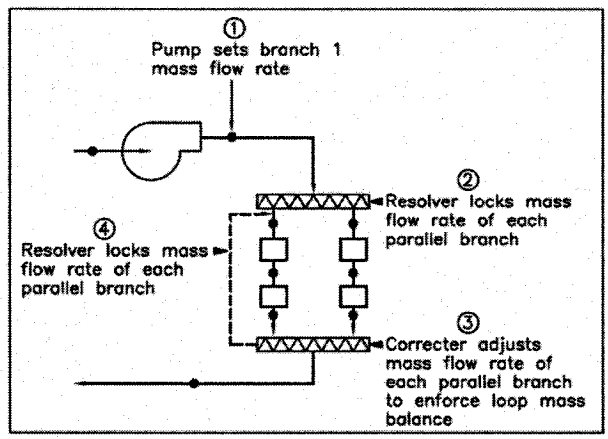

Figure 3.5: Plant Supply-Side Solution Scheme [29]

The interaction between all components involved in the plant simulation is shown in Figure 3.6.

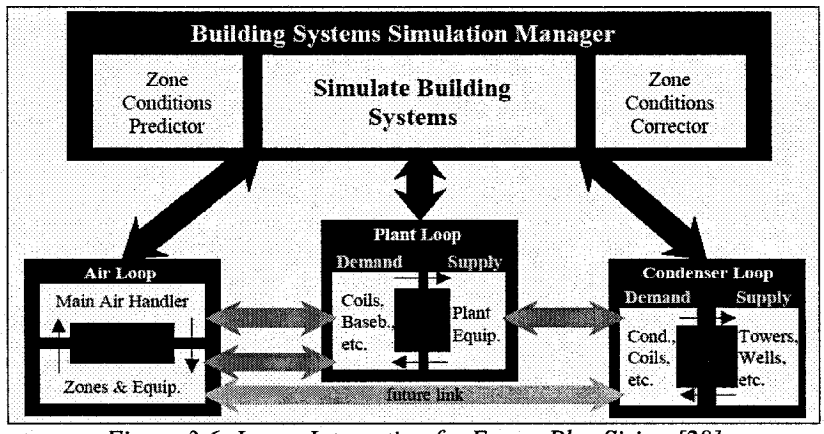

Figure 3.6: Loops Interaction for EnergyPlus Sizing [28]

To avoid the use of a complex solver, there are restrictions on the pump locations. They are not allowed on the demand sub-loop of either the plant or condenser loop [29]. The various sub-loops are solved for the supply side to meet a particular load based on the demand side loops simuation. Different plant equipment components are available in EnergyPlus to give the designer the flexibility required to properly simulated the building central plant.

For example, an electric chiller with heat recovery is simulated as a standard vapour compression refrigeration cycle with a double bundled condenser. Two separate flow paths are considered through the condenser [29]. One path is used to reflect heat through the cooling tower, while the other recovers heat from the condenser and use it for heating the perimeter zones (Figure 3.7).

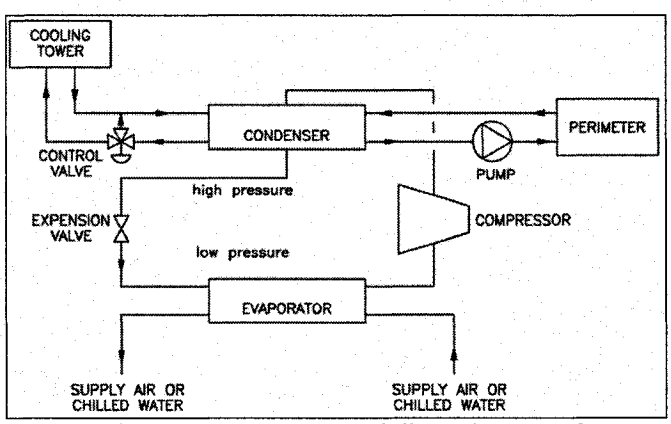

Figure 3.7: Diagram of Vapour Compression Chiller: Electric with Heat Recovery [29]

The vapour compression chiller: electric uses the model developed in the ASHRAE HVAC toolkit [11] as presented in Chapter 2. For each plant components, EnergyPlus recommend default input parameters based on the model used and the operating conditions. Various plant scenarios are presented in the EnergyPlus example

files to help the designer set up the model components adequately. However, the user may input more relevant data, if available.

3.3 Verification and Use

Since the first distribution of the energy analysis program EnergyPlus, several versions were released with new features and increased accuracy of simulation results. Version 1.4.0 of the program was released on October 14th, 2006. However, this study was performed with version 1.3.0, which was released on April 28th, 2006. Several researchers have compared and evaluated particular features of the program in specific context. Winkelmann [31] modeled different window types and configurations, and concluded that EnergyPlus allows for the analysis of windows impact on peak load, thermal comfort, condensation, natural ventilation, and daylighting. Methat [32] evaluated the natural ventilation of an office building with open atrium using the COMIS module coupled with EnergyPlus. Fisher and Rees [33] presented results from the simulation of ground source heat pump systems. Zhou et al. [34] implemented and evaluated different optimization algorithms to determine the best control strategies that utilize thermal energy storage in a typical office building, in order to reduce electrical energy charges, electrical demand charges, and total electricity charges. Mithraratne et al. [35] evaluated thermal behaviour of a high thermal mass residential building based on the anisotropic model of solar radiation implemented in EnergyPlus. They concluded that although EnergyPlus has a detailed solar distribution model for a single zone, it treats the inter-zone solar transfer as diffuse radiation. This tends to underestimate the internal air temperatures in colder months and overestimates the same in the warmer months.

In spite of this, only a limited amount of information, related to the simulation of large buildings, has been published so far. Bellemare et al. [36] modeled an institutional building with 54 interior zones and related VAV systems. They compared results predicted by EnergyPlus with monitored data, and with those predicted by the DOE-2 program. The first comparison, between EnergyPlus predicted results and monitored data, show similar trends. Comparisons between predictions made by EnergyPlus and DOE-2 program also show similar trends when the EnergyPlus input was modified to respect the limits encountered in the DOE-2 program, such as the constant room temperature to determine the heating/cooling load for each zone. Ellis and Torcellini [37] have simulated a tall building having an overall floor area of 240,000 m^2. Their analysis was mainly focused on stack effects and the use of floor multipliers, while HVAC systems were entered through the simple purchased air option. This approach reduces the computing time since it calculates cooling and heating loads without taking into account the performance of HVAC equipments. Witte et al. [38] evaluated EnergyPlus for a base case building with mechanical systems using BESTEST guideline. The test helped to identify errors and documentation deficiencies. Most problems encountered were related to system cycling mode and humidity. All issues encountered were investigated and fixed in later versions of the program. By performing various tests, which included analytical, comparative, sensitivity, range and empirical tests, the program is improved and its credibility among the scientific community is enhanced [38].

EnergyPlus is under constant review and its capabilities are constantly improving. However, since the program is still under development, the debugging process is long

and complex. Also, even though the program offers a wide variety of features, the modeling of some mechanical systems is still under expansion. Various components used for heating purposes, such as water-to-water heat exchanger, are missing in EnergyPlus and thus simulating large buildings with complex mechanical systems for cold climate is a challenge (refer to Chapter 4 for strategies used to develop the computer model).

4. DEVELOPMENT OF THE COMPUTER MODEL

4.1 Methodology

The building under study was submitted for Commercial Building Incentive Program (CBIP) to Natural Resources Canada to obtain funding based on building energy savings [5]. The CBIP file generates the input file for the DOE-2 program, which is the engine for the EE4 program, to estimate the annual energy cost and consumption of the proposed building versus the performance of a reference building. The files provided by the mechanical consultant, Pageau, Morel et Associés (PMA), were helpful to create the initial input file in this study. The DOE-2 file, that contains the building description, is translated into an "idf" input file compatible with the EnergyPlus program. This conversion is realized through the use of a utility program named DOE2Translator provided as a pre-process program by EnergyPlus. The translation program provides incomplete design object information, and therefore many modifications are required to obtain a working input file for the EnergyPlus program.

The initial phase in the development of the computer model consists of collecting the architectural, electrical, and mechanical data to prepare the input file. The input file reflects the geometry of the building and its characteristics having an impact on thermal loads as well as the description of HVAC systems. The accurate modeling of the components/subsystems of the building and mechanical systems have a significant impact on the building energy use. Data obtained from the simulation are compared with monitored data, which were collected from March 13th to June 30th 2006, to calibrate the model.

4.2 Short Description of the Sciences Building

The Concordia Sciences building is located on the Loyola campus in Montréal and has a total floor area of 32,000 m^2. The building is divided in three main sectors: sector A, B and C (Figure 4.1). Sector A is the heart of the building and mainly consists of laboratories and offices. Sector C is located on the south-west side of the building and the sector B is the Bryan wing, an existing building that is integrated to the Sciences building. The majority of the envelope infrastructure has been conserved and the interior has been redesigned to accommodate the new university needs.

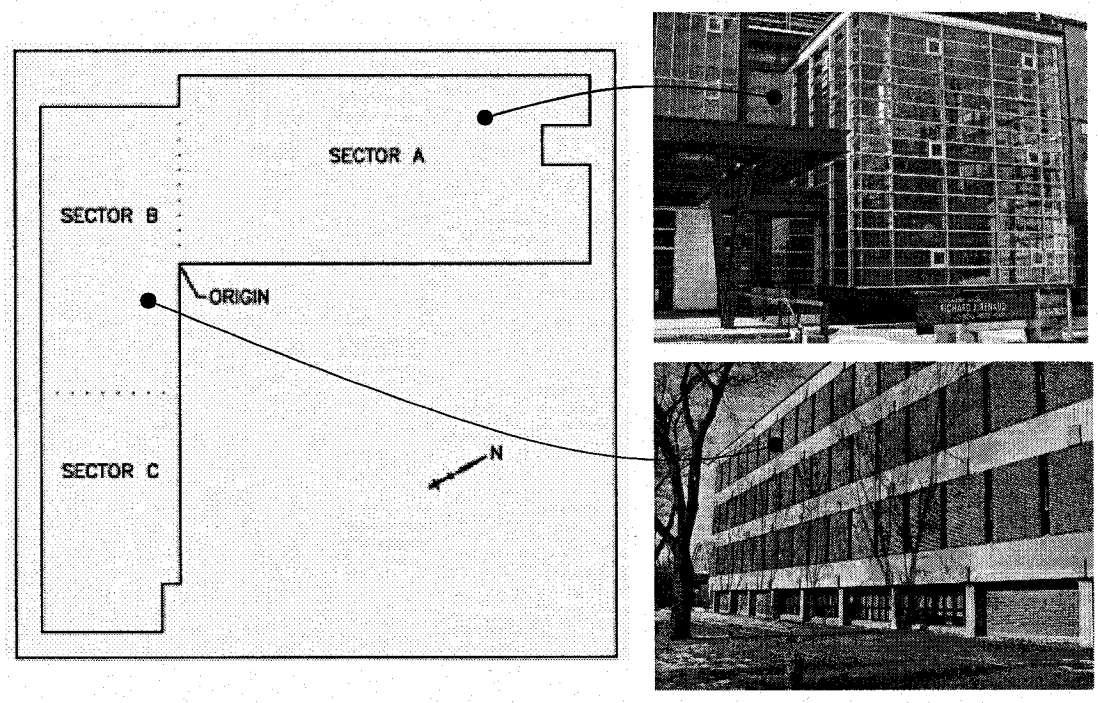

Figure 4.1: General Building Layout

The floor plans of sector A are divided between office spaces and laboratories. Offices are principally located along the south-east and south-west perimeters. The main entrance is along the south façade of the building. The building is eight stories high. There are two basements with storage areas, testing labs and classrooms. Staff offices and teaching areas are located on the five floors above ground. The sixth floor is a

mechanical penthouse where most of the HVAC equipment is located. This sector also includes an atrium located on the west portion of the wing that acts as a transition area between the existing structure and the new structure.

Sector B is the renovated section of the building. The existing Bryan building has been integrated to the new complex. The building is four stories high. There is one basement where offices and lockers are located. The three floors above ground are essentially used for office spaces.

Sector C is the south-west wing of the Sciences building. There are four stories above ground and one basement floor. Research labs, computer labs, and machine shops are located in the basement. The fourth floor is a mechanical penthouse where mechanical systems for both sectors B and C are installed. Offices are located along the east façade and labs occupied the remaining of the floor space.

4.2.1 Building Exterior Envelope

According to the design specifications, the building has walls with the overall thermal resistance varying between 2.6 and 3.1 m^2 °C/W and roofs between 2.8 and 4.2 m^2 °C/W. Most walls are insulated brick or aluminium panels completed with an air space, a vapour barrier and one or two layers of gypsum board. The roofs are built-up of a bitumen membrane, a concrete layer, two types of insulation, a plywood panel, a vapour barrier and another concrete layer. Two types of glazing are present: double low-E clear with film 6mm/6mm air gap (glazing 0) and double low-E clear 6mm/13mm air gap (glazing 1). The glazing accounts for about 32% of the total area of exterior walls [39].

The fenestration assemblies are either curtain walls with aluminium framing completed with thermal break or fixed aluminium with thermal break frames. The ceiling height varies between 2.4 and 2.6 meters.

4.2.2 Heating and Cooling Space Loads

Equipment loads and lighting loads are defined from data specified for the CBIP incentive program, which is given in terms of installed load per zone floor area (W/m^2). Schedules of operation and loads are taken from the original DOE-2 file. The lighting installed load is between 7 and 10 W/m^2, and the equipment load is between 2 and 10 W/m^2.

4.2.3 HVAC Systems

Mechanical systems are designed to maintain the indoor thermal parameters within the comfortable range. Since the main activities of the building are teaching and research in fields such as biology, chemistry and biochemistry, the size and system requirements are quite large. To reduce the zone loads, motion detectors were installed in all rooms of the Sciences building. The motion detector shut off lights after an adjustable delay of no activity. When lights shut off, a signal is also sent to the building automated system to reduce the amount of air sent to the room. For laboratories, the supply airflow rate is changed from 10 air changes per hour (ACH) during occupied hours to 6 ACH while unoccupied. This is further reduced to 3 ACH at night time. The ventilation is brought back to 10 ACH whenever occupants are present [40]. Other room types are restricted to a minimum of 3 ACH, if located on the perimeter, and 1.5 ACH if it is an interior zone [39].

Two identical air handling units serve sectors B and C (AHU-7 and AHU-8). The design airflow rate for the whole system is 75.5 m^3/s, the cooling capacity is 1655 kW and the heating capacity is 2340 kW. Sector A is served by four identical air handling units (AHU-1 to AHU-4), each having a design airflow rate of 37.75 m^3/s. The overall cooling and heating capacity for this sector is 3310 kW and 4580 kW, respectively. The animal laboratories, which are located in the second basement west wing of sector A are supplied by a separate 100% outside air system (AHU-5 and AHU-6). The zone requirements of the animal laboratories are satisfied by two identical 11.8 m^3/s systems having a total cooling capacity of 550 kW and a total heating capacity of 1150 kW.

Laboratories require large amount of fresh air and thus a large amount of energy is required to heat and cool the outdoor air introduced into the building. To reduce the energy burden, heat recovered from the exhaust air streams by a run around glycol loop is used to pre-heat or pre-cool the outdoor air. For all units, filters and coils are selected for a face velocity of 2.03 m/s [40]. This reduces the total system pressure loss and allows the use of smaller electric motors. Variable frequency drives are also installed on fans to improve efficiency at part load operation.

4.2.4 Primary Systems

A thermal central plant serves all sectors of the building, where different systems have been installed, to increase the performance of the building. Figure 4.2 is a simplified schematic representation of the systems present in the central plant and in the building.

Plate heat exchangers recuperate the heat rejected from chillers and from exhaust gases from two existing boilers (Point A) to pre-heat the heating water (Figure 4.2). During the summer season, the heating water system, which is used for re-heat purposes only, operates on 35 °C supply and 29.4°C return water temperatures. The water temperature is increased to 51.7 °C supply and 29.4°C return during the winter season. The heating water is also pre-heated via a plate heat exchanger (Point D) using the condenser water that is circulated between the cooling towers and central plant chillers (CH-1 and CH-2). If heat recuperated via the heat recovery system is insufficient to achieve the required water temperature, a tube and shell heat exchanger is used to further heat up the water using steam produced by a 96% efficient natural gas boiler having a capacity of 815 kW (Point B). Steam is also supplied from the central plant boiler to the humidifiers installed in the air handling units (Point C).

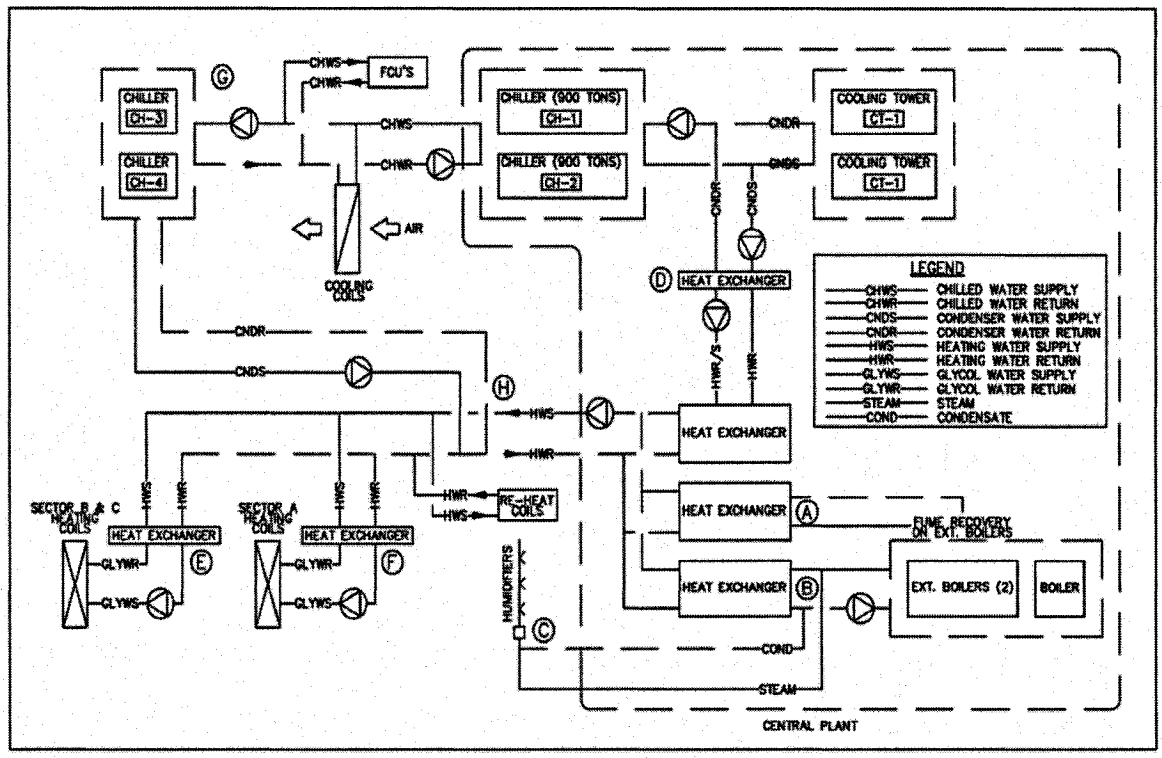

Figure 4.2: Simplified Schematic of HVAC Systems and Central Plant

Variable air volume (VAV) boxes, installed in most offices and laboratories areas, have re-heat water coils working between 51.7/29.4°C water temperatures supplied by the central plant. The heating water also serve the plate heat exchangers that warm up a 50% glycol solution from 26.7°C to 48.9°C to be supplied to the glycol heating coils installed within each of the air handling units (Points E and F). The chillers have the cooling capacity of 3165 kW (900 tons) each, and a coefficient of performance (COP) of 5.76. Chilled water cooling coils operating between 5.6/13.3°C water temperatures provide the cooling required within the building. Two additional chillers (CH-3 and CH-4) are included within the building to serve the fan coil units, during the winter and part of the shoulder seasons (Point G). Fan coils units are located mainly in electrical rooms, telecom rooms and cold rooms, and run all year around. The condensers of chillers CH-3 and CH-4 are also connected to the heating water loop to pre-warm the heating water (Point H).

The combination of energy efficient measures and operating strategies has led to a 50% reduction in energy consumption compared to the Model of National Energy Code of Canada for Buildings (MNECB), and thus, the Sciences building qualified for the CBIP application [40].

4.3 Modeling Approach

The Concordia Sciences building has a good combination of architectural and mechanical complexity and thus, is a challenging building to model. A thorough approach is required to understand the interaction between all the building components and obtain suitable predictions for thermal and system loads from the model.

4.3.1 Architectural Systems

The complexity of the building has led to many modeling issues related to the determination of space loads. Given the size of the building and its vocation, a large number of thermal zones and building surfaces (walls, roofs, partitions, floors), with a significant impact of heat transfer phenomenon, are used to develop the input file (Table 4.1).

Table 4.1: Zone Distribution by Sector

Sector	Number of conditioned zones	Plenums	Number of surfaces
A	58	14	1154
B	18	4	286
C	21	8	333
Animal Labs	6	N/A	79
TOTAL	103	26	1852

The origin of each zone must be defined in reference to the origin of the building/floor, using x, y, z-coordinates. The origin is located at the ground floor level of the lower left corner of sector A (Figure 4.1). In order to obtain more accurate results, it is recommended to include every surface within a zone. In the case of one interior partition that separates two zones, the vertices of this partition must be defined in both zones. This condition helps in obtaining the same surface area on both sides of the partition. This way, the conservation of energy principle applied to the partition is respected. Two adjacent zones – zone 13 and 14 – are used to demonstrate the vertices identification process for a particular partition belonging to both zones. Figure 4.3 shows the zones general information.

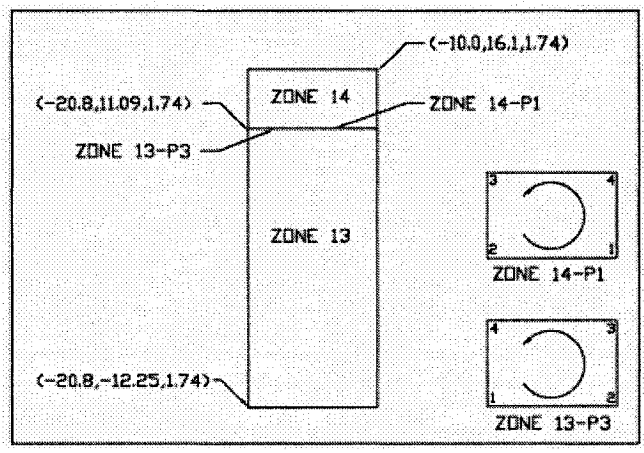

Figure 4.3: Definition of the Partition Wall between two Adjacent Zones

Surfaces must be defined in terms of x, y, z-coordinate starting from the lower left corner and continuing counter clockwise from the outside. Thus, directly copying a partition belonging to one zone to its adjacent zone to have corresponding partitions is not possible. Coordinates reordering is required to achieve correct partition identification. As shown in the above figure, if directly copying partition Zone 13-P3 to define partition Zone 14-P4, the vertices numbering is inadequate. Table 4.2 shows the appropriate vertices definition for both partitions as enter in the input file.

Table 4.2: Definition of Partition Vertices

Zone13-P3,	**Zone14-P1,**	!- User Supplied Surface Name
ZONE-13,	ZONE-14,	!- InsideFaceEnvironment
Zone14-P1,	Zone13-P3,	!- OutsideFaceEnvironment Object
0.5,	0.5,	!- View Factor to Ground
4,	4,	!- Number of Surface Vertex Groups
-10,	-20.8,	!- Vertex 1 X-coordinate {m}
11.09,	11.09,	!- Vertex 1 Y-coordinate {m}
1.74,	1.74,	!- Vertex 1 Z-coordinate {m}
-20.8,	-10,	!- Vertex 2 X-coordinate {m}
11.09,	11.09,	!- Vertex 2 Y-coordinate {m}
1.74,	1.74,	!- Vertex 2 Z-coordinate {m}
-20.8,	-10,	!- Vertex 3 X-coordinate {m}
11.09,	11.09,	!- Vertex 3 Y-coordinate {m}
4.14,	4.14,	!- Vertex 3 Z-coordinate {m}
-10,	-20.8,	!- Vertex 4 X-coordinate {m}
11.09,	11.09,	!- Vertex 4 Y-coordinate {m}
4.14;	4.14;	!- Vertex 4 Z-coordinate {m}

Since most of the building has plenum spaces, several plenum zones are created to estimate the variable air temperature inside each plenum and corresponding zone loads. Temperature within a zone is controlled and kept close to its set point temperature, while plenum temperature is uncontrolled and fluctuates depending on heat gains and losses between the plenum and surroundings. By modeling plenum spaces, the simulated thermal behaviour of a zone is a closer representation of actual conditions. Based on the design specifications, the zone summer temperature set point is 24°C during occupancy and should not exceed 35°C at night. During winter, the zone set point is 22°C during occupancy and should not be lower than 18°C at night time. However, the collected data indicated that the zone set point temperature is not changed at night (see Chapter 5). The zone temperature is thus set to 24°C under cooling mode and 22°C under heating mode.

Figures 4.4 and 4.5 show the predicted variation of the air temperature in the plenum and few adjacent zones on the third floor of sector B for summer design day (July 21st) and winter design day (January 21st). The plenum is a common return plenum for all given zones with exterior walls, and it is located on the sector top floor, thus it has a roof and exterior walls in contact with the outdoor environment. Zone-23-Common is a zone that includes all corridors and common rooms located in that area. Figures 4.4 and 4.5 clearly show higher plenum temperature in the summer and lower values in the winter. The room conditions are barely fluctuating around the zone temperature set point.

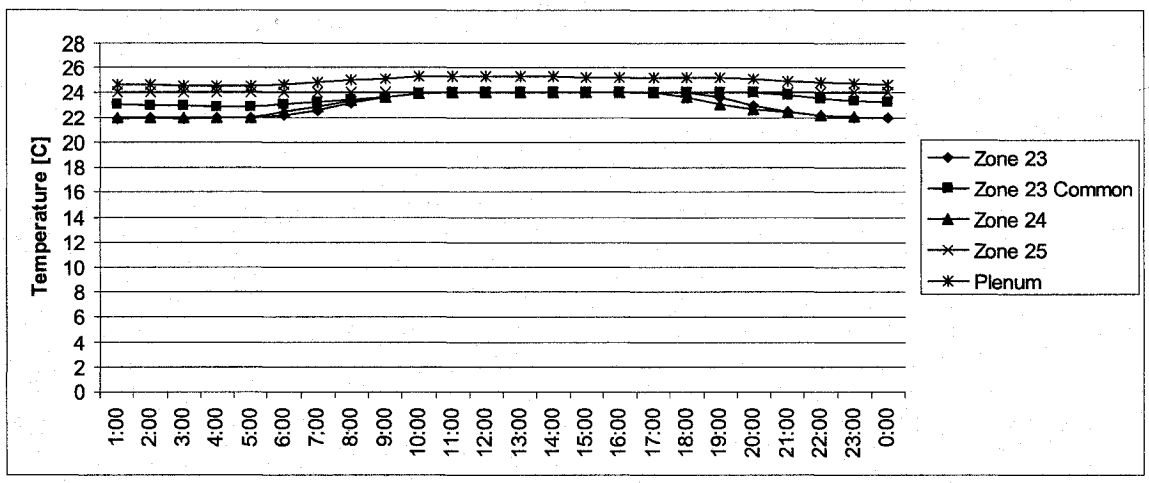

Figure 4.4: Plenum and Zone Temperature Variation during the Summer Design Day

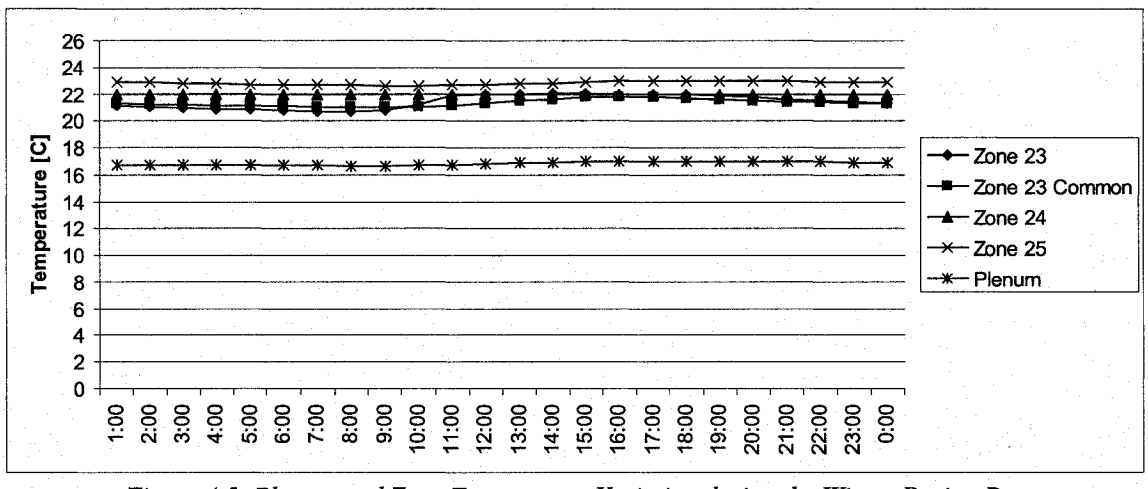

Figure 4.5: Plenum and Zone Temperature Variation during the Winter Design Day

Initially, plenums were only created for zones with return air plenums. The ceiling height for direct exhaust zones were specified in the zone entry object only, no dummy plenum zones were created above direct exhaust rooms. After investigation and simulating both approaches, it was decided to create plenum for direct exhaust zone too. The loads obtained with the additional plenums were lower than the ones obtained with entering the ceiling heights only, thus, better representing actual zone conditions. Plenum and zone temperature variations for an interior zone with direct exhaust for summer and winter design day are shown in Figures 4.6 and 4.7.

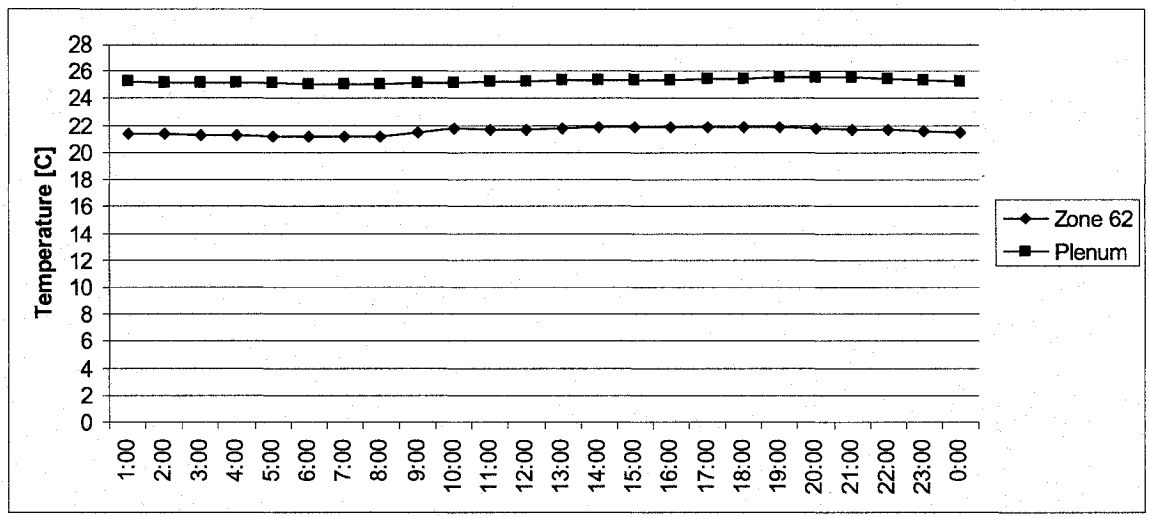

Figure 4.6: Direct Exhaust Plenum and Zone Temperature Variation during the Summer Design Day

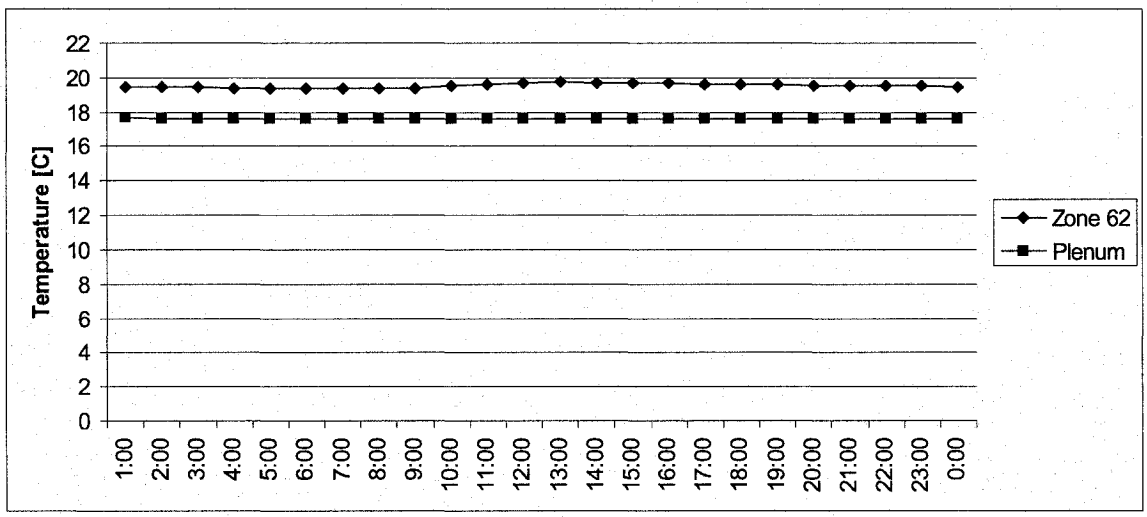

Figure 4.7: Direct Exhaust Plenum and Zone Temperature Variation during the Winter Design Day

Data obtained and presented in Figures 4.6 and 4.7 show that there is a difference between the plenum and zone temperatures even under direct exhaust situation. Modeling the direct exhaust plenum as a dummy thermal zone, that defines surfaces for heat transfer and storage purposes, leads to more accurate results. To limit the total number of zones, all the direct exhaust plenum located on the same floor and same sector are grouped together.

The use of plenums has increased the complexity of the input file, but it has also simplified the definition of ceiling/floor as an internal surface. The floor layout being considerably different from one floor to another, it is a challenge to define ceilings and floors with identical superficies, in order to meet the program condition for respecting the conservation of energy principle. The problem is resolved by defining a plenum between two surfaces (a ceiling and a floor). The floor of each plenum is divided in pieces to match the ceilings of the zone located below. Similarly, the ceiling of each plenum is divided in pieces to match the floor of the zones located above. In zones where there is no plenum, such as mechanical rooms, the ceiling towards adjacent spaces is left unfilled. By leaving the information blank, no heat transfer between zones is taken into consideration, however, the heat storage capacity of the object is still taken into account. The floor slab having a high thermal mass and the temperature difference between the two zones being relatively small, the amount of heat transfer between two zones located on two adjacent floors is minimal and can be neglected. This approach simplifies the model by limiting the total number of surfaces to be included in the input file.

In terms of loads, the EnergyPlus program requires the information to be entered as the total installed power (W) for each zone. Thus, the required data for EnergyPlus program are calculated using the zone area as defined through the x, y and z-coordinates and information provided in the converted file.

Infiltration is evaluated only for above ground perimeter zones. Air tightness in large building is extremely hard to evaluate. As a guideline for model input, Kaplan and

Canner [17] recommend using 0.2 (l/s)/m^2 of gross exterior wall area, while calculations based on the Model National Energy Code for Buildings are based on 0.25 (l/s)/m^2 [5] as natural infiltration rate. Since the later value is also used as default in EE4/DOE-2 for CBIP applications, the same value is input in EnergyPlus. Infiltration is assumed to occur only when the HVAC systems is OFF. When the system is ON, no infiltration occurs due to building pressurization. For this building, the systems are always ON and thus no infiltration should occur. Therefore, the air infiltration rate is set to zero in the input file. The impact of this assumption will be tested through the sensitivity analysis (Chapter 6.2).

4.3.2 HVAC Systems

A number of runs were required to achieve practical results. To ease the entry process for HVAC systems in EnergyPlus, compact HVAC systems were originally used. Compact HVAC objects provide a shorthand way of describing standard HVAC system configurations. Those models include built-in default data and user input data entry for basic system options. A typical compact zone system input is presented in Figure 4.8.

```
COMPACT HVAC:ZONE:VAV,
    ZONE-8,                  !- Zone Name
    Bryan-Sud,               !- Air Handling System Name
    Thermostat H,            !- Thermostat Name
    0.376,                   !- Zone Supply Air Max Flow Rate {m3/s}
    0.21,                    !- Zone Supply Air Min Flow Fraction
    flow/person,             !- Zone Outside Air Flow Type
    0.015,                   !- Zone Outside Air Flow Rate {m3/s}
    Hot Water,               !- Reheat Coil Type
    ,                        !- Reheat Coil Availability Schedule
    Reverse Action;          !- Zone Damper Heating Action
```

Figure 4.8: Compact Zone System Inputs

EnergyPlus automatically sets up loops, branches and node names for the specified objects. Each object can be expanded in the following runs to detail each component. This approach abbreviates and simplifies the initial modeling. The

information about schedules and HVAC systems is based on data obtained from the original EE4/DOE-2 file. Expanded inputs generated from the compact zone system inputs are presented in Figures 4.9, 4.10 and 4.11. The expanded inputs can be grouped in three different categories: 1) zone sizing inputs (Figure 4.9), which set the design requirements of the zone; 2) water-side equipment inputs, which set the re-heat design requirements and branches (Figure 4.10); and 3) air-side zone equipment inputs, which describe the air side connections, the equipment installed (VAV with re-heat) and the room set point (Figure 4.11).

```
ZONE SIZING,
        ZONE-8,          !- Name of a zone
        16.1,            !- Zone cooling design supply air temperature {C}
        23.9,            !- Zone heating design supply air temperature {C}
        0.006,           !- Zone cooling design supply air humidity ratio {kg-H2O/kg-air}
        0.006,           !- Zone heating design supply air humidity ratio {kg-H2O/kg-air}
        flow/person,     !- outside air method
        0.015,           !- outside air flow per person {m3/s}
        0,               !- outside air flow {m3/s}
        1,               !- zone sizing factor
        flow/zone,       !- cooling design air flow method
        0.376,           !- cooling design air flow rate {m3/s}
        flow/zone,       !- heating design air flow method
        ;                !- heating design air flow rate {m3/s}
```

Figure 4.9: Zone Sizing Inputs

```
COIL:Water:SimpleHeating,
        ZONE-8 Reheat Coil,              !- Coil Name
        Reheat-Coil Schedule H,          !- Available Schedule
        autosize,                        !- UA of the Coil {W/K}
        autosize,                        !- Max Water Flow Rate of Coil {m3/s}
        ZONE-8 Reheat Coil HW Inlet,     !- Coil_Water_Inlet_Node
        ZONE-8 Reheat Coil HW Outlet,    !- Coil_Water_Outlet_Node
        ZONE-8 Damper Outlet,            !- Coil_Air_Inlet_Node
        ZONE-8 Supply Inlet;             !- Coil_Air_Outlet_Node
BRANCH,
        ZONE-8 Reheat Coil HW Branch,    !- Branch Name
        ,                                !- Maximum Branch Flow Rate {m3/s}
        COIL:Water:SimpleHeating,        !- Comp1 Type
        ZONE-8 Reheat Coil,              !- Comp1 Name
        ZONE-8 Reheat Coil HW Inlet,     !- Comp1 Inlet Node Name
        ZONE-8 Reheat Coil HW Outlet,    !- Comp1 Outlet Node Name
        ACTIVE;                          !- Comp1 Branch Control Type
```

Figure 4.10: Water-Side Zone Equipment Inputs

```
CONTROLLED ZONE EQUIP CONFIGURATION,
        ZONE-8,                         !- Zone Name
        ZONE-8 Equipment,               !- List Name: Zone Equipment
        ZONE-8 Supply Inlet,            !- Node List or Node Name: Zone Air Inlet Node(s)
        ,                               !- Node List or Node Name: Zone Air Exhaust Node(s)
        ZONE-8 Zone Air Node,           !- Zone Air Node Name
        ZONE-8 Return Outlet;           !- Zone Return Air Node Name
ZONE EQUIPMENT LIST,
        ZONE-8 Equipment,               !- Name
        AIR DISTRIBUTION UNIT,          !- KEY--Zone Equipment Type 1
        ZONE-8 ATU,                     !- Type Name 1
        1,                              !- Cooling Priority 1
        1;                              !- Heating Priority 1
AIR DISTRIBUTION UNIT,
        ZONE-8 ATU,                     !- Air Distribution Unit Name
        ZONE-8 Supply Inlet,            !- Air Dist Unit Outlet Node Name
        SINGLE DUCT:VAV:REHEAT,         !- KEY--System Component Type 1
        ZONE-8 VAV Reheat;              !- Component Name 1
SINGLE DUCT:VAV:REHEAT,
        ZONE-8 VAV Reheat,              !- Name of System
        VAV Schedule,                   !- System Availability schedule
        ZONE-8 Damper Outlet,           !- DAMPER Air Outlet Node
        ZONE-8 Damper Inlet,            !- UNIT Air Inlet Node
        0.376,                          !- Maximum air flow rate {m3/s}
        0.21,                           !- Zone Minimum Air Flow Fraction
        ZONE-8 Reheat Coil HW Inlet,    !- Control node
        COIL:Water:SimpleHeating,       !- Reheat Component Object
        ZONE-8 Reheat Coil,             !- Name of Reheat Component
        autosize,                       !- Max Reheat Water Flow {m3/s}
        0,                              !- Min Reheat Water Flow {m3/s}
        ZONE-8 Supply Inlet,            !- UNIT Air Outlet Node
        0.001;                          !- Convergence Tolerance
ZONE CONTROL:THERMOSTATIC,
        HeatCoolSetPt-Zone8,            !- Thermostat Name
        ZONE-8,                         !- Zone Name
        Control Schedule,               !- Control Type SCHEDULE Name
        Dual Setpoint with Deadband,    !- Control Type #1
        Thermostat H;                   !- Control Type Name #1
```

Figure 4.11: Air-Side Zone Equipment Inputs

For simplification, all air handling units providing air to a specific sector are combined into one large unit having an equivalent capacity of all the air handling units for that sector. Two identical units are installed to serve sectors B and C; however, in the model they are combined as one unit. In sector A, four identical units are installed while only one unit having the total capacity of installed units is simulated in EnergyPlus. Conditioned air to the animal labs is provided by two additional 100% outside air units that are combined together for simulation purposes.

4.3.3 Primary Systems

The complex structure of the central plant cannot be directly simulated by EnergyPlus. Therefore, the approximation used in the model is described here. The building is provided with steam boilers and steam-to-water heat exchangers to provide heating water to the VAV re-heat coils and the heating coils of the air handling units (Figure 4.12: Installed Heating Water Loop). Two independent loops are modeled: a glycol (heating) loop for heating coils of the air handling unit (Figure 4.12: Modeled Heating Water Loop) and a heating water loop (low and high temperature varying throughout the seasons) which is connected to the heat recovery loop and provides heating water to the VAV re-heat coils (Figure 4.13). Heating coils located in the air handling units use a 50% ethylene glycol mixture. Steam-to-water or water-to-water heat exchangers are not yet available in EnergyPlus. Therefore, the heating loops are both set up as heating water loops and boiler efficiencies are adjusted to take into account the combined effect of the boiler and heat exchanger efficiencies (Figure 4.12).

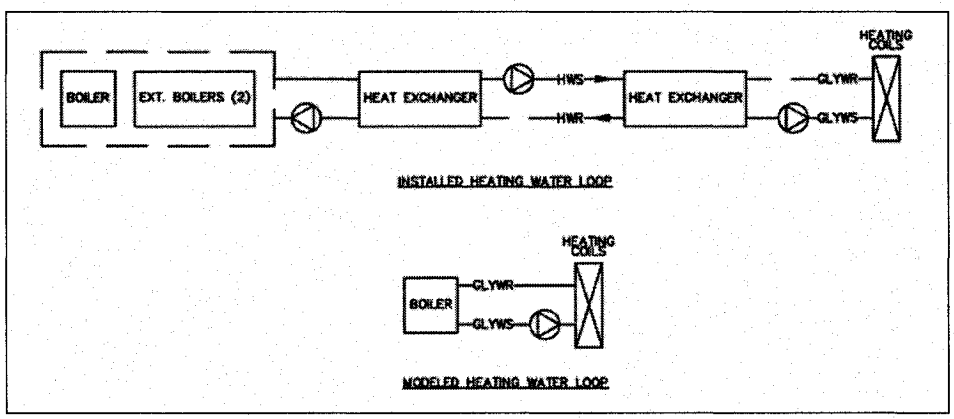

Figure 4.12: Heating Water Loop Schematic

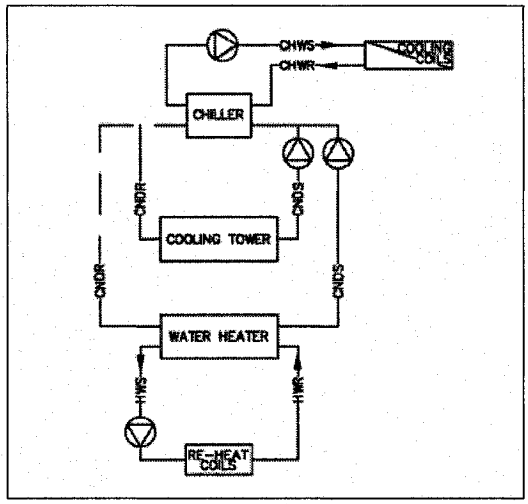

Figure 4.13: Cooling and Reheat Simulation Schematic

To simulate the heat recovery, the heating water boiler is replaced by a water heater. The water heater recuperates the heat rejected by the condenser and provides the additional heat required to maintain the supply heating water set point temperature for the re-heat coils. The condenser is connected to the water heater and to the cooling tower (Figure 4.13). In the actual building, two sets of chillers are installed: one set of two chillers (CH-3 and CH-4) operate during the winter and part of the shoulder season, providing cooling to electrical/utilities rooms during the winter months, and the second set of chillers (CH-1 and CH-2) is in the central plant and provide additional cooling to the building during the summer and shoulder seasons, if required. Since the two sets of chillers never operate simultaneously, only one large chiller, having the capacity of chillers CH-1 and CH-2, is included in the model. The supply and return temperatures for chilled and condenser water loops are modified throughout the seasons to reflect the actual on-site operating conditions.

Additional heat recovery measures are present in the building but are left out for simplification purposes. The heat recovery on the exhaust using glycol coils is not included in the model because of the absence of glycol heating loop. Also, the steam humidifiers are replaced by electrical humidifiers in the input file since it is the only available option in EnergyPlus. Predictions made by EnergyPlus are evaluated and compared with collected data to verify the correctness of the model (see Chapter 6).

4.3.4 Computing Time

The development of the computer model required a thorough approach to properly include all the components present in the building. The size and complexity of the building has a direct impact on the computing time required to perform the simulations. Two different computers were used to perform the simulations: 1) laptop with Dell Latitude D600 Pentium M of 1.4 GHz, and 512 MB of RAM, and 2) desktop with Dell Precision 360 Pentium 4 of 2.8 GHz, and 2.0 GB of RAM. Computation times for the two computers, for both the calibration period (spring season) and annual simulation, are presented in Table 4.3.

Table 4.3: Computing Time

Computer Type	Sector A		Sectors B & C	
	Spring	Annual	Spring	Annual
Laptop	3h16 min	8h38 min	31 min	1h56 min
Desktop	2h18 min	7h22 min	21 min	1h09 min

4.4 Summary

The complexity of the building has led to many modeling issues related to the determination of space and system loads. The computer model was developed using 129 thermal zones and 1852 surfaces, and information from the design specifications and

operating data. Secondary systems were initially defined using compact HVAC systems, and then refined by adding the missing HVAC components present in the building. The number of air branches required to simulate the building as one entity is not supported by EnergyPlus. Consequently, sectors B and C and sector A are modeled separately, which add to the complexity in evaluating the performance of the central plant. The modeling of the primary system itself was also challenging. In the existing central plant, the design of the heating and cooling equipments is complex and can not directly be simulated by the EnergyPlus program. For instance, there are many heat recovery systems present in the building that are not included in the model. Consequently, no attempt is made to estimate the plant performance due to differences between the building and EnergyPlus model operating conditions. Most of the calibration process and system analysis is limited to the performance of the HVAC systems. Overall the development of the model was time consuming and required the use of multiple assumptions and simplifications.

5. AS-OPERATED PERFORMANCE OF THE SCIENCES BUILDING

Information about the as-built and as-operated thermal performance of the Sciences building is obtained from the Monitoring and Data Acquisition System through the collaboration of the Physical Plant of Concordia University. The system uses Siemens Insight version 3.7 and allows for the collection of 49 points every 30 minutes (Table 5.1). The precision on the temperature collectors is ± 0.1% at 0°C, while no data are available for the precision on the airflow rate and humidity collectors. Data used in this study were collected from March 13th to June 30th, 2006.

Table 5.1: Description of Monitored Data

Description of Measured Variable	Acronym	Description of Measured Variable	Acronym [unit]
Air Side		AHU-1 Supply Air Relative Humidity	RH [%]
AHU-1 Supply Airflow Fan 1	S/A [m^3/s]	AHU-2 Supply Air Relative Humidity	RH [%]
AHU-1 Supply Airflow Fan 2	S/A [m^3/s]	AHU-3 Supply Air Relative Humidity	RH [%]
AHU-2 Supply Airflow Fan 1	S/A [m^3/s]	AHU-4 Supply Air Relative Humidity	RH [%]
AHU-2 Supply Airflow Fan 2	S/A [m^3/s]	AHU-5 Supply Air Relative Humidity	RH [%]
AHU-3 Supply Airflow Fan 1	S/A [m^3/s]	AHU-6 Supply Air Relative Humidity	RH [%]
AHU-3 Supply Airflow Fan 2	S/A [m^3/s]	AHU-7 Supply Air Relative Humidity	RH [%]
AHU-4 Supply Airflow Fan 1	S/A [m^3/s]	AHU-8 Supply Air Relative Humidity	RH [%]
AHU-4 Supply Airflow Fan 2	S/A [m^3/s]	Outdoor Air Temperature	$T_{O/A}$ [C]
AHU-7 Supply Airflow Fan 1	S/A [m^3/s]	**Water Side**	
AHU-7 Supply Airflow Fan 2	S/A [m^3/s]	Heating Water Supply Temperature	HWS [°C]
AHU-8 Supply Airflow Fan 1	S/A [m^3/s]	Heating Water Return Temperature	HWR [°C]
AHU-8 Supply Airflow Fan 2	S/A [m^3/s]	Sector A Glycol Water Supply Temperature	GLYWS [°C]
AHU-1 Supply Air Temperature	$T_{S/A}$ [°C]	Sector A Glycol Water Return Temperature	GLYWR [°C]
AHU-2 Supply Air Temperature	$T_{S/A}$ [°C]	Sector B & C Glycol Water Supply Temperature	GLYWS [°C]
AHU-3 Supply Air Temperature	$T_{S/A}$ [°C]	Sector B & C Glycol Water Return Temperature	GLYWR [°C]
AHU-4 Supply Air Temperature	$T_{S/A}$ [°C]	Chiller CH-3 Chilled Water Supply Temperature	CHWS-3 [°C]
AHU-5 Supply Air Temperature	$T_{S/A}$ [°C]	Chiller CH-3 Chiller Water Return Temperature	CHWR-3 [°C]
AHU-6 Supply Air Temperature	$T_{S/A}$ [°C]	Chiller CH-3 Condenser Water Supply Temperature	CNDS-3 [°C]
AHU-7 Supply Air Temperature	$T_{S/A}$ [°C]	Chiller CH-3 Condenser Water Return Temperature	CNDR-3 [°C]
AHU-8 Supply Air Temperature	$T_{S/A}$ [°C]	Chiller CH-4 Chilled Water Supply Temperature	CHWS-4 [°C]
AHU-1 Return Air Temperature	$T_{R/A}$ [°C]	Chiller CH-4 Chiller Water Return Temperature	CHWR-4 [°C]
AHU-2 Return Air Temperature	$T_{R/A}$ [°C]	Chiller CH-4 Condenser Water Supply Temperature	CNDS-4 [°C]
AHU-3 Return Air Temperature	$T_{R/A}$ [°C]	Chiller CH-4 Condenser Water Return Temperature	CNDR-4 [°C]
AHU-4 Return Air Temperature	$T_{R/A}$ [°C]		
AHU-7 Return Air Temperature	$T_{R/A}$ [°C]		
AHU-8 Return Air Temperature	$T_{R/A}$ [°C]		

5.1 Average Monitored Data at the Sciences Building

During the spring season, the outdoor air temperature is in the vicinity of the designed supply air temperature and thus, since the air systems are completed with a

100% outside air economizer, the cooling/heating coils are not operating whenever possible. If $T_{O/A} \approx T_{S/A}$, the outdoor air is introduced directly to the building to maintain the design supply air set point temperature without using the mechanical cooling. The systems still runs on a 100% outdoor air when $T_{S/A} \leq T_{O/A} \leq T_{R/A}$, but the cooling coils need to be operational to maintain the design supply air temperature.

Outdoor air dry-bulb temperature is collected on-site for comparison with the normal and average weather data at Trudeau airport that is used by EnergyPlus for simulation purposes (see Chapter 6). The outdoor air dry-bulb temperature variations over the month of May are presented in Figure 5.1. The monitored outdoor air temperature is greater than the average Typical Meteorological Year (TMY) value measured at the airport. Table 5.2 presents the average measured values near the building as well as those measured at the Trudeau airport over the month of April, May and June.

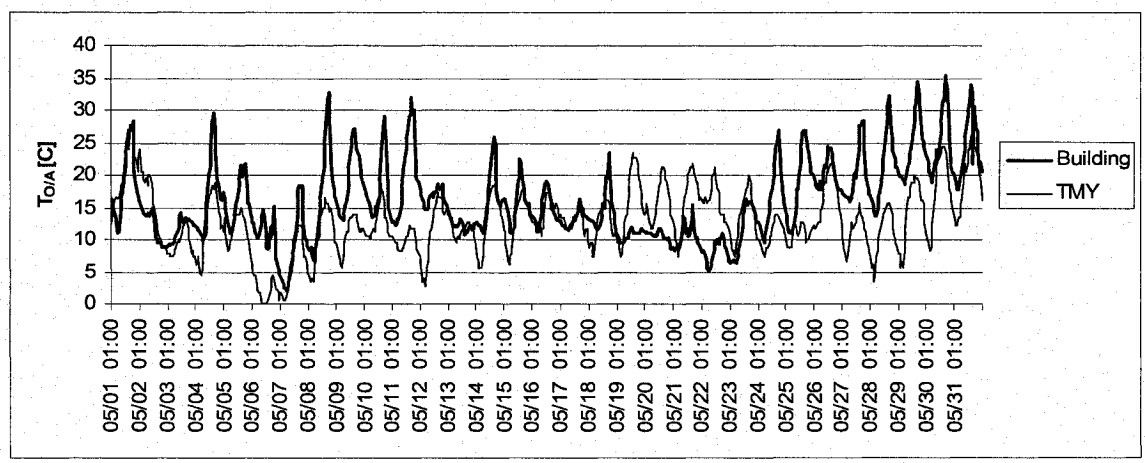

Figure 5.1: Outdoor Air Temperature for the month of May

Table 5.2: Monthly Average of the Outdoor Air Temperature

Month	Measured Average [°C]	Trudeau Airport Average (TMY value) [°C]	Temperature Difference [°C]
April	9.3	5.2	+ 4.1
May	15.9	12.9	+ 3.0
June	18.5	18.6	- 0.1

Different air and water systems are present in the building. Chilled water, heating water and steam are provided to the building by the central plant. On the air side, there are three major groups of air handling units: 1) AHU-1 to AHU-4 for sector A; 2) AHU-7 and AHU-8 for sectors B and C; 3) AHU-5 and AHU-6 for animal labs. Detailed collected data are only presented for sectors B and C. These sectors are served by two identical air handling units, AHU-7 and AHU-8. Components of each unit are shown in Figure 5.2. Each unit has a return fan, a mixing box, heating coils, a humidifier, cooling coils, filters, and supply fans. The measured point of the return air is located before the return fan, while the measured supply air points (temperature, relative humidity and airflow) are located after the supply fan. The measured points of the water temperature (glycol, heating and chilled) are located at the inlets and outlets of heat exchangers and chillers.

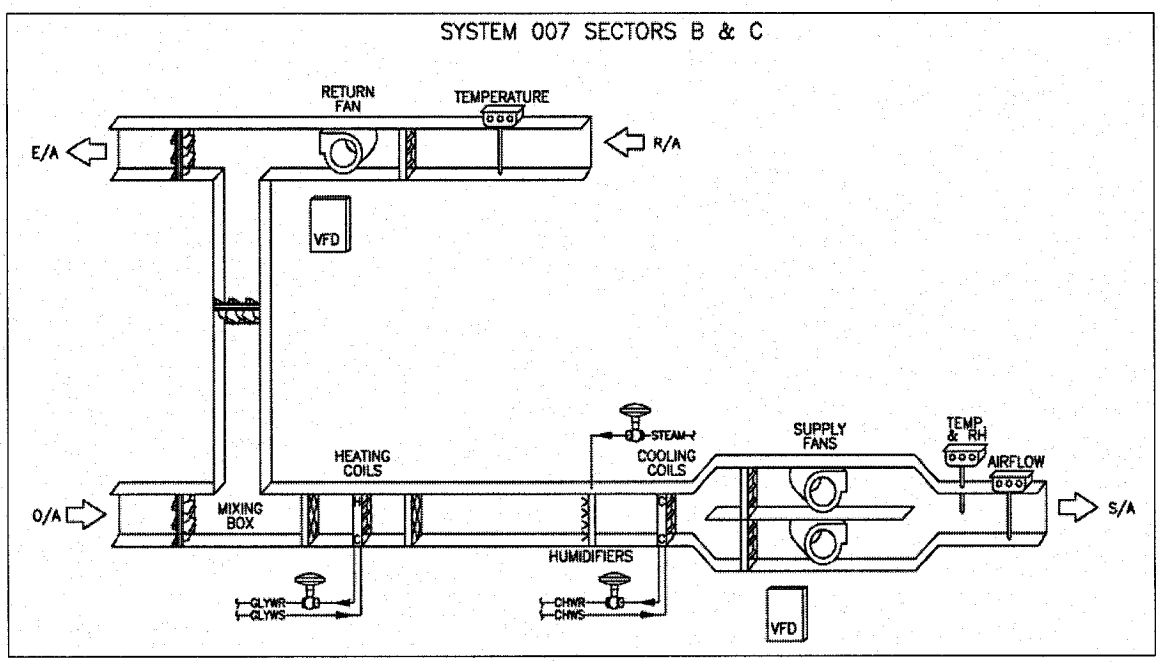

Figure 5.2: Capture of Display Software for Sectors B & C Air Handling Unit

In the computer model, AHU-7 and AHU-8 are combined together as one large unit; hence the total airflow of AHU-7 and AHU-8 is presented in this chapter, and also

in Chapter 6 for comparison with the simulation results. Supply air (S/A) and return air (R/A) temperatures are collected for all units located in the building (Table 5.3). Since the air systems in EnergyPlus are entered as one large system, the average weighted values, based on the airflow rates of each AHU, are used for comparison. Table 5.3 and Figure 5.3 present some sample measurements for the month of May.

Table 5.3: Daily Average Measurements on the Air-Side Loop for the Month of May; Sectors B & C

Month/Day	Airflow [m^3/s]			$T_{O/A}$ [°C]	$T_{S/A}$ [°C]			$T_{R/A}$ [°C]		
	B	C	Total		B	C	Average	B	C	Average
05/01	10.13	12.64	22.78	19.1	15.7	15.3	15.4	22.1	22.2	22.2
05/02	10.14	12.65	22.79	12.1	16.4	15.2	15.7	22.0	22.1	22.0
05/03	10.13	12.66	22.79	11.5	16.6	15.1	15.7	21.9	22.0	22.0
05/04	10.11	12.70	22.81	16.8	15.9	15.2	15.5	22.0	22.1	22.0
05/05	10.10	12.72	22.82	15.8	16.5	15.6	16.0	22.0	22.1	22.1
05/06	10.10	12.74	22.84	10.6	16.0	14.8	15.2	21.7	21.8	21.7
05/07	10.10	12.76	22.86	8.5	16.0	15.1	15.4	21.2	21.7	21.6
05/08	10.09	12.79	22.88	16.6	16.0	15.4	15.6	21.9	22.0	22.0
05/09	10.09	12.82	22.91	19.3	15.7	15.2	15.4	22.1	22.2	22.2
05/10	10.11	12.85	22.96	17.9	16.8	16.0	16.3	22.2	22.3	22.2
05/11	10.10	12.88	22.99	20.2	15.7	15.3	15.4	22.0	22.2	22.1
05/12	10.09	12.91	23.00	16.7	17.2	16.3	16.7	22.2	22.2	22.2
05/13	10.09	12.95	23.04	12.3	16.2	15.2	15.5	21.7	21.7	21.7
05/14	10.10	12.97	23.06	16.2	15.9	15.4	15.6	21.7	21.8	21.8
05/15	10.10	12.99	23.08	15.7	16.8	15.8	16.2	22.0	22.1	22.1
05/16	10.10	13.01	23.11	14.6	16.8	15.6	16.1	22.0	22.1	22.1
05/17	10.10	13.03	23.13	13.2	16.5	15.3	15.8	21.9	22.0	22.0
05/18	10.09	13.05	23.14	14.6	16.9	15.8	16.2	21.8	22.0	21.9
05/19	10.06	13.05	23.11	10.7	16.7	15.7	16.1	21.8	21.9	21.9
05/20	10.02	13.06	23.09	10.6	16.4	15.0	15.6	21.5	21.6	21.6
05/21	9.98	13.07	23.05	10.6	16.3	15.2	15.6	21.4	21.5	21.4
05/22	9.95	13.07	23.03	8.1	16.6	15.3	15.8	21.4	21.5	21.5
05/23	9.95	13.08	23.03	11.5	16.7	15.6	16.1	21.8	21.9	21.8
05/24	9.97	13.09	23.07	16.5	17.7	16.5	17.0	22.0	22.1	22.0
05/25	9.99	13.09	23.08	18.6	16.0	15.4	15.6	22.0	22.1	22.1
05/26	9.99	13.08	23.07	20.0	15.1	15.1	15.1	22.1	22.2	22.2
05/27	10.00	13.06	23.05	20.3	15.1	15.1	15.1	22.1	22.2	22.2
05/28	10.01	13.09	23.10	21.0	15.2	15.1	15.1	22.2	22.4	22.3
05/29	10.02	13.12	23.14	24.4	15.0	15.0	15.0	22.3	22.5	22.4
05/30	10.04	13.16	23.19	24.7	15.3	15.2	15.3	22.4	22.6	22.5
05/31	10.05	13.17	23.22	24.2	15.0	15.0	15.0	22.4	22.6	22.5
Average			20.57	15.9			15.7			22.0
Std. Dev.			8.09	6.1			1.0			0.3

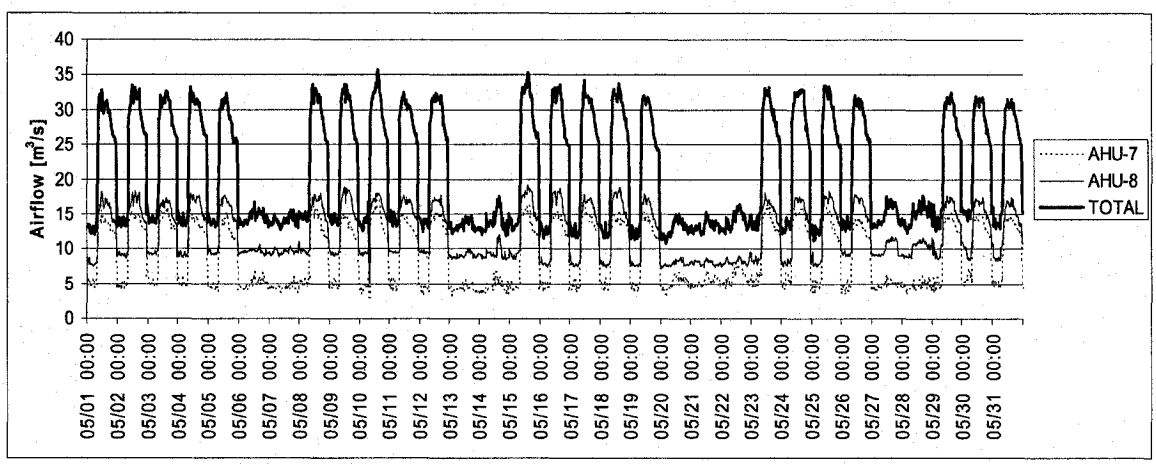

Figure 5.3: Airflow Variation for the Month of May; Sectors B & C

Figure 5.4 shows the outdoor air (O/A), the supply air (S/A) and return air (R/A) temperatures variation throughout the month of May for sectors B and C.

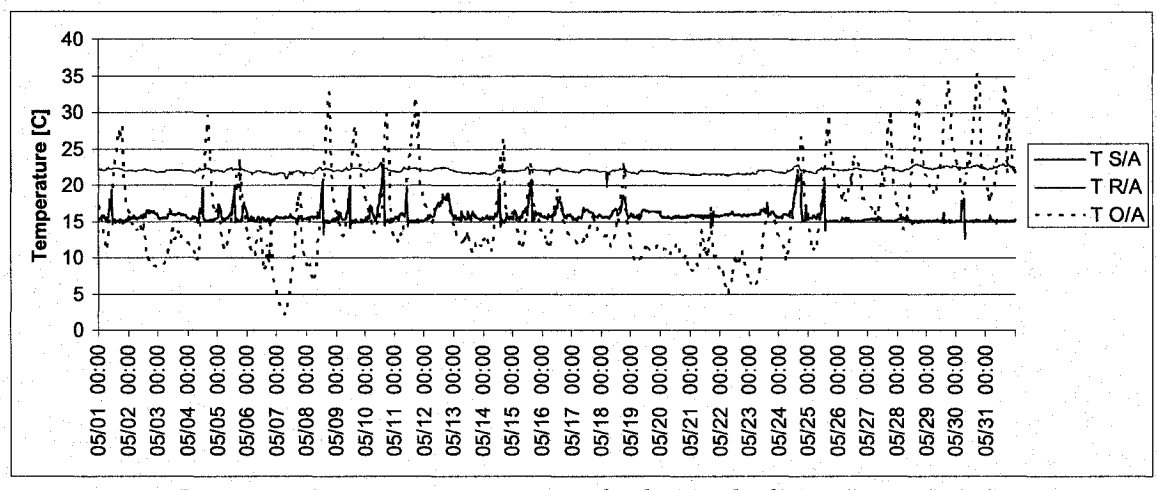

Figure 5.4: Air Temperature Variation for the Month of May; Sectors B & C

On the water side, the chilled water (CHW), the steam and the heating water (HW) are provided by the university central plant. Additional chillers (CH-3 and CH-4) are installed within the building to supply cooling to the utilities room during the winter and shoulder seasons. Chillers CH-1 and CH-2 have been in operation from April 20th to 22nd and then from May 4th on. Data are presented for the month of May for chillers CH-

3 and CH-4, the heating water and the glycol loop to the air handling units of sectors B and C (Table 5.4).

Table 5.4: Daily Average Water Temperature [°C] for the Month of May; Sectors B & C

Month/ Day	HWS	HWR	GLYWS	GLYWR	CHILLER CH-3				CHILLER CH-4			
					CHWS	CHWR	CNDS	CNDR	CHWS	CHWR	CNDS	CNDR
05/01	33.1	30.9	26.5	25.8	16.3	15.1	29.0	30.0	6.5	7.6	26.9	27.5
05/02	31.5	29.8	27.1	25.8	15.8	15.1	28.4	29.9	8.9	11.0	26.9	26.6
05/03	32.4	31.2	28.3	26.5	12.8	15.1	32.1	31.3	11.9	13.0	24.9	25.7
05/04	32.6	30.5	27.4	26.2	OFF	OFF	OFF	OFF	OFF	OFF	OFF	OFF
05/05	32.2	30.9	26.8	25.8	OFF	OFF	OFF	OFF	OFF	OFF	OFF	OFF
05/06	32.8	31.8	28.7	26.4	OFF	OFF	OFF	OFF	OFF	OFF	OFF	OFF
05/07	34.7	33.2	30.9	27.4	OFF	OFF	OFF	OFF	OFF	OFF	OFF	OFF
05/08	32.9	31.0	28.3	26.9	OFF	OFF	OFF	OFF	OFF	OFF	OFF	OFF
05/09	32.6	30.5	24.9	24.4	OFF	OFF	OFF	OFF	OFF	OFF	OFF	OFF
05/10	31.7	30.3	23.8	23.6	OFF	OFF	OFF	OFF	OFF	OFF	OFF	OFF
05/11	31.7	29.3	23.3	23.2	OFF	OFF	OFF	OFF	OFF	OFF	OFF	OFF
05/12	32.4	32.0	23.0	23.0	OFF	OFF	OFF	OFF	OFF	OFF	OFF	OFF
05/13	31.8	31.0	24.7	23.6	OFF	OFF	OFF	OFF	OFF	OFF	OFF	OFF
05/14	31.0	29.9	27.3	25.6	OFF	OFF	OFF	OFF	OFF	OFF	OFF	OFF
05/15	30.5	29.8	26.5	25.2	OFF	OFF	OFF	OFF	OFF	OFF	OFF	OFF
05/16	30.5	29.9	26.2	25.2	OFF	OFF	OFF	OFF	OFF	OFF	OFF	OFF
05/17	30.6	29.7	24.1	23.7	OFF	OFF	OFF	OFF	OFF	OFF	OFF	OFF
05/18	31.0	30.4	22.8	22.6	OFF	OFF	OFF	OFF	OFF	OFF	OFF	OFF
05/19	32.0	30.5	28.8	25.7	OFF	OFF	OFF	OFF	OFF	OFF	OFF	OFF
05/20	31.9	30.8	28.9	25.3	OFF	OFF	OFF	OFF	OFF	OFF	OFF	OFF
05/21	32.4	31.3	29.3	26.0	OFF	OFF	OFF	OFF	OFF	OFF	OFF	OFF
05/22	33.7	32.3	30.6	27.4	OFF	OFF	OFF	OFF	OFF	OFF	OFF	OFF
05/23	31.9	30.6	29.0	26.5	OFF	OFF	OFF	OFF	OFF	OFF	OFF	OFF
05/24	32.9	32.2	27.6	26.1	OFF	OFF	OFF	OFF	OFF	OFF	OFF	OFF
05/25	31.5	29.9	26.6	25.6	OFF	OFF	OFF	OFF	OFF	OFF	OFF	OFF
05/26	31.5	29.1	25.1	24.5	OFF	OFF	OFF	OFF	OFF	OFF	OFF	OFF
05/27	31.1	29.5	24.5	24.1	OFF	OFF	OFF	OFF	OFF	OFF	OFF	OFF
05/28	31.2	29.4	24.4	24.2	OFF	OFF	OFF	OFF	OFF	OFF	OFF	OFF
05/29	30.8	28.4	24.9	24.8	OFF	OFF	OFF	OFF	OFF	OFF	OFF	OFF
05/30	32.1	29.2	25.8	25.7	OFF	OFF	OFF	OFF	OFF	OFF	OFF	OFF
05/31	32.7	29.6	26.5	26.5	OFF	OFF	OFF	OFF	OFF	OFF	OFF	OFF
Average	32.0	30.5	26.5	25.3								
Std. Dev.	1.0	1.1	2.2	1.3								

5.2 Analysis

Data collected over the spring season are analyzed for a better understanding of how the air and water systems interact together.

5.2.1 Airflow Rates

As previously mentioned, three major groups of air handling units are installed in the building. The airflow rate analysis is presented for the air handling units for sectors A, B and C.

5.2.1.1 Sectors B and C

During occupancy, the average supply airflow rate is 30.0 m^3/s, and it is reduced to an average of 14.0 m^3/s at night time and during week-ends (Figure 5.3). This corresponds to about 4.5 air changes per hour (ACH) during the occupied period, and 2.1 ACH during the unoccupied period. The design specifications indicate that in laboratories the supply air must be equal to about 10 ACH during occupancy, 6 ACH during occupancy while unoccupied, and 3 ACH at night time. All other zone types are restricted to a minimum of 3 ACH, if located on the perimeter, and 1.5 ACH, if it is an interior zone [39]. Laboratories occupy about 40% of the total floor area of sectors B and C, while perimeter and interior spaces occupy approximately 25% and 35% of the remaining floor area. Based on this information, the average required ACH is estimated at 5.3 ACH when all laboratories are fully occupied, at 4.5 ACH when 50% are occupied and 50% are unoccupied during occupied hours, and at 2.5 ACH while the building is unoccupied. The measurements indicate that during the full occupancy and when 50% of the laboratories are occupied, the airflow rate satisfied the design requirements. When the building is unoccupied, the HVAC systems supply only 2.1 ACH while the design is for 2.5 ACH.

The design specifications, as presented in the CBIP file, gives a total airflow of 46.5 m^3/s. This value does not include the supply compensation for the exhaust requirements of laboratories. The additional airflow required to accommodate all exhaust hoods located in sector C is calculated based on the design specifications of all the Variable Air Volume (VAV) units installed on the ventilation hoods. The total airflow for all installed hoods (~ 60 hoods) in sector C is around 25.0 m^3/s. By considering the coefficient of simultaneous usage (diversity factor) of hoods for each room (Table 5.5), the maximum airflow rate required by the hoods is 18.5 m^3/s. Hence, the total required supply airflow rate is about 65.0 m^3/s. Since the design fan capacity of sectors B and C is 75.5 m^3/s, the measurements indicate that during the occupied period, the fans work on average at 40% (30.0/75.5 m^3/s) of total capacity, and during the night at 18.5% (14.0/75.5 m^3/s) of capacity. During the spring season, the maximum supply fans capacity is 50% (37.5/75.5 m^3/s).

Table 5.5: Design Assumptions for Exhaust Hoods [39]

Number of hoods per room	Percentage of hoods running at full capacity
1	100%
2-3	90%
4-5	80%
6-7	70%
8-9	60%
10+	50%

5.2.1.2 Sector A

During occupancy the average supply airflow rate is 73.5 m^3/s, and it is reduced to an average of 52.0 m^3/s at night time and during week-ends. This corresponds to about 6.0 ACH during the occupied period and 4.25 ACH during the unoccupied period. Based on the design criteria presented earlier (10/6/3 ACH for laboratories and 3/1.5 ACH for other zones), the average required ACH is estimated at 6.3 ACH when all laboratories are fully occupied, at 5.3 ACH when 50% are occupied and 50% are unoccupied during

occupied hours, and at 2.8 ACH while the building is unoccupied. Hence, the occupied ACH is consistent with the design specifications. However, the measured unoccupied value (4.25 ACH) is higher than the minimum estimated value of 2.8 ACH. This denotes that during unoccupied hours, some of the research laboratories are being used, thus increasing the ACH requirements for sector A.

The design specification gives a total airflow of 91.5 m^3/s, which excludes the exhaust requirements of the laboratories. The design fan capacity for sector A is set to 151.0 m^3/s. Laboratories occupy 50% of the occupied floor area of sector A, and thus a large amount of supply air must be provided to these rooms. Based on the VAV specifications, a total airflow for all installed hoods (~170 hoods) of 75.0 m^3/s is required to accommodate all exhaust hoods located in sector A. By considering the coefficient of simultaneous usage (diversity factor) of hoods for each room (Table 5.5), the maximum airflow required by the hoods is 45.5 m^3/s. Based on the VAV specifications, the value calculated using the diversity factor is about 60% of the total exhaust requirements for sector A. The maximum coincident use of laboratory hoods the system can accommodate is 80%. Based on this value, the supply airflow rate is 151.0 m^3/s. Measurements indicate that during the occupied period, supply fans work on average at 50% (73.5/151.0 m^3/s) of total capacity, and during the night at 35% (52.0/151.0 m^3/s) of capacity. During the spring season, the maximum supply fans capacity is 60% (90.5/151.0 m^3/s). Table 5.6 summarizes the air systems information.

Table 5.6: Summary of Airflow Rates

ITEM		SECTOR A	SECTORS B & C
Specifications			
Design airflow for cooling/heating [m^3/s]		91.5	46.5
Maximum hood exhaust [m^3/s], including diversity factor		59.5	25.0
Total required airflow [m^3/s]		151.0	71.5
Installed capacity [m^3/s]		151.0	75.5
Measured			
Average airflow rate[m^3/s]	Occupied	73.5	30.0
	Unoccupied	52.0	14.0
	Average	60.4	20.3
	Std. Dev.	11.6	8.0
Air changes per hour [ACH]	Occupied	6.0	4.5
	Unoccupied	4.25	2.1
Flow per unit area [$L/s/m^2$]	Occupied	4.2	3.1
	Unoccupied	2.9	1.5

In terms of airflow per surface area, ASHRAE recommends a minimum supply airflow rate of 3.8 $L/s/m^2$ for laboratories and 0.66 $L/s/m^2$ for offices [41]. The average airflow rate per unit area is 4.2 $L/s/m^2$ during occupancy for sector A, which is above the recommended value made by ASHRAE for laboratories. For sectors B and C, 40% of the floor area is occupied by laboratories, while the remaining 60% is mainly occupied by offices. Based on the weighted average, the recommended airflow per unit area is 1.9 $L/s/m^2$. Therefore, the average measured airflow rate per unit area for sectors B and C, of 3.1 $L/s/m^2$ during occupancy, is 163% higher than the value recommended by ASHRAE.

The variation of supply airflow rate with outdoor air temperature is presented in Figure 5.5. There is a clear separation of measured data for both sets (occupied versus unoccupied for each sector). The impact of outdoor air temperature on the supply airflow rate is minimal. Hence, one can conclude that the heating/cooling loads due to heat losses/gains through the exterior envelope are smaller compared with the building internal gains.

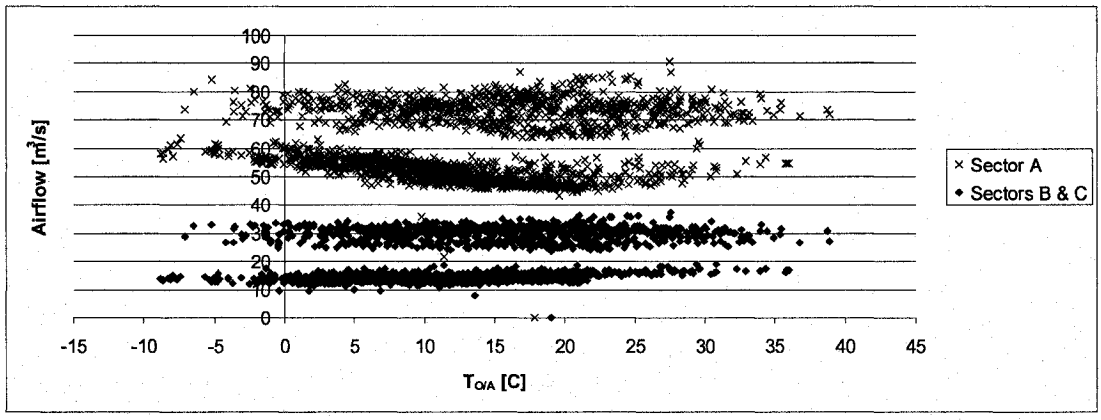

Figure 5.5: Variation of the Supply Airflow Rate with Outdoor Air Temperature for the Spring Season

5.2.2 Supply and Return Air Temperatures

On average, for sectors B and C, during the month of May, the supply air temperature is 15.7°C ±1°C. Based on the specifications, the leaving heating coil air temperature is 12.8°C, and the leaving cooling coil air temperature is 11.2°C. The increase in temperature due to the fan can be calculated as follow [42].

$$\Delta T_F = \frac{0.811\ W_F}{V_F} \qquad (5.1)$$

where,

ΔT_F in the increase in temperature due to the fan [°C];

W_F is the electric power of fan motor [kW];

V_F is the fan airflow rate [m^3/s].

Based on this equation and the fan data collected from the manufacturer [43] for AHU-7 and 8, the rise in air stream temperature is about 2.2 °C. When adding this value to the leaving heating and cooling coil air temperatures, the supply air temperatures are respectively 15.0°C and 13.4°C, which are close to the measured values of 15.7°C ±1°C, for the month of May.

Throughout most of the spring season, the supply air temperature is kept close to its set point (Figures 5.6 and 5.7). However, for sector A, the supply air temperature is above the supply air set point for about 70 hours during the spring season, and about 55 hours for sectors B and C. Most of the hours where the temperature is above 20°C occur during the afternoons of March 31st, April 12th, 18th and 19th. This situation occurs because the cooling coils are not in operation and the outdoor air is introduced directly into the building. Once the central plant chillers (CH-1 and CH-2) are in operation (May 4th), the supply air temperature is around the design supply set point of 16.3°C ± 1.5°C for sector A, and 15.9°C ± 1.4°C for sectors B and C.

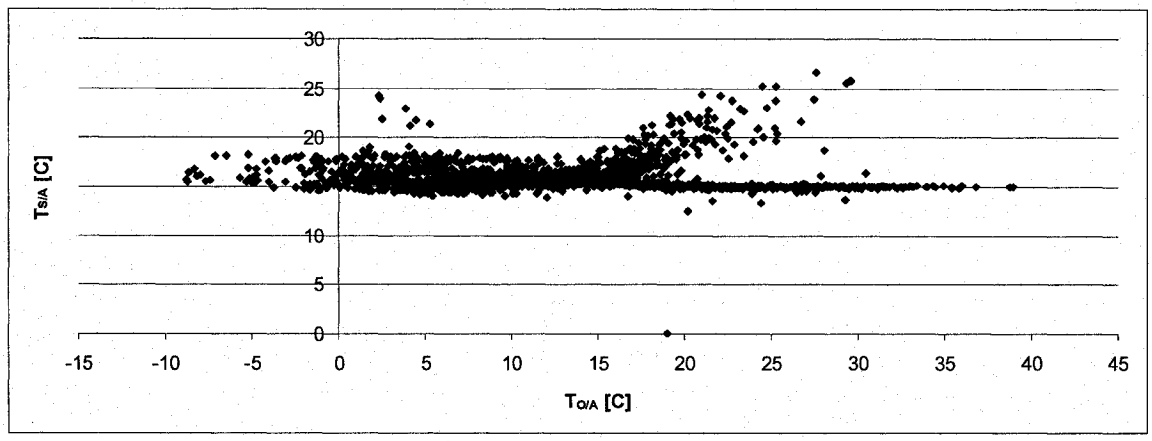

Figure 5.6: Hourly Values of Supply Air Temperature versus Outdoor Air Temperature for the Spring Season; Sectors B & C

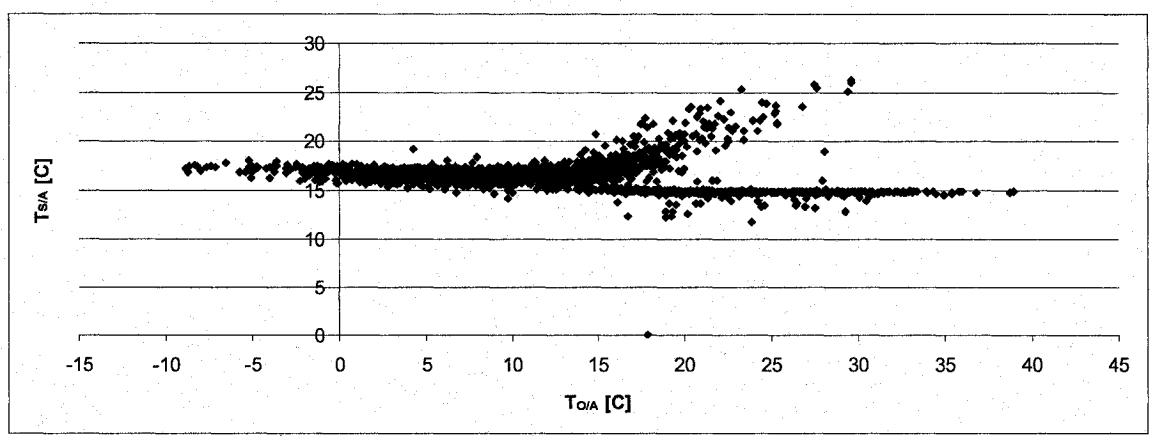

Figure 5.7: Hourly Values of Supply Air Temperature versus Outdoor Air Temperature for the Spring Season; Sector A

On the return side, the air temperature is around 22°C ± 0.3°C (Table 5.3 and Figure 5.4). A constant return air temperature implies that no setback or setup on the zone temperature set point is implemented in the building. The supply air temperature is maintained constant at all time, while the airflow rate varies depending on the level of occupancy in the building. These conclusions are also valid for sector A.

5.2.3 Air-Side Thermal Load

The air-side thermal loads for each sector are estimated from the measured data as follows:

$$Q_{Sector} = V_a \cdot \rho_a \cdot C_{p,a} \cdot (T_{R/A} - T_{S/A}) \qquad (5.2)$$

where

Q_{Sector} is the sector load [kW];

V_a is the measured airflow rate for each sector [m^3/s];

ρ_a is the density of air, $\rho_a = 1.169$ kg/m^3;

$C_{p,a}$ is the specific heat of air, $C_{p,a} = 1.004$ kJ/kg · K;

$T_{R/A}$ is the weighted average return air temperature [°C];

$T_{S/A}$ is the weighted average supply air temperature [°C].

For both sectors, cooling is required most of the spring season. For sectors B and C, the monthly average load is between 131.2 and 168.5 kW, and for sector A it is between 337.9 and 476.1 kW. Summary of the seasonal loads are presented in Table 5.7. The seasonal total cooling load is 33 kWh/m^2 for sectors B and C, and 48 kWh/m^2 for sector A. Occupancy has a major impact on the sector load, while the increase in outdoor air temperature has a limited impact on the load (Figures 5.8 and 5.9).

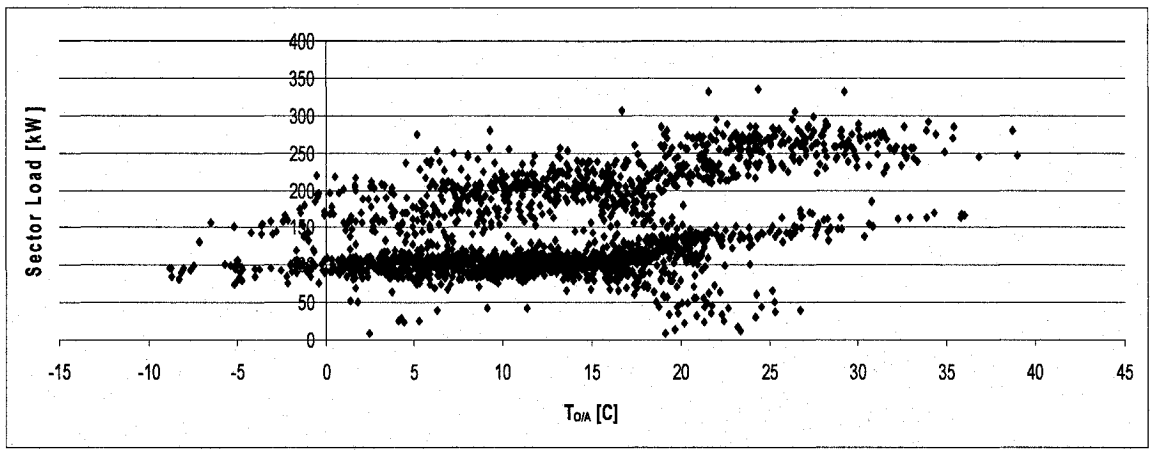

Figure 5.8: Sector Cooling Load versus Outdoor Air Temperature for the Spring Season; Sectors B and C

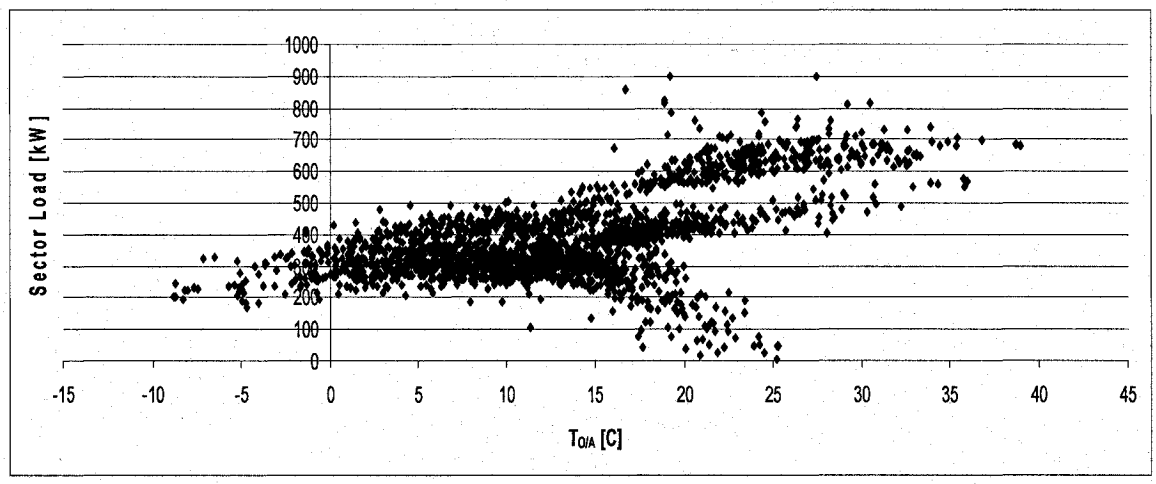

Figure 5.9: Sector Cooling Load versus Outdoor Air Temperature for the Spring Season; Sector A

Before May 4th, the cooling coils are not operational, and outdoor air is directly introduced to the building. Consequently, the supply air temperature is above 20°C during the afternoons of March 31st, April 12th, 18th and 19th. The average return air temperature for both sectors is 22°C, thus, when the supply air temperature is above the average return air temperature there is no cooling load (Figures 5.8 and 5.9).

Table 5.7: Overview of Air Systems Data

			SECTOR A			SECTOR B & C		
			APRIL	MAY	JUNE	APRIL	MAY	JUNE
AIRFLOW [m^3/s]		Average	60.6	59.9	57.8	19.3	20.4	20.3
		Std. Dev.	10.7	11.8	11.8	7.9	8.1	7.2
S/A Temp [°C]		Average	16.8	16.2	15.4	16.0	15.7	15.3
		Std. Dev.	1.6	1.4	1.3	1.8	1.0	0.8
R/A Temp [°C]		Average	21.5	21.8	22.4	21.9	22.0	22.4
		Std. Dev.	0.6	0.5	0.4	0.5	0.3	0.3
Sector Load	Cooling [kW]	Average	337.9	395.7	476.1	131.2	149.7	168.5
		Std. Dev.	99.3	137.4	146.9	54.1	64.0	67.4
	Heating [kW]	Average	78.7	25.3		48.4		
		Std. Dev.	65.9	N/A		31.5		
	Cooling [W/m^2]		19.1	22.4	26.9	13.7	15.7	17.6
	Heating [W/m^2]		4.5	1.4		5.1		

5.2.4 Water Systems

Throughout the spring season, the chillers (CH-1 and/or CH-2) installed in the central plant are in operation from April 20th to 22nd and then from May 4th on. Therefore, chillers CH-3 and CH-4 are operational until May 4th. Figures 5.10 and 5.11 present the water temperatures variation over the spring season for chillers CH-3 and CH-4. It is noticed that water temperature variations are still monitored after May 4th, which is when chillers CH-3 and CH-4 are not in operation. For instance, on May 21st, the chilled water temperatures at chiller CH-3 is 6.7°C (supply) and 10.6°C (return) (Figure 5.10). At the same time, the chilled water temperature at chiller CH-4 is about 7.1°C (both supply and return) (Figure 5.11). These data raise questions about the location of sensors and what temperatures are actually measured. They indicate the chilled water temperatures when CH-1 and CH-2 are in operation. Based on the monitored information collected after May 4th, the chilled water supply temperature is around 5.6°C and the condenser water supply temperature is around 35°C, as per the design specifications.

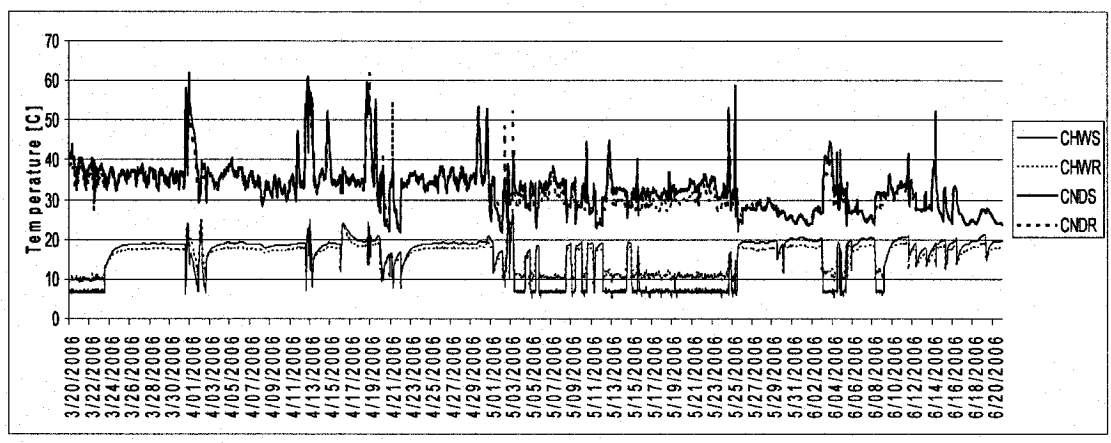

Figure 5.10: Water Temperatures at Chiller CH-3 over the Spring Season

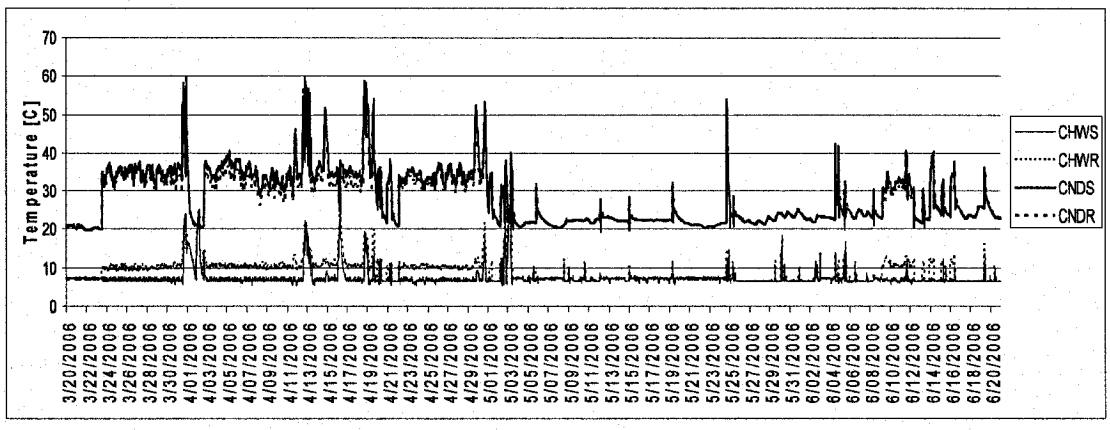

Figure 5.11: Water Temperatures at Chiller CH-4 over the Spring Season

Based on collected information, only one chiller, either chiller CH-3 and CH-4, is providing cooling to the building until May 4th. Thus, the cooling load of the chiller in operation can be calculated using the following formula:

$$Q_{chiller} = V_P \cdot \rho_w \cdot C_{p,w} \cdot \Delta T_w \qquad (5.3)$$

where

$Q_{chiller}$ is the load [kW];

V_P is the rated design flow for the pump, which is 10.7 L/s or 0.0107 m^3/s;

ρ_w is the density of water at 9.45°C, which is the average design temperature, $\rho_w = 998.9$ kg/m^3;

$C_{p,w}$ is the specific heat of water at 9.45°C, $C_{p,w} = 4.21$ kJ/kg K;

ΔT_w is the temperature difference between the chilled water return (CHWR) and the chilled water supply (CHWS) [°C].

Figure 5.12 shows the variation of chiller load up to May 4th. From March 20th to May 4th, the average chiller load is 145 ± 35 kW. Over the same period, the average total air-side building thermal load (total of sectors A, B and C) is 360 ± 55 kW. If the outdoor air temperature is low, the mixed air temperature is close to the design supply air temperature and no mechanical cooling is required. However, if the outdoor air temperature is between 16°C and 24°C, the system is working at a 100% outside air, hence the design supply air temperature is above the supply set point, and mechanical cooling is required. If mechanical cooling is required and the measured supply air temperature is above the design set point, either the cooling coil is not in operation or the cooling provided by the chiller (CH-3 or CH-4) is not sufficient to meet the cooling requirements of the building for that period. Since chillers CH-3 and CH-4 are only providing chilled water to fan coil units located in telecom, electrical and utilities rooms, one can conclude that the cooling coils are not in operation for that period, thus

explaining the raise in supply air temperature when the outdoor air temperature is above the design supply air temperature (Figures 5.6 and 5.7).

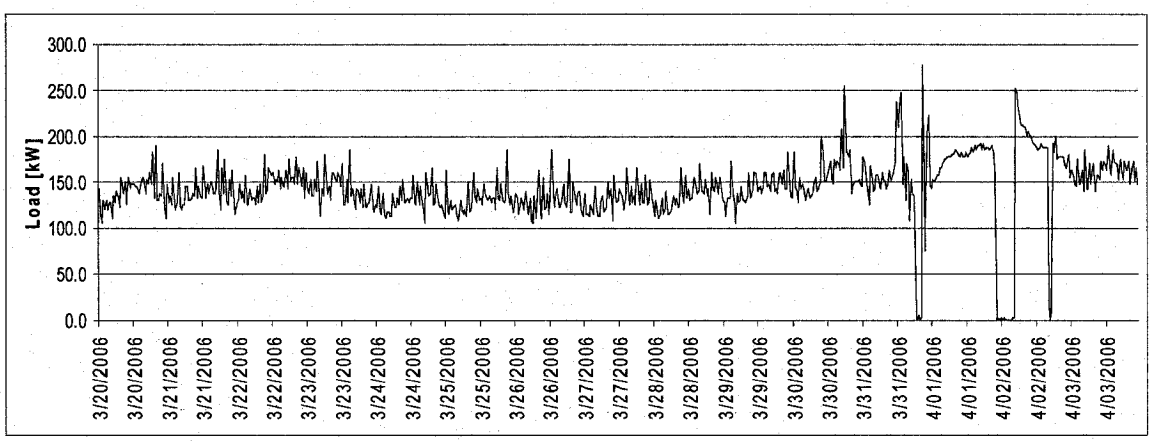

Figure 5.12: Variation of Chiller Load from March 20th to May 4th.

Figure 5.13 presents the outdoor air and corresponding supply air temperature variation for two consecutive days, March 30th and 31st, when the cooling coils are not in operation. On March 30th, the outdoor air temperature is always below the supply air temperature set point and thus, the design supply air temperature is met. On March 31st, the outdoor air temperature is higher than the supply air set point during the afternoon, and consequently the supply air temperature is higher than the design set point. Therefore, the measured data support the assumption that the cooling coils are not in operation before May 4th.

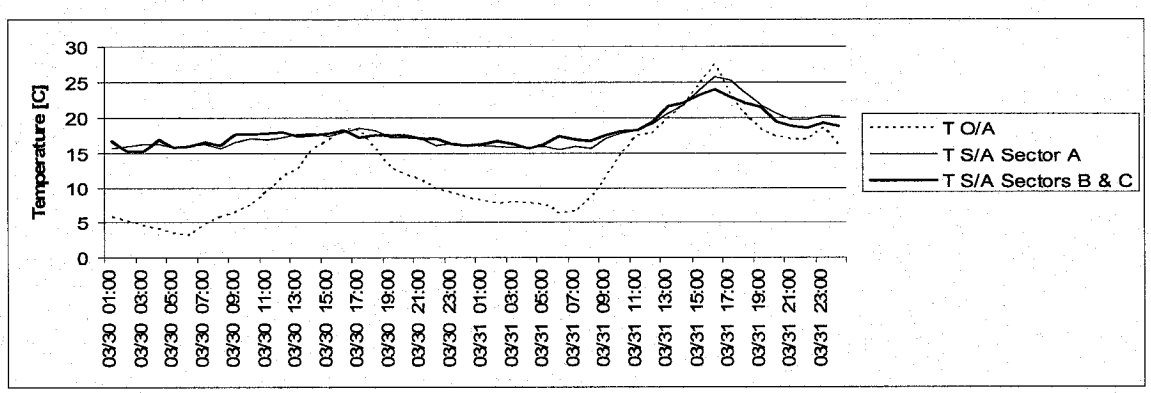

Figure 5.13: Air Temperature Variation for March 30th and 31st, 2006

The total building cooling load is between 250 kW and 500 kW (building load axis), while the chiller load is around 145 kW (Figure 5.14). The building load increases at higher outdoor air temperature (Figures 5.8 and 5.9), while the outdoor air temperature has less impact on the chiller load (Figure 5.15). The chiller load slightly increases at higher outdoor air temperatures, supporting the assumption that the cooling coils located in the air handling units are not in operation and that the chiller only provides cooling to the fan coil units from March 20th to May 4th, which was confirmed by the building operators.

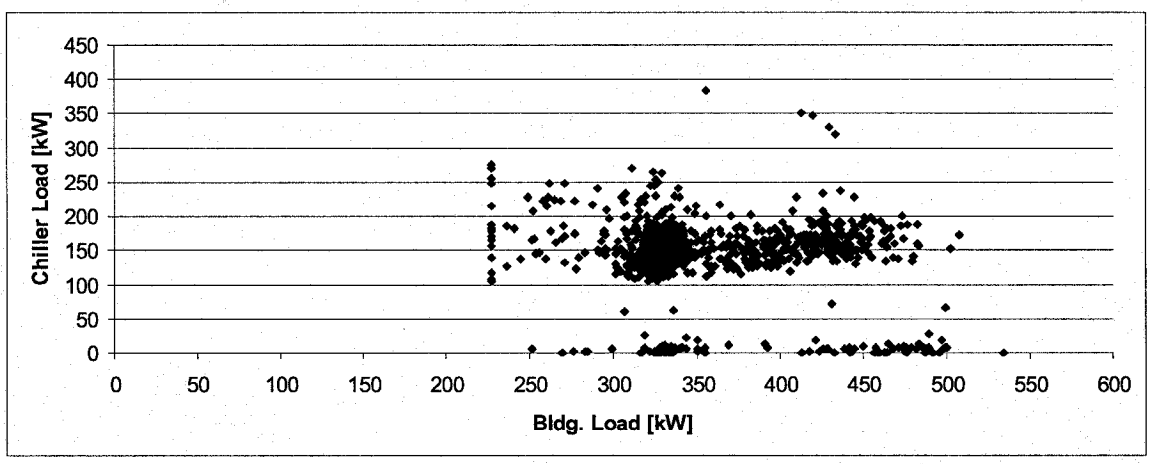

Figure 5.14: Chiller Load versus Building Load; March 20th to May 4th, 2006

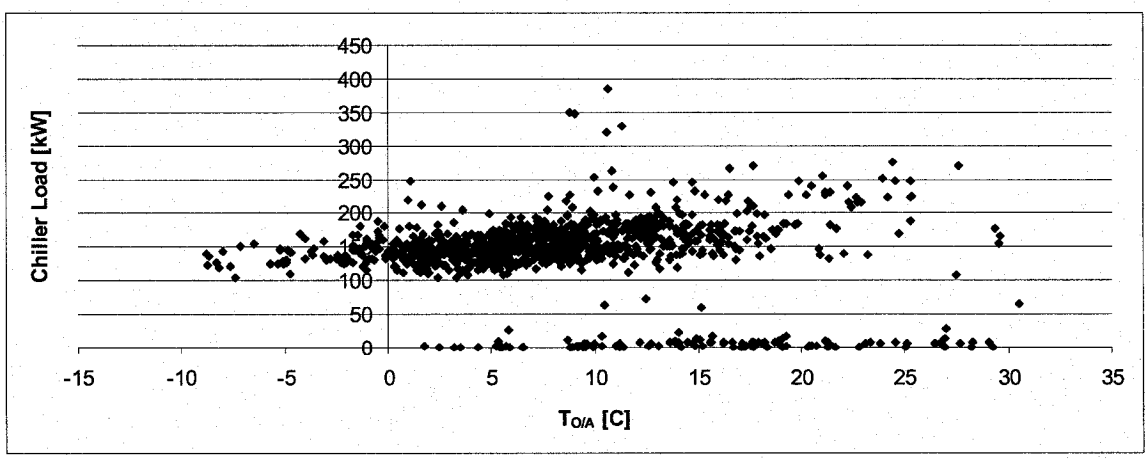

Figure 5.15: Chiller Load versus Outdoor Air Temperature; March 20th to May 4th, 2006

The condenser water is connected to the heating water loop for heat recovery purposes. When comparing the condensed water temperature of chiller CH-3 (or chiller CH-4, which ever is operational) and the heating water supply temperature, the two closely correspond (Figure 5.16). Hence, for most of the spring season, the condensed water temperature is high enough to meet the required heating water supply temperature of the re-heat coils.

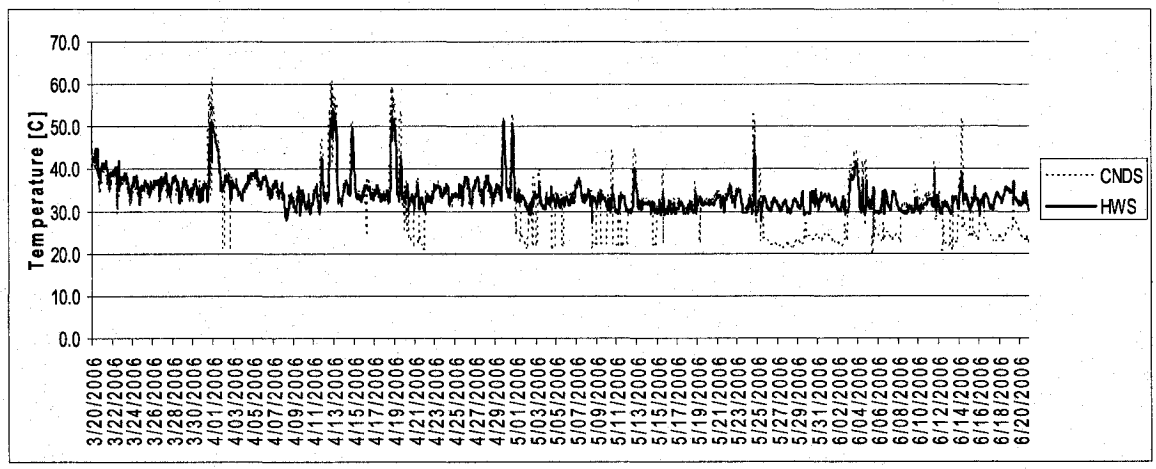

Figure 5.16: Water Temperature of CNDS and HWS over the Spring Season

At outdoor air temperatures below 5°C, the heating water temperature increases from about 35°C to 45°C with the decrease in outdoor air temperatures, while being relatively constant at 30-35°C for outdoor air temperatures above 5°C (Figure 5.17). For the condenser water temperatures, the temperature decreases with the increase in outdoor air temperature, for outdoor air temperatures below 20°C (Figure 5.18). For higher outdoor air temperatures, which are mainly occurring when chillers CH-1 and CH-2 are in operation, the condenser supply water temperature is around 25°C, which is close to the heating water supply temperature.

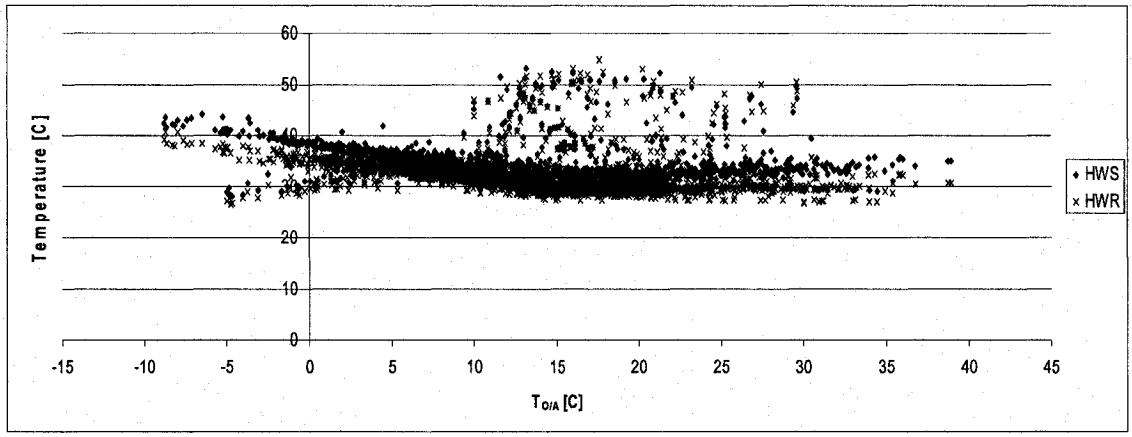

Figure 5.17: Heating Water Temperature versus Outdoor Air Temperature over the Spring Season

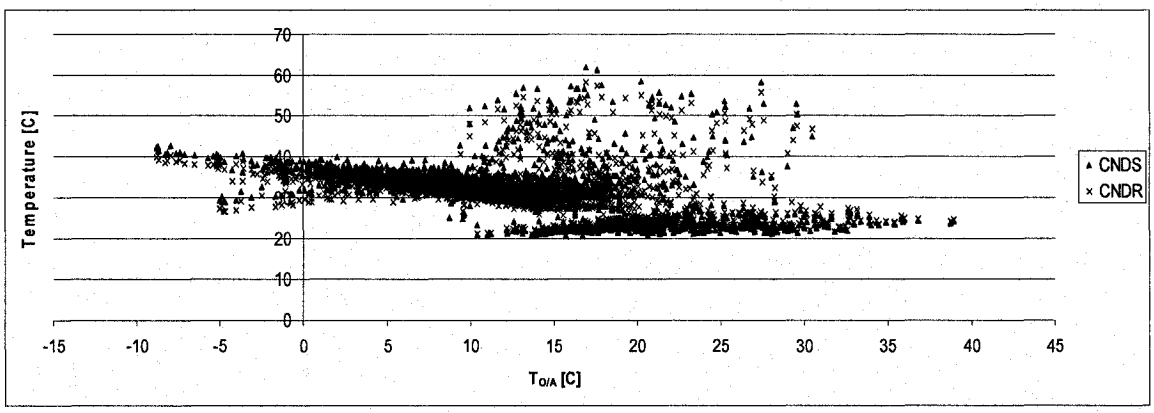

Figure 5.18: Condenser Water Temperature versus Outdoor Air Temperature over the Spring Season

For sector B and C, the difference between the glycol supply and return water temperatures is close to zero, which indicates that the heating coils are mostly off during the spring season (Figure 5.19). Since sector A has more laboratories than sectors B and C, the outdoor air requirement is higher and consequently the mixed air temperature is lower than the design supply air temperature for longer period of time. The heating requirements for sector A are thus higher than for sectors B and C. Consequently, larger difference in glycol water temperatures are noticed for sector A (Figure 5.20).

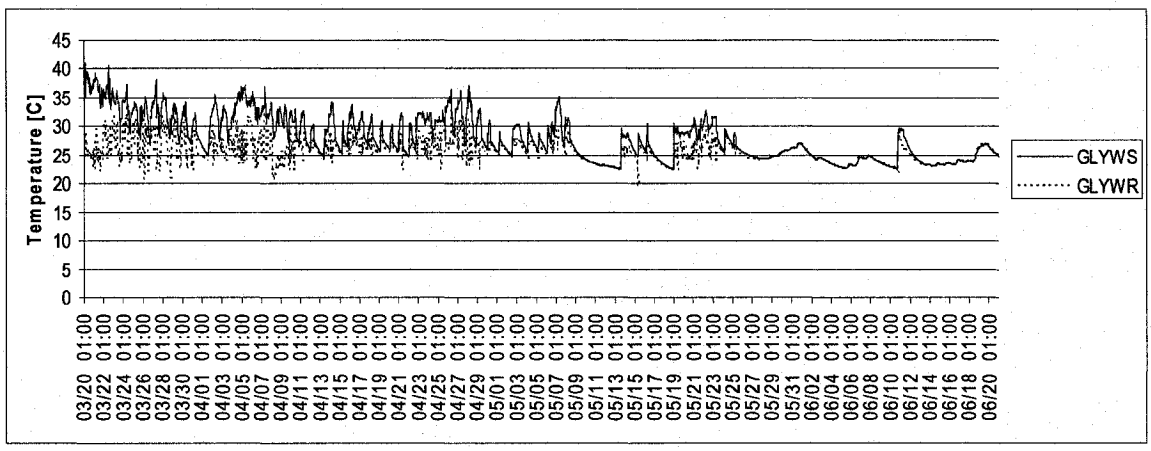

Figure 5.19: Glycol Water Temperature Variation for the Spring Season; Sectors B & C

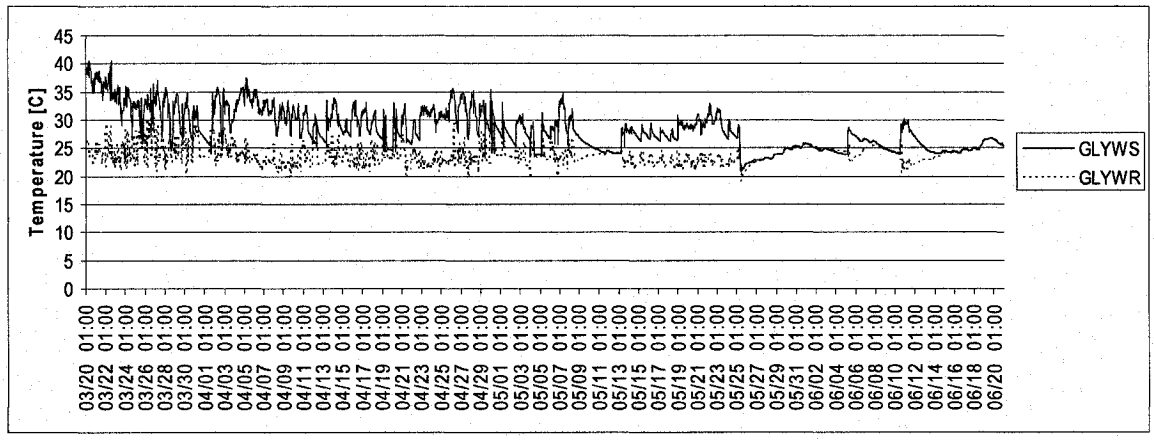

Figure 5.20: Glycol Water Temperature Variation for the Spring Season; Sector A

For sectors B and C, the glycol water temperature difference is close to zero for outdoor air temperatures above 10°C (Figure 5.21). Thus, the heating coils for sectors B and C are not operational at outdoor air temperatures above 10°C. Similarly, the cut-off temperature for the heating coils of sector A is 12°C (Figure 5.22). The higher outdoor air level for sector A explains the higher outdoor air temperature limit for the heating coils to be non-operational.

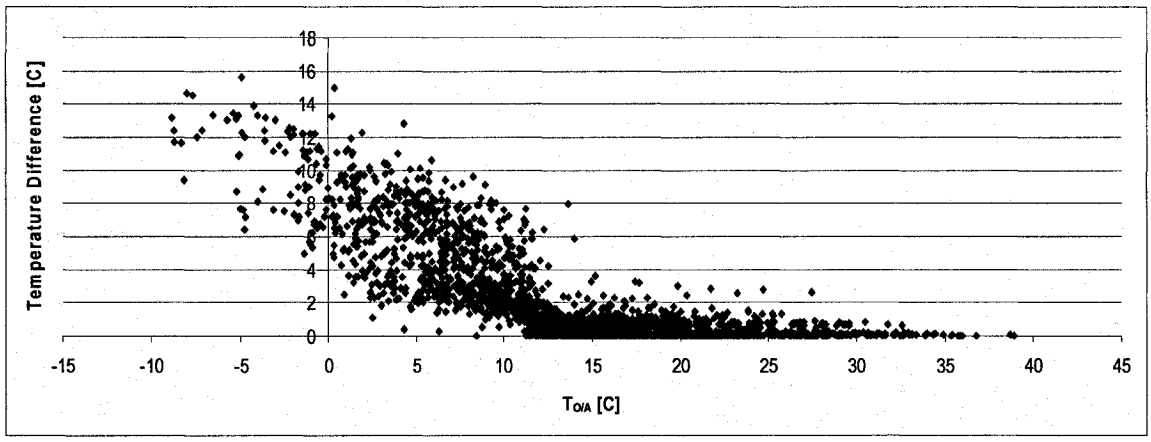

Figure 5.21: Glycol Temperature Difference versus Outdoor Air Temperature over the Spring Season; Sectors B and C

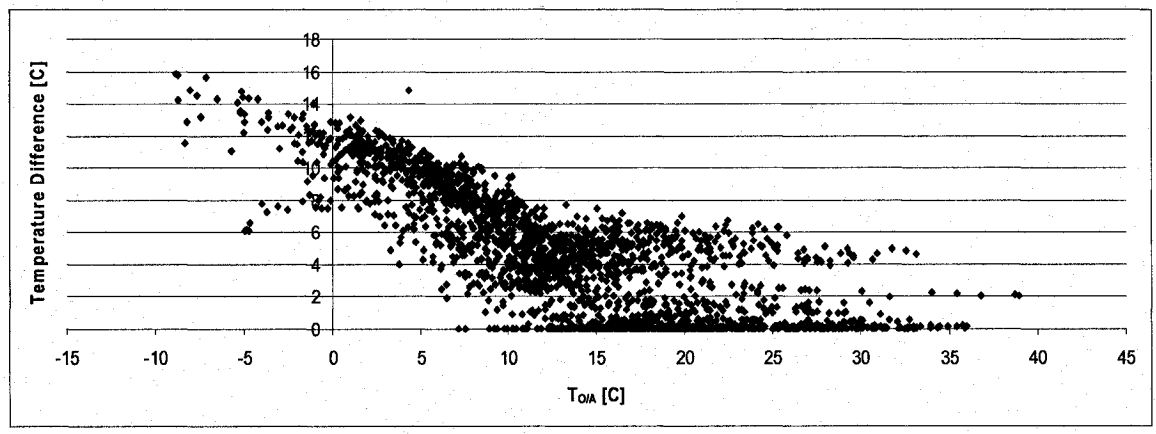

Figure 5.22: Glycol Temperature Difference versus Outdoor Air Temperature over the Spring Season; Sector A

5.3 Detailed Analysis of Monitored Data for Selected Weeks

In order to better understand the system operations, data monitored at smaller time steps for one week per month are presented. Weeks are starting on Mondays and ending on Sundays, thus the airflow for the last two days of the week is lower than during occupied hours. The airflow rates for all sectors are similar for all weeks (Figures 5.23, 5.28, 5.33 and 5.37). The air handling units are operating at higher capacity during occupied hours (9:00 to 22:00). During unoccupied hours – nights, week-ends and holidays – the airflow rates are reduced to around 70% of the occupied airflow rates for

sector A, and around 50% of the occupied airflow rates for sectors B and C. For all four weeks the variation of airflow rate is minimal, thus showing the limited impact the outdoor air temperature has on the system airflow rates.

5.3.1 March 20th to March 26th 2006

Measured data for the week of March 20th to the 26th 2006 are presented in Figures 5.23 to 5.27.

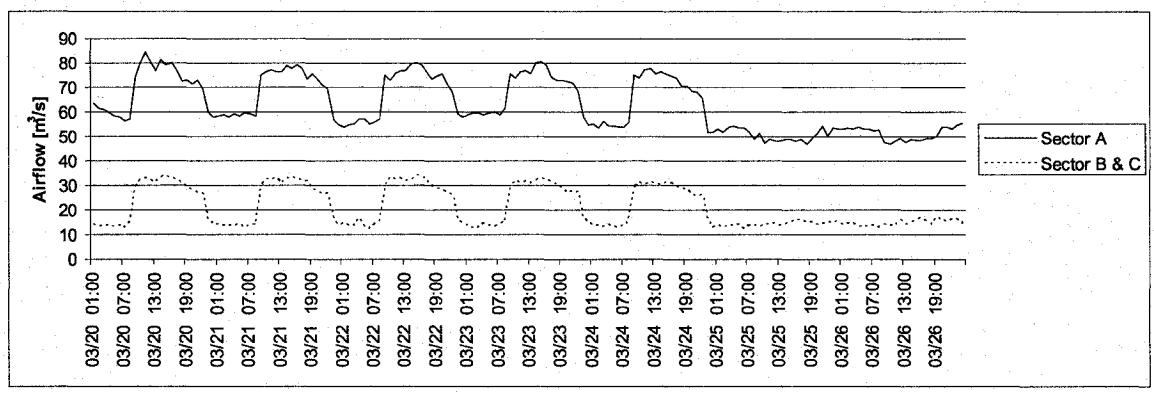

Figure 5.23: Airflow Variation for the Week of March 20th to March 26th

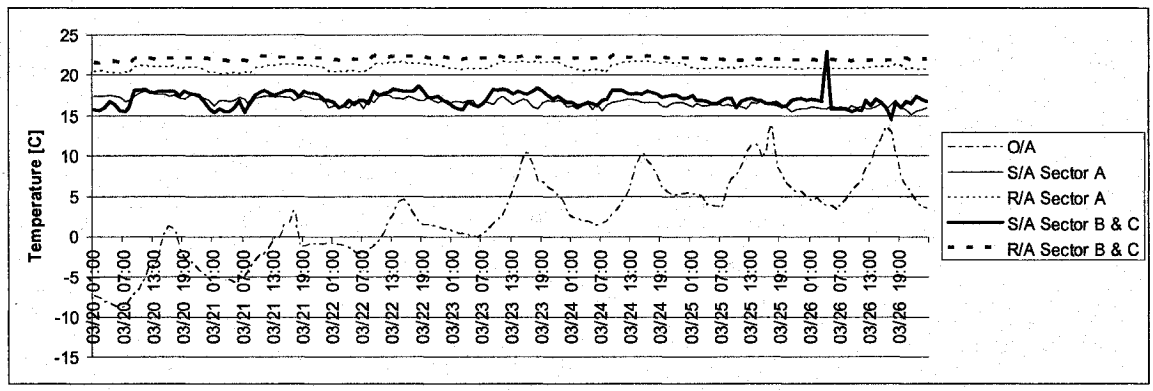

Figure 5.24: Air Temperature Variation for the Week of March 20th to March 26th

The outdoor air temperature is below the supply air temperature for the whole week. For all sectors, the supply air temperature is close to the design set point (Figure 5.24). The return air temperature is higher than the supply air temperature due to internal heat gains within each zone.

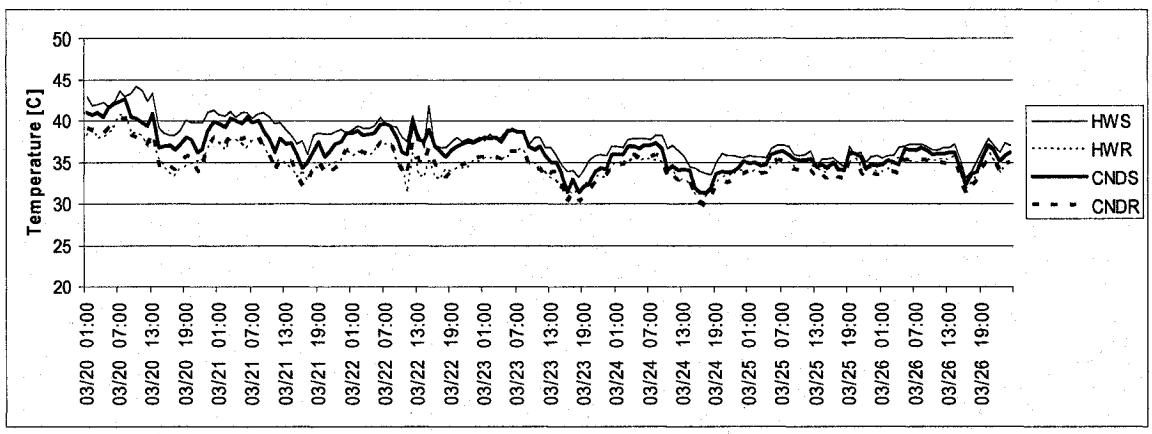

Figure 5.25: HW and CND Water Temperature Variation for the Week of March 20th to March 26th

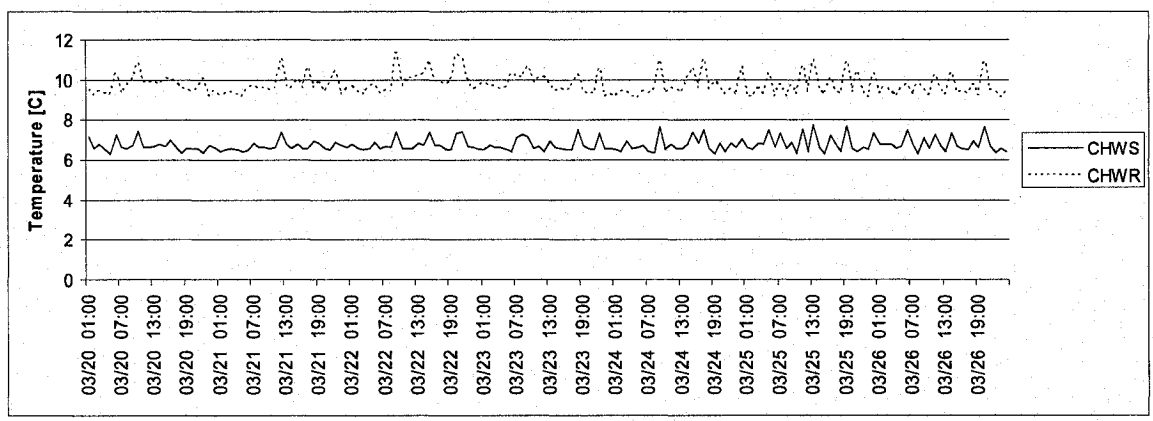

Figure 5.26: Chilled Water Temperature Variation for the Week of March 20th to March 26th

On the water side, the condenser water and the heating water temperatures are close to each other (Figure 5.25). Thus, the heating required for the re-heat coils is met by recuperating the heat from the condenser loop. The supply chilled water temperature is above the design set point of 5.6°C, while the return chilled water temperature is lower than the design set point (Figure 5.26). The heating coils located in sector A units are mainly operating at night time, while the ones located in sectors B and C units are not in operation, thus reducing the heating requirement for the whole building (Figure 5.27).

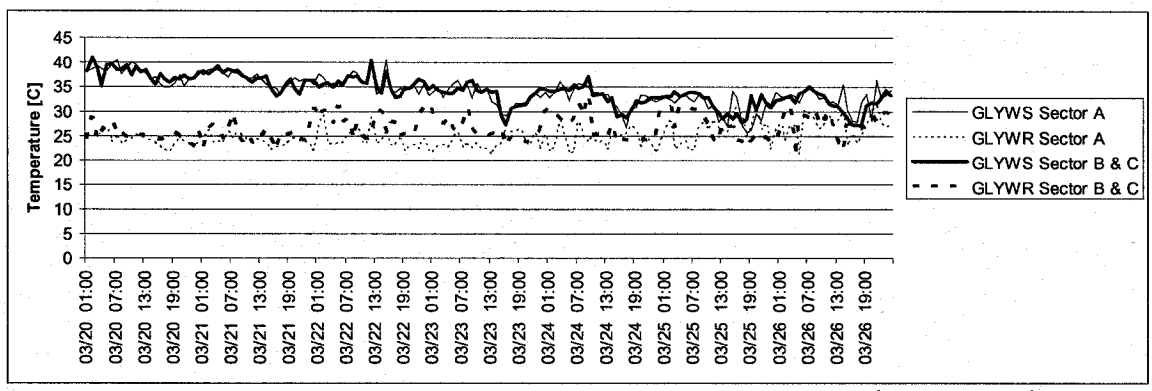

Figure 5.27: Glycol Temperature Variation for the Week of March 20th to March 26th

5.3.2 April 24th to April 30th 2006

Measured data for the week of April 24th to the 30th 2006 are presented in Figures 5.28 to 5.32.

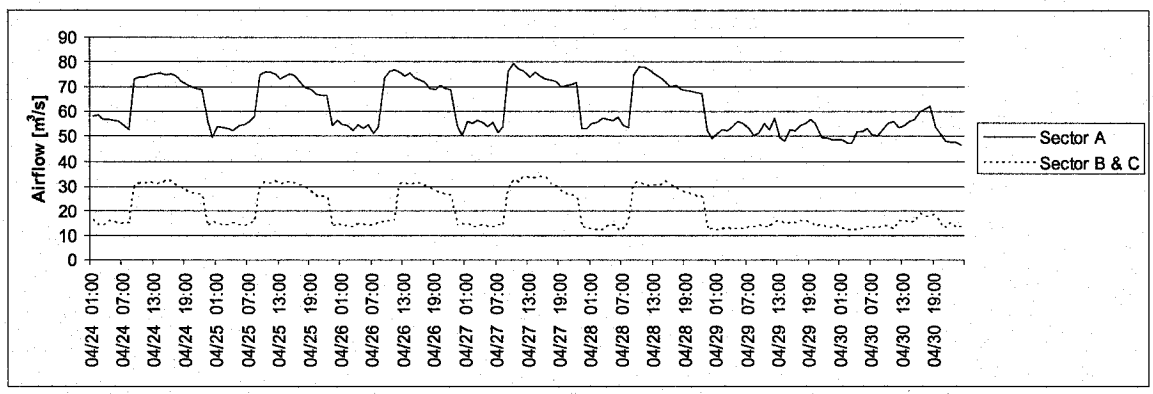

Figure 5.28: Airflow Variation for the Week of April 24th to April 30th

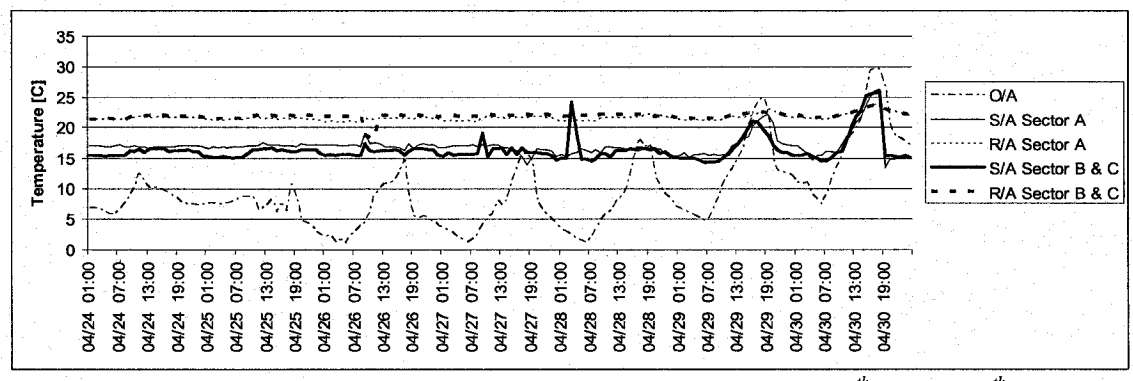

Figure 5.29: Air Temperature Variation for the Week of April 24th to April 30th

During the shown period, chillers CH-1 and CH-2 are not in operation and thus the cooling coils of the air handling units are not operational. When the outdoor air

temperatures are below 24°C, the air handling units work under economizer mode, and the outdoor air is directly introduced to the building. Therefore, for outdoor air temperatures above 16°C, the supply air temperature is close to the outdoor air temperature, supporting the assumption that the cooling coils are not in operation for that period (Figure 5.29). For instance, this occurs on April 29th between 13:00 and 19:00. The return air temperature is relatively constant throughout the week at 22°C.

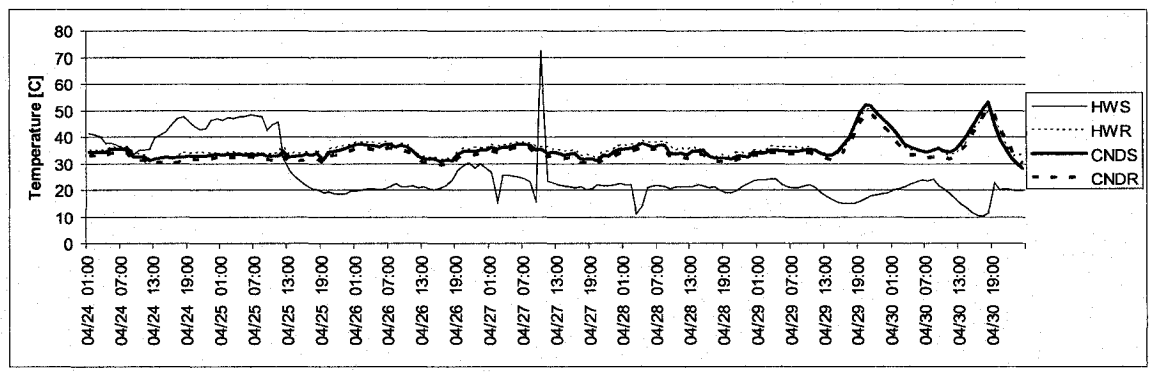

Figure 5.30: HW and CND Water Temperature Variation for the Week of April 24th to April 30th

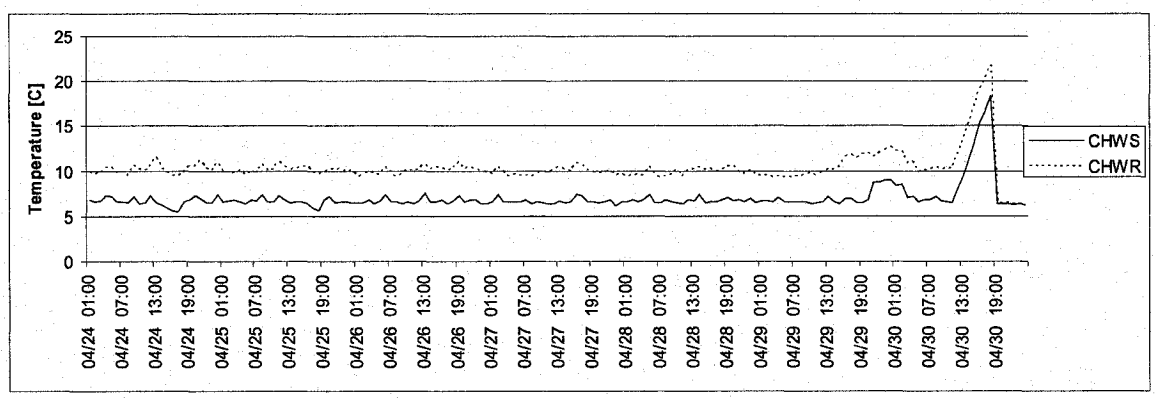

Figure 5.31: Chilled Water Temperature Variation for the Week of April 24th to April 30th

On the water side, the heating water temperatures fluctuate throughout the week (Figure 5.30). The condenser water temperature is not sufficient to meet the re-heat coils loads, and thus additional heating is provided to the heating water loop. The chilled water supply temperature is around 6°C, which is close to the design set point, while the

chilled water return temperature is around 10°C (Figure 5.31). From April 24th to the 30th, there is a water temperature difference on the sector A glycol loop, thus the heating coils for that sector are in operation most of the time, while the one located in sectors B and C units are not. Sectors B and C glycol water supply and return temperatures are almost identical. Sector A has higher outdoor air requirements; therefore, the mixed air temperature of sector A is below the supply air set point more frequently than in sectors B and C, thus inducing a heating load (Figure 5.32).

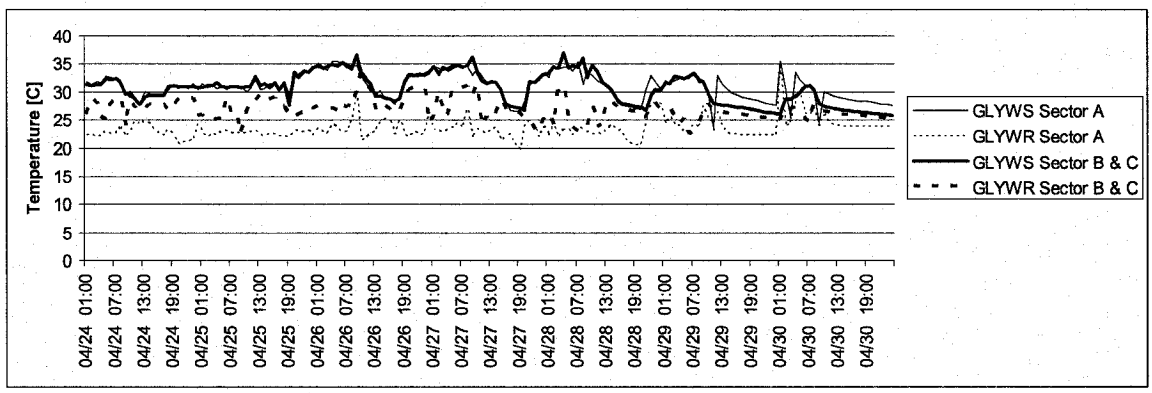

Figure 5.32: Glycol Temperature Variation for the Week of April 24th to April 30th

5.3.3 May 15th to May 21st 2006

Measured data for the week of May 15th to the 21st 2006 are presented in Figures 5.33 to 5.36.

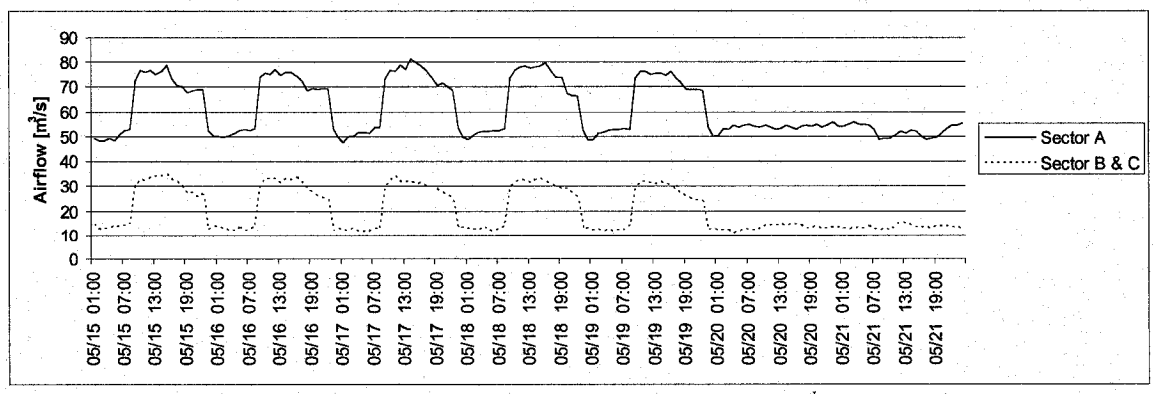

Figure 5.33: Airflow Variation for the Week of May 15th to May 21st

For the month of May, chillers CH-1 and CH-2 are in operation and thus the supply air temperature is close to the design set point (Figure 5.34). The return air temperature is relatively constant throughout the week.

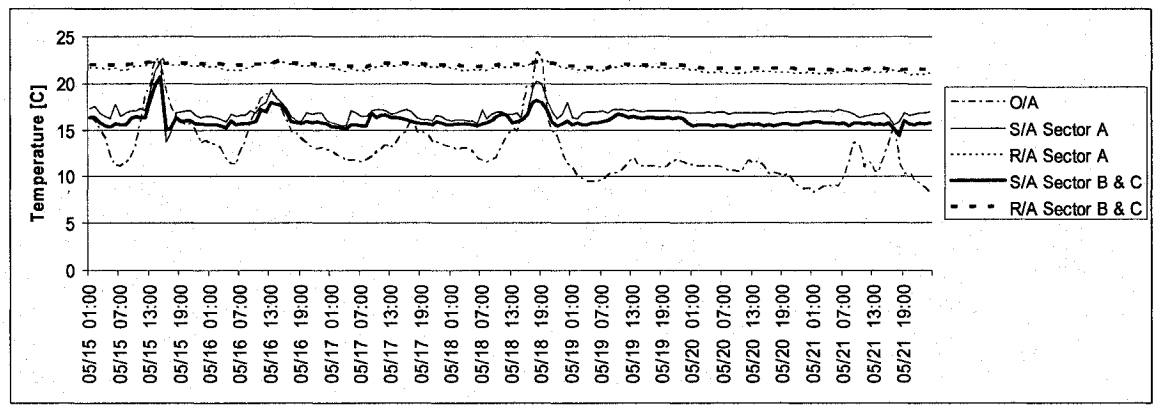

Figure 5.34: Air Temperature Variation for the Week of May 15th to May 21st

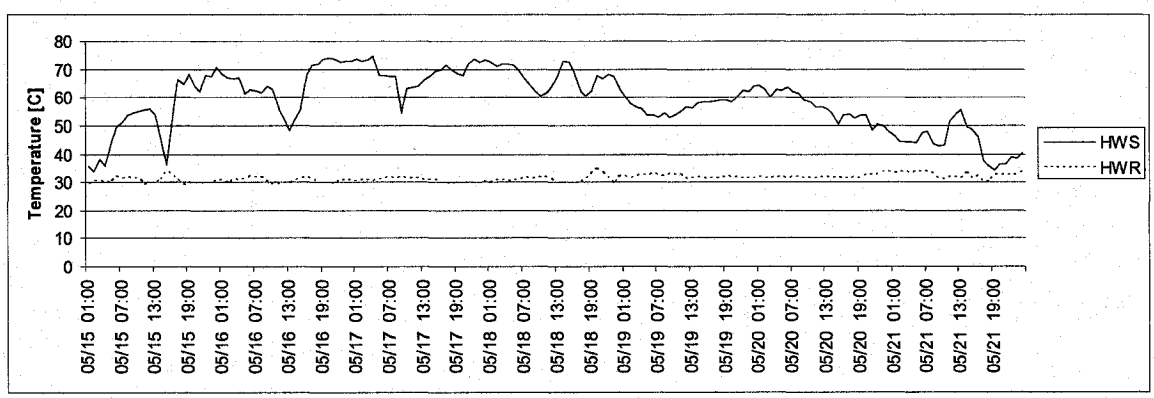

Figure 5.35: Water Temperature Variation for the Week of May 15th to May 21st

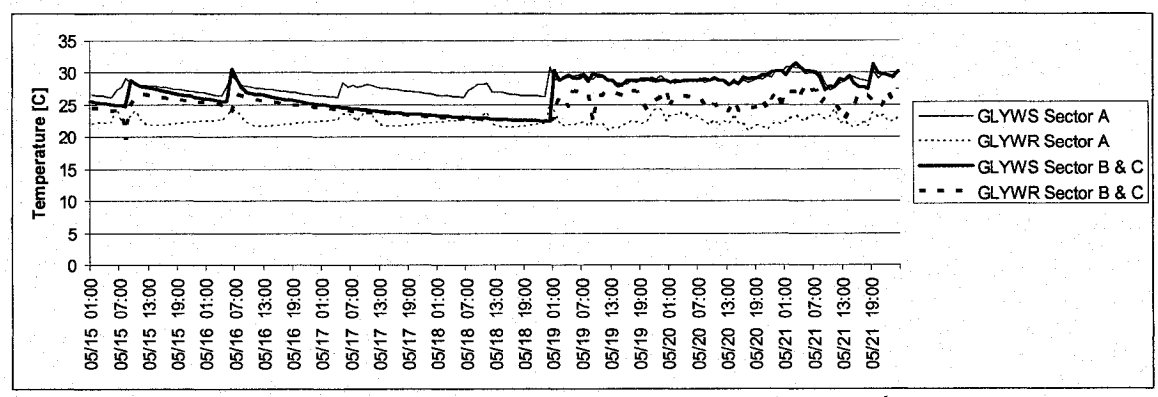

Figure 5.36: Glycol Temperature Variation for the Week of May 15th to May 21st

On the water side, the heating water supply (HWS) temperature fluctuates throughout the week, while the heating water return (HWR) temperatures is around 30°C (Figure 5.35). No heating is required at the air handling units of sectors B and C (Figure 5.36). In sector A, when the outdoor air temperature is lower than 12°C, heating is required at the air handling units (Figure 5.36).

5.3.4 June 12th to June 18th 2006

Measured data for the week of June 12th to the 18th 2006 are presented in Figures 5.37 to 5.39.

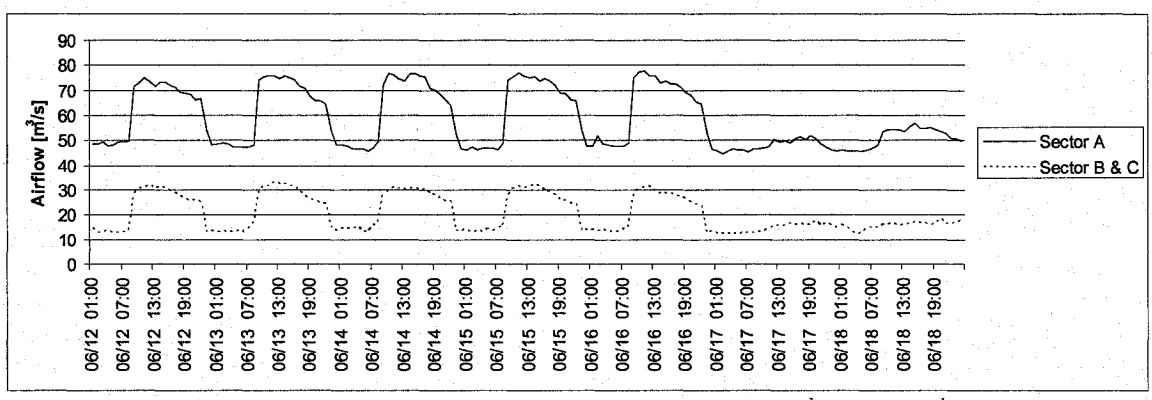

Figure 5.37: Airflow Variation for the Week of June 12th to June 18th

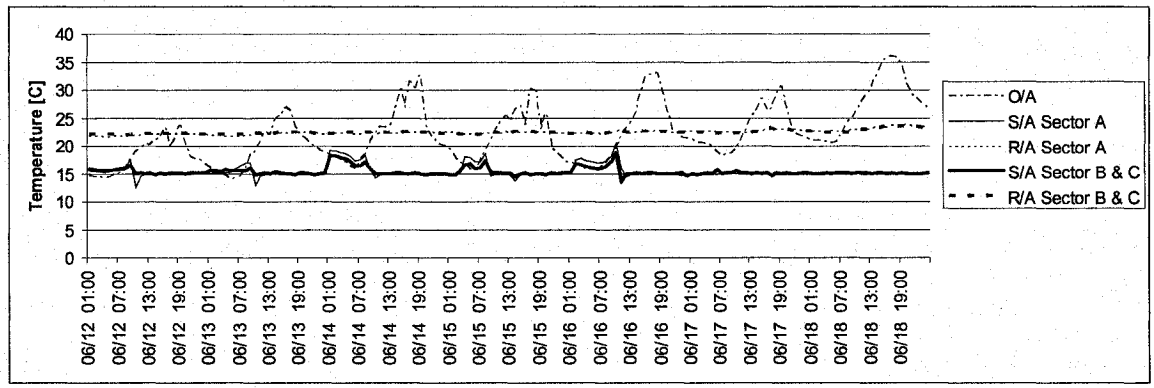

Figure 5.38: Air Temperature Variation for the Week of June 12th to June 18th

In June, chillers CH-1 and CH-2 are in operation and consequently the supply air temperature is close to the design set point (Figure 5.38). The return air temperature is relatively constant throughout the week.

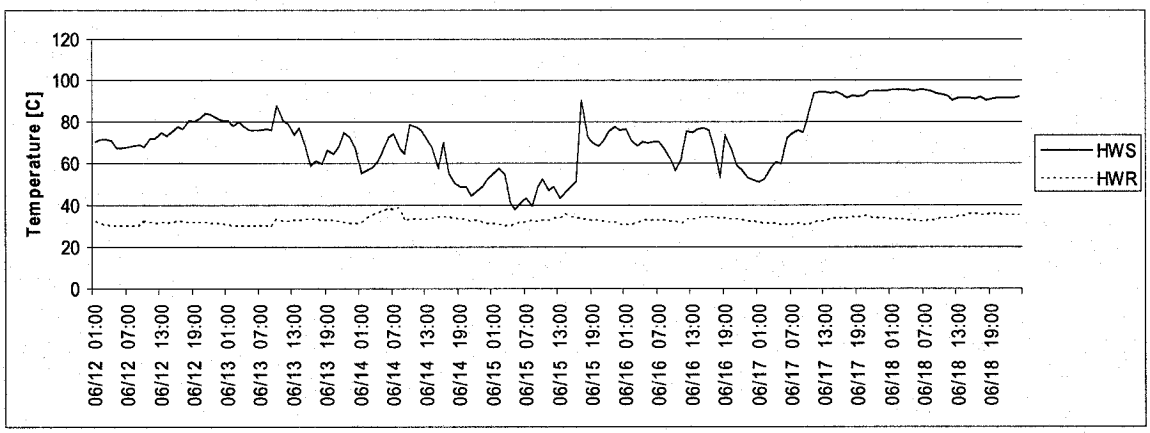

Figure 5.39: Water Temperature Variation for the Week of June 12th to June 18th

In June, the outdoor air temperature is above the supply air temperature (Figure 5.38), and the heating coils located in the air handling units are not operational. The heating water supply (HWS) temperature fluctuates throughout the week, while the heating water return (HWR) temperature is around 30°C (Figure 5.39).

5.4 Summary

- For sectors B and C, the average airflow rate during the occupied period is 30.0 m^3/s and the average airflow rate during the unoccupied period is 14.0 m^3/s. The supply fans work on average at 40% of total capacity during occupied period, and during unoccupied period at 18.5% of capacity. During the spring season, the maximum supply airflow rate is 50% of the fans capacity.
- For sector A, the average airflow rate during the occupied period is 73.5 m^3/s and the average airflow rate during the unoccupied period is 52.0 m^3/s. During occupied

period, the supply fans work on average at 50% of total capacity, and during unoccupied period at 35% of capacity. During the spring season, the maximum supply airflow rate is 60% of the fans capacity.

- For all sectors, the supply air temperature is maintained constant at all time, around 16°C during the spring season, while the airflow rate varies depending on the level of occupancy in the building. For sector A, the airflow rate during unoccupied period is 70% of the occupied airflow rate. For sectors B and C, the unoccupied to occupied airflow rate ratio is 46%.
- The supply airflow rate does not significantly vary with the variation of outdoor air temperature; hence, one can conclude that the heating/cooling load due to heat losses/gains through the exterior envelope are smaller compared to the building internal gains.
- For all sectors, the return air temperature is around 22°C for all hours of the day. Constant return air temperature implies no setback or setup on the room temperature set point.
- Chillers CH-1 and CH-2 enter into operation on May 4th. Based on the monitored data, it seems that the cooling coils installed in the air handling units are not in operation before this date. Consequently, from March 20th to May 4th, the supply air temperature is above the supply air set point when the outdoor air temperature is above 16°C, which is the design supply air temperature.
- Over the spring season, the condenser water temperature of chiller CH-3 (or chiller CH-4, which ever is operational) and the heating water supply temperature closely

correspond. The temperature of the heat recovery loop is adequate to meet the required supply heating water temperature of the re-heat coils.

- The glycol water temperature difference is close to zero for outdoor air temperatures above 10°C for sectors B and C, and for temperatures above 12°C for sector A. Thus, for outdoor air temperatures above the specified values, the heating coils located in the air handling units are not in operation.

6. COMPUTER MODEL CALIBRATION

Information about the as-built and as-operated thermal performance of the Sciences building is obtained from the Monitoring and Data Acquisition System through the collaboration of the Physical Plant of Concordia University. Data collected from that system are compared with simulation results. The model is calibrated over the spring season, from March 20th to June 20th. Since the annual or daily electrical and/or gas consumption information are not available, comparison is performed in terms of supply airflow rates, and supply and return air temperatures.

6.1 Comparison with Monitored Data

The outdoor air dry-bulb temperature variations over the month of May are presented in Chapter 5 (Figure 5.1). The monitored outdoor air temperature is greater than the average Typical Meteorological Year (TMY) value measured at the airport. These differences may affect calculations of the heating and cooling loads, and the economizer systems operation for the calibration period.

Therefore, the weather file, which uses TMY weather format, is modified to reflect the on-site conditions for the calibrated period. For all days, the dry-bulb temperature in the original weather file is replaced by the outdoor air temperature measured on site, while the relative humidity is kept as per the original weather file. However, when the psychometric calculations give state of moist air with more than 100% relative humidity, the program calculations do not converge. Hence, for those particular hours, the relative humidity and the atmospheric pressure are modified based

on hourly data collected by Environment Canada at the Montréal Pierre-Elliott-Trudeau airport. Figure 6.1 shows the revised dry-bulb outdoor air temperature for the month of May.

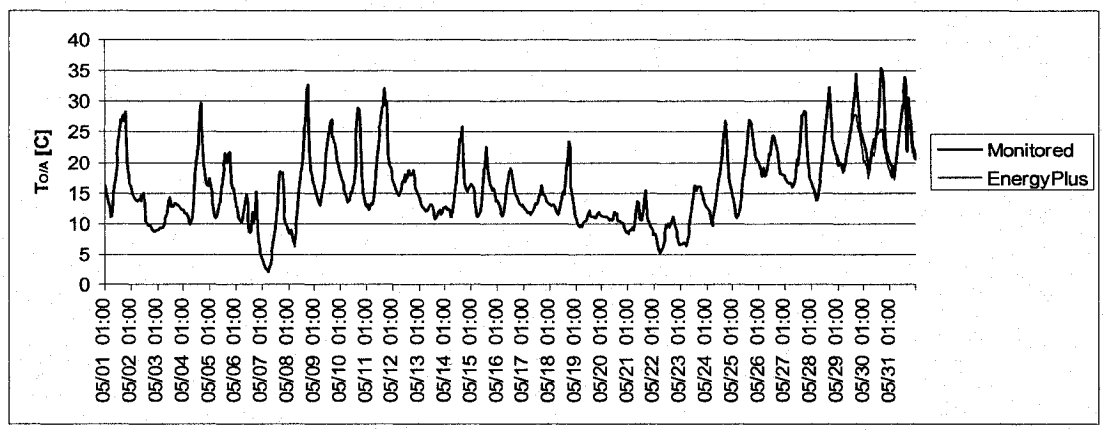

Figure 6.1: Revised Outdoor Air Temperature for the Month of May

The calibration analysis is performed over the spring season, which is from March 20th to June 20th. The analysis is performed over two intervals: (1) period A, from May 4th to June 20th, when the mechanical cooling system is in operation, and (2) period B, from March 20th to May 4th, which corresponds to the heating and shoulder portion of the spring season, when the mechanical cooling is not in operation.

6.1.1 Analysis of Period A

The monitored data revealed that the cooling coils located within the air handling units are operational from May 4th to June 20th. Data are analyzed for most of the month of May and June for all sectors.

6.1.1.1 Sectors B & C

The initial input file is prepared using information collected from the original CBIP file. In this file, the zone summer temperature set point is 24°C during occupancy and 35°C at night, while during winter, the zone set point is 22°C during occupancy and

18°C at night time. All temperature set points (heating, chilled, condenser and glycol water) are entered based on the design specifications. Figure 6.2 shows the variation of supply airflow rate that is required to satisfy the cooling load of sectors B and C.

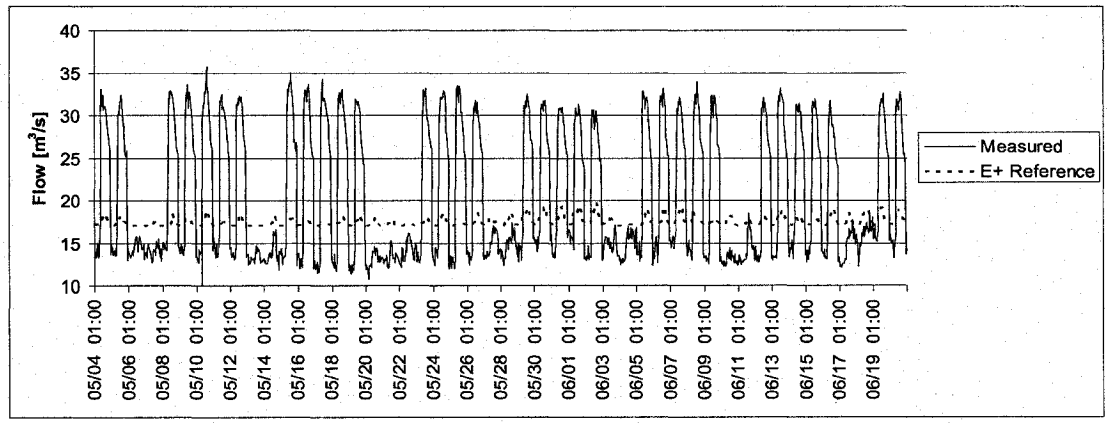

Figure 6.2: Airflow Rate Variation from May 4th to June 20th; Sectors B & C

There is no significant variation of the predicted supply airflow rates, while the minimum airflow rate is higher than the measured values. The underprediction of the supply airflow rate may be explained by the fact that the airflow rate supply to compensate for the laboratories exhaust air is not included in the input file.

The supply and return air temperatures are also compared (Figure 6.3). For sectors B and C, the supply air temperature is set to 16 °C in EnergyPlus. A similar value is measured in the actual building (15.6°C ± 1.0°C). The return air temperature is overestimated in EnergyPlus, which could be explained by the assumption of the presence of set back/up temperature that was used in the EnergyPlus file.

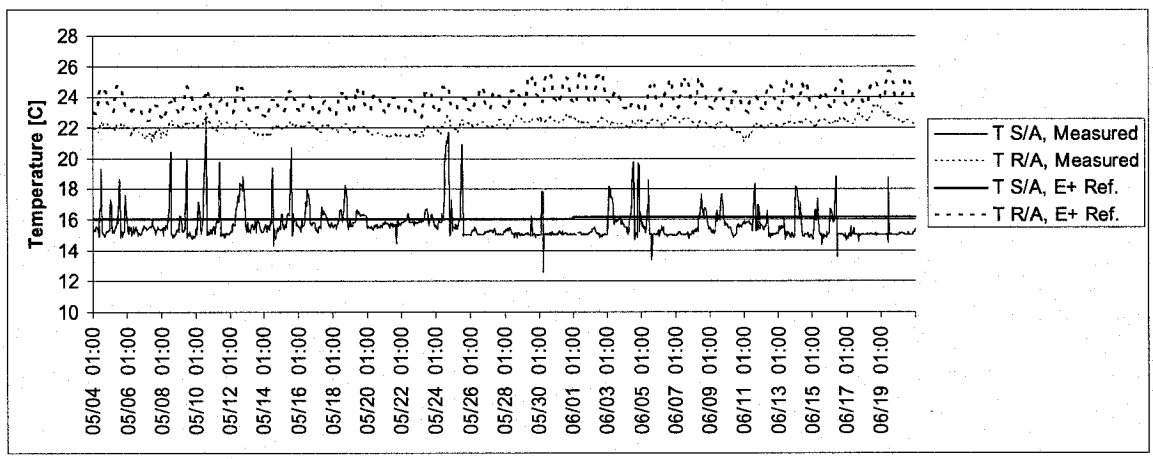

Figure 6.3: Air Temperature Variation from May 4th to June 20th; Sectors B & C

To improve the model, the input file is modified to reflect the actual building behaviour. Thus, the assumption about the space set back/up temperature is removed, and replaced by a constant set point temperature (22°C for heating and 24°C for cooling). The water temperatures are adjusted to match the building operating conditions (refer to Chapters 4 and 5 for design and measured values). The minimum supply airflow rate is also modified to match the minimum supply airflow rate for sectors B and C, which is approximately 20% of the maximum supply airflow rate measured over the spring season. Figures 6.4 and 6.5 present the predicted air temperatures and supply airflow rate based on the modified input file.

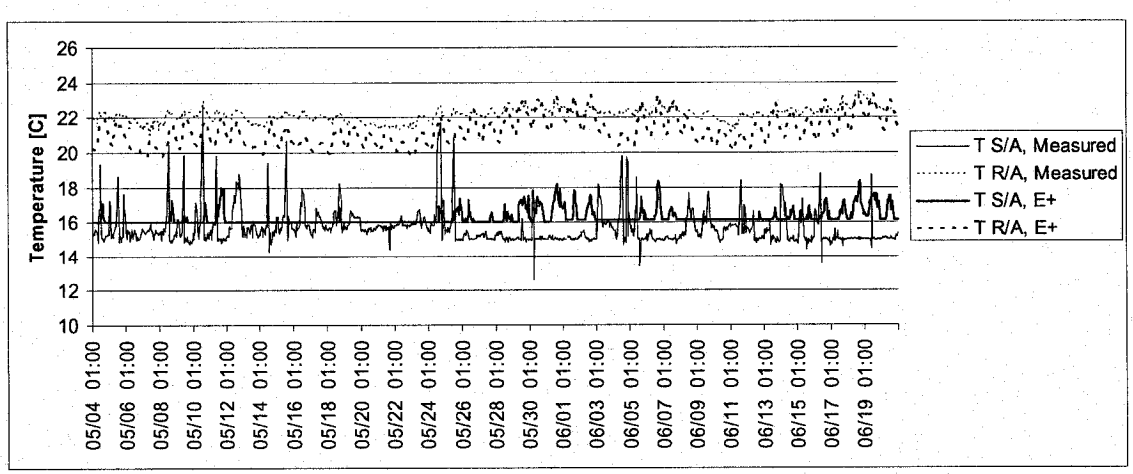

Figure 6.4: Revised Air Temperature Variation from May 4th to June 20th; Sectors B & C

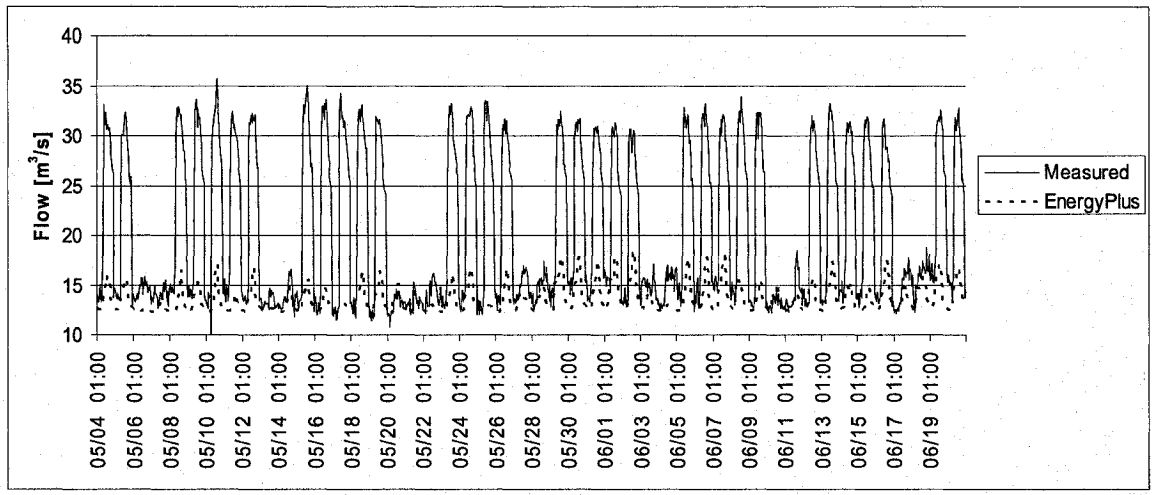

Figure 6.5: Revised Airflow Rate Variation from May 4th to June 20th; Sectors B & C

On the air-side, the revised simulated air temperatures are closer to the monitored data (Figure 6.4). The average measured return air temperature is 22.1°C, while the average predicted value is 23.1°C. On the supply air side, the average measured and predicted air temperatures are both close to 15.6°C.

In terms of supply airflow rates, the measured and predicted values show similar trend. However, during occupied hours, the simulated results are much lower. During the unoccupied period, the supply airflow rate is close to the monitored values (Figure 6.5). The supply airflow rate calculated by the EnergyPlus program corresponds to the space cooling/heating loads. Since the laboratories exhaust airflow rate is not included in the EnergyPlus model, the additional airflow rate must be added to the simulation results. The additional airflow, which is required to accommodate all exhaust hoods located in sector C, is 18.5 m^3/s when considering the coefficient of simultaneous usage (refer to Chapter 5). Hence, the airflow rate of 18.5 m^3/s is added to the results obtained using EnergyPlus during the occupied period (Figure 6.6).

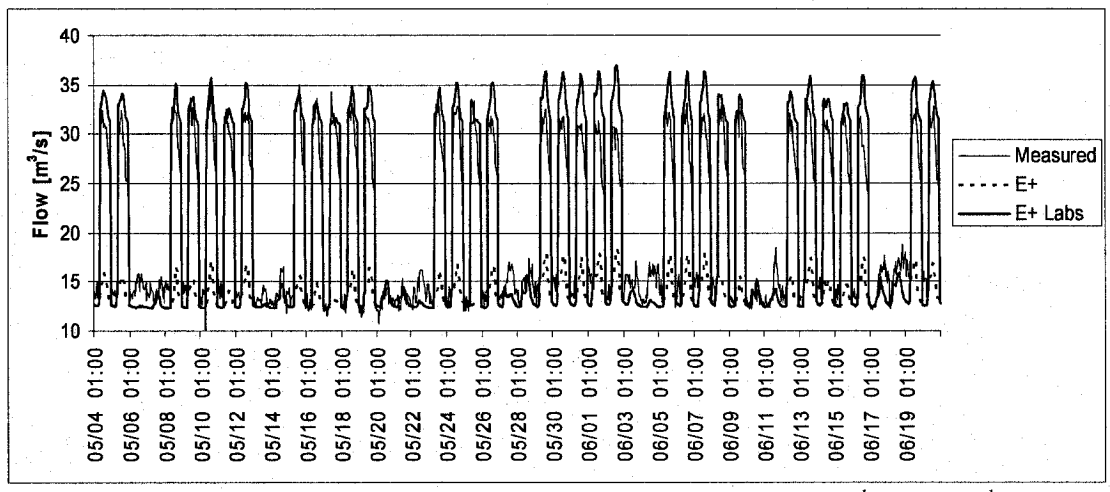

Figure 6.6: Supply Airflow Rate including Laboratories Requirements from May 4th to June 20th; Sectors B & C

The addition of the exhaust requirements for the laboratories hoods reduces the difference between the simulated results and the monitored data.

The comparison of sector air-side thermal loads is a good indication if the simulation results are in agreement with the measured data. By assuming that the latent loads are negligible, the whole building (sector) air-side thermal loads are estimated as follows:

$$Q_{Sector} = V_a \cdot \rho_a \cdot C_{p,a} \cdot (T_{R/A} - T_{S/A}) \qquad (5.2)$$

where

Q_{Sector} is the sector load [kW];

V_a is the measured airflow rate for each sector [m^3/s];

ρ_a is the density of air, $\rho_a = 1.169$ kg/m^3;

$C_{p,a}$ is the specific heat of air, $C_{p,a} = 1.004$ kJ/kg · K;

$T_{R/A}$ is the weighted average return air temperature [°C];

$T_{S/A}$ is the weighted average supply air temperature [°C].

The building is completed with a heat recovery system on the exhaust air. From the design specification, the heat recovery efficiency (HRE) of the system is estimated to be approximately 40%. The additional thermal load due to the outdoor air requirements for the laboratory hoods is calculated using equation (6.2).

$$Q^*_{Sector} = Q_{Sector,\ hoods} \cdot (1 - HRE) \qquad (6.2)$$

where

Q^*_{Sector} is the additional thermal load due to the ventilation air for laboratories requirements if the heat recovery is counted for [kW];

$Q_{Sector,\ hoods}$ is the thermal load calculated using the outdoor air airflow rate and equation (6.1) [kW];

HRE is the efficiency of the heat recovery system installed on the exhaust stream.

The total sector thermal load is calculated as the sum of Q_{Sector} (equation 6.1) and Q^*_{Sector} (equation 6.2) for measured data and is compared with the estimated thermal load from the EnergyPlus program (Figure 6.7). The total estimated thermal load, including the laboratories load, show similar trend with the thermal load calculated from measured data. For sectors B and C, the average measured load is 155 ± 67 kW, while the average estimated load is 160 ± 64 kW. The relative error is 3.5% between both sets of data. Therefore, the measured and estimated thermal loads are in agreement.

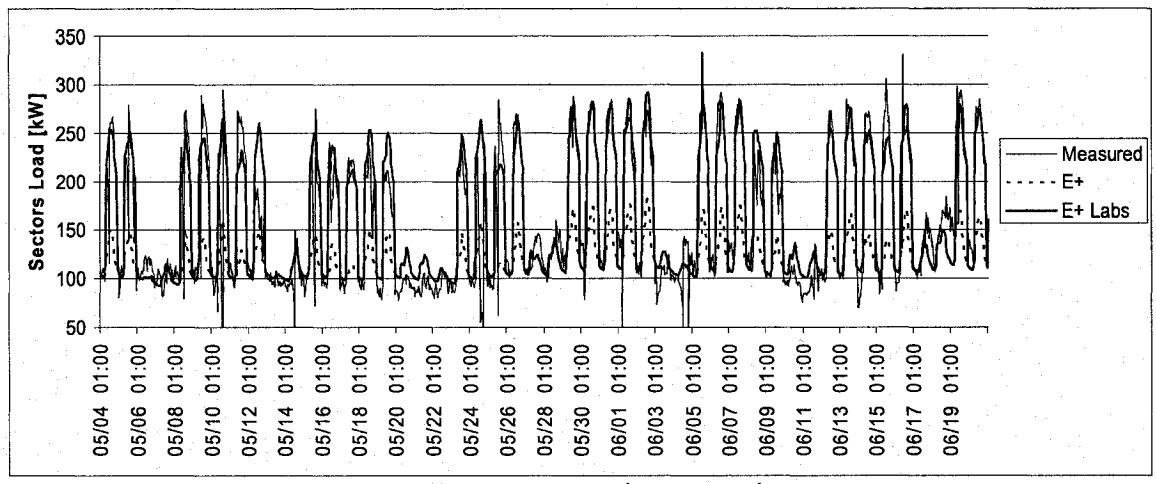

Figure 6.7: Sector Load from May 4th to June 20th; Sectors B & C

The estimated thermal load calculated on the air-side using equations (6.1) and (6.2) is also compared to the summation of all the zone thermal loads and the cooling coil load estimated by EnergyPlus. The calculated sector thermal load varies between 90 and 180 kW (Figure 6.8), while the summation of all the zone thermal loads estimated by EnergyPlus varies between 60 and 180 kW (Figure 6.9). The distribution pattern shows a similar trend for both sets of data: the load increases with the increase in outdoor air temperature.

The cooling coil load also increases with the increase in outdoor air temperature for temperatures above 16°C, which is the design supply air temperature for the system (Figure 6.10). For outdoor air temperatures below 16°C, the cooling coil is not operational. At outdoor air temperatures between 22°C and 24°C, some points are outside the linear pattern noticed for increase in outdoor air temperature. At those air temperatures, the system is still working under economizer mode, i.e. the system uses a 100% outside air, and thus the cooling requirements are higher. At outdoor air temperatures above 24°C, the level of fresh air is set to the minimum requirement and the

cooling coil load (~ 250 kW) is close to the sector thermal load (Figure 6.8) and zones thermal load (Figure 6.9). The closeness of the results for the estimated thermal loads, the summation of the zone thermal loads and the cooling coil load shows that EnergyPlus results are plausible.

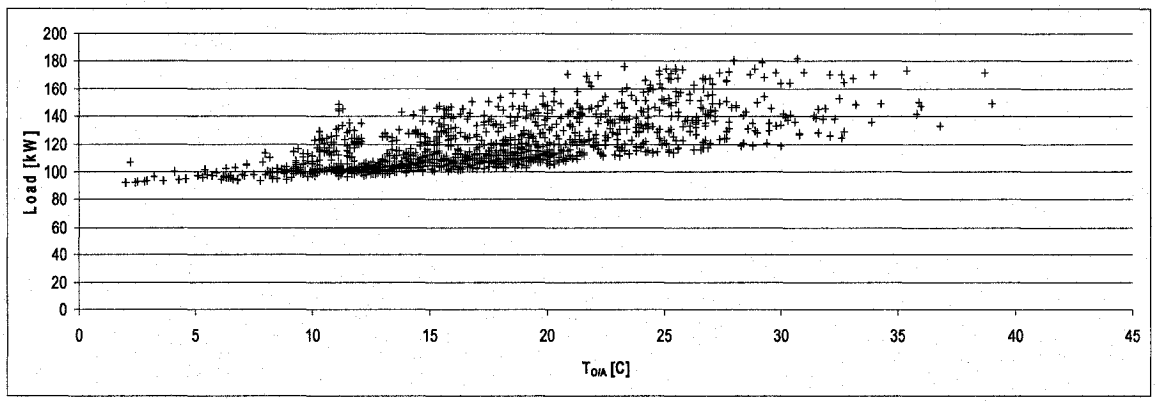

Figure 6.8: Estimated Sector Air-Side Thermal Load versus Outdoor Air Temperature from May 4th to June 20th; Sectors B & C

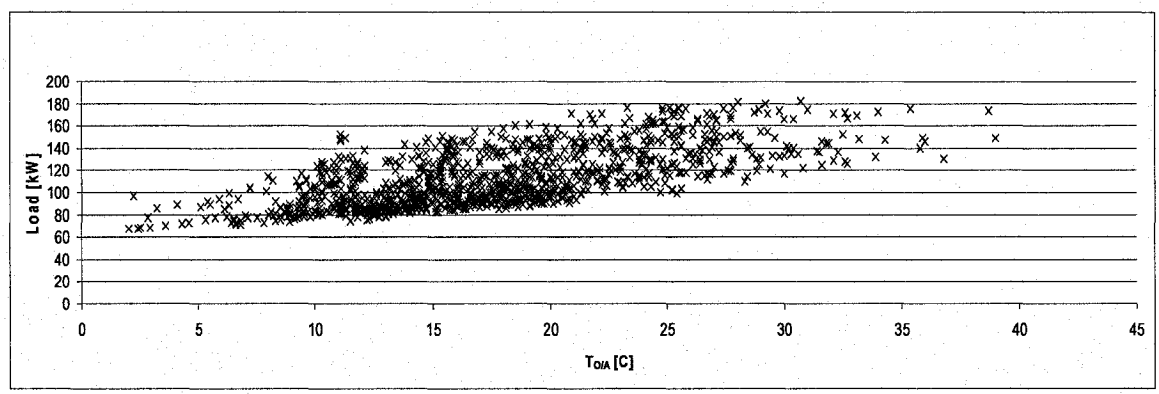

Figure 6.9: Estimated Zone Thermal Load of all Zones versus Outdoor Air Temperature from May 4th to June 20th; Sectors B & C

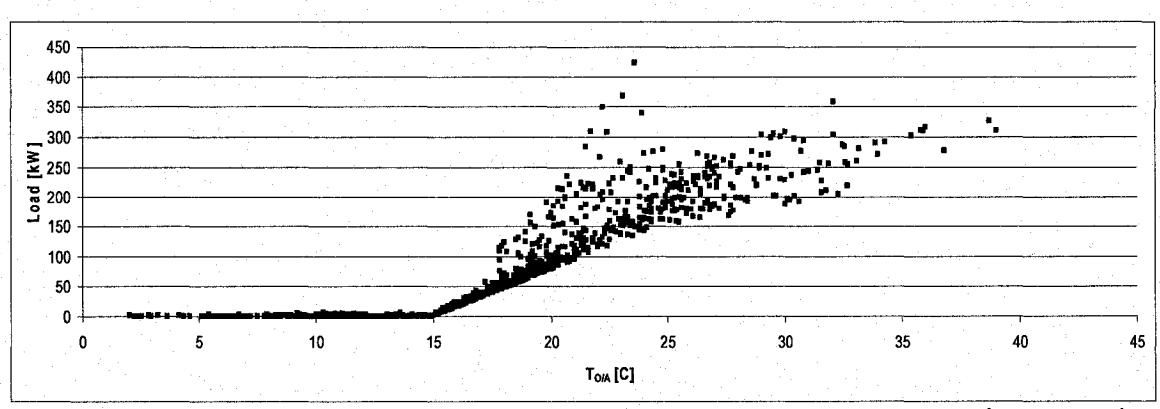

Figure 6.10: Estimated Cooling Coil Load versus Outdoor Air Temperature from May 4th to June 20th; Sectors B & C

6.1.1.2 Sector A

Similarly, for sector A, the initial input file is prepared using information collected from the original CBIP file. All temperature set points (heating, chilled, condenser and glycol water) are entered based on the design specifications. Figure 6.11 shows the airflow rate variation for the cooling portion of the analysis as obtained using the initial input file. The variation in airflow rates is much lower in EnergyPlus, but a similar trend is noticed over the shown period. The underprediction of the supply airflow rate may be explained by the absence of the laboratories exhaust air requirement in the input file.

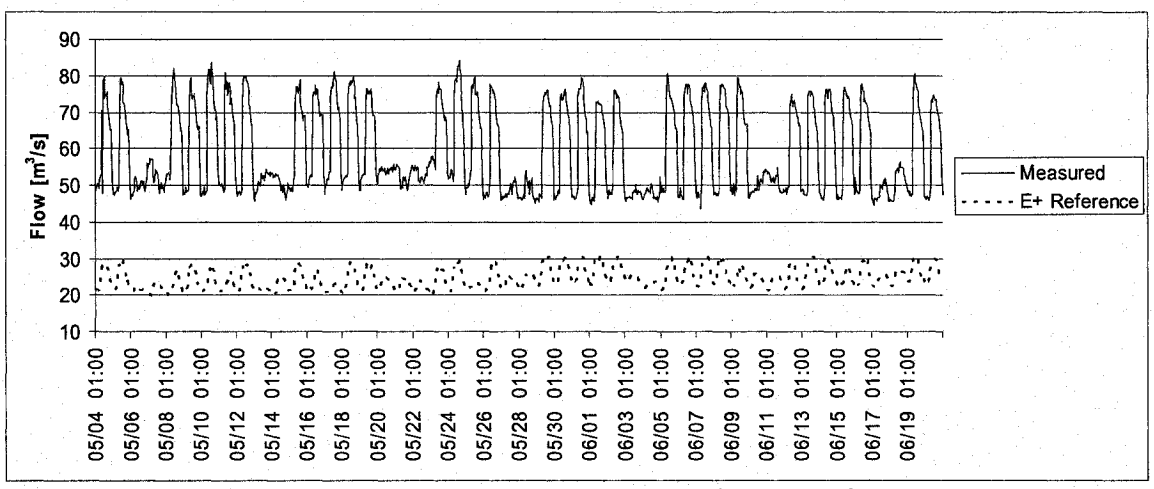

Figure 6.11: Airflow Rate Variation from May 4th to June 20th; Sector A

The supply and return air temperatures are also compared (Figure 6.12). For sector A, the supply air temperature is set to 16°C in EnergyPlus. A similar value is measured in the actual building (15.9 ± 0.4°C). The return air temperature is overestimated in EnergyPlus over 24 hours, which could be explained by the assumption of the presence of set back/up temperature that was used in the EnergyPlus input file.

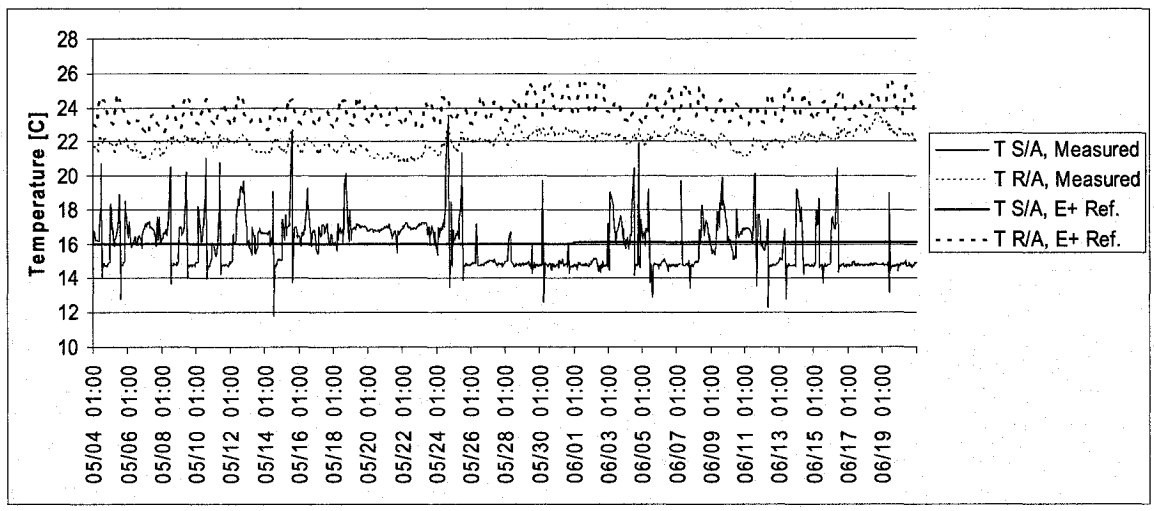

Figure 6.12: Air Temperature Variation from May 4th to June 20th; Sector A

To improve the model, the input file is modified to reflect the actual building behaviour. Thus, the assumption about the space set back/up is removed and replaced by a constant set point temperature (22°C for heating and 24°C for cooling) and the water temperatures are adjusted to match the building operating conditions (refers to chapters 4 and 5 for design and measured values). The minimum supply airflow rate is also modified to include the continuous exhaust required for some of the laboratories. The additional minimum airflow required to accommodate the continuous exhaust rate in sector A is calculated based on the design specifications of the Variable Air Volume (VAV) units installed on the ventilation hoods. The total airflow for continuous exhaust is 17.0 m^3/s. Hence, a minimum airflow rate of 17.0 m^3/s is included in the input file. Figures 6.13 and 6.14 present the predicted air temperatures and supply airflow rate variation based on the modified input file.

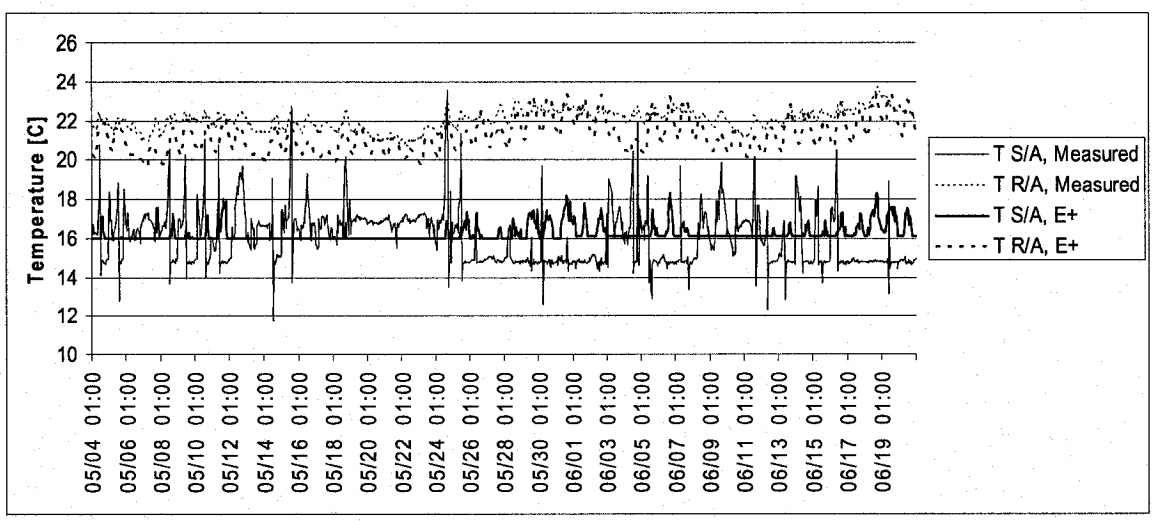

Figure 6.13: Revised Air Temperature Variation from May 4th to June 20th; Sector A

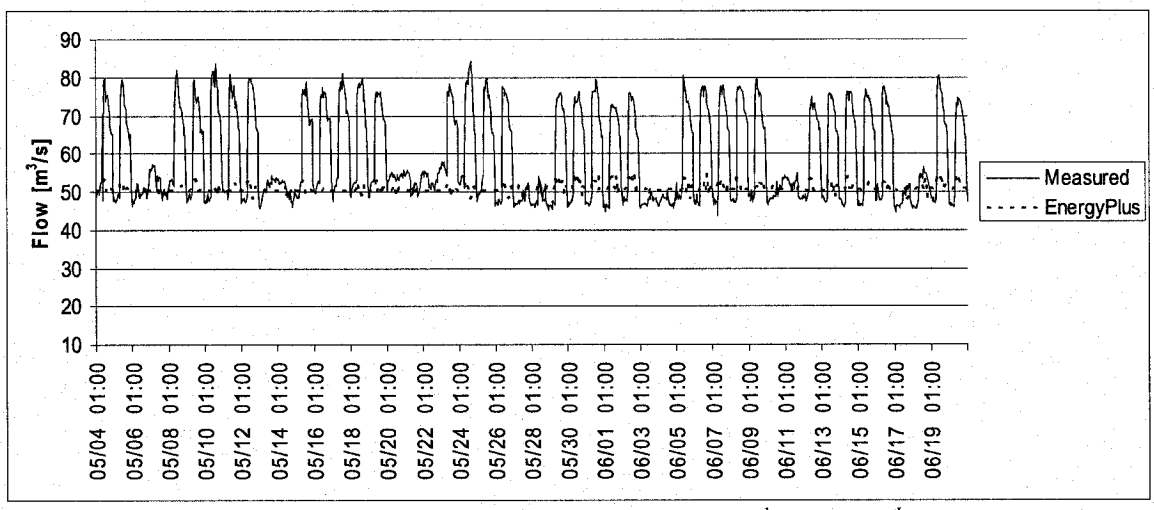

Figure 6.14: Revised Airflow Rate Variation from May 4th to June 20th; Sector A

On the air-side, the revised simulated air temperatures are close to the monitored information (Figure 6.13). Based on the average return air temperature for the shown period, the measured value is 22.0 °C, while the predicted value is 21.2°C. For the supply air temperature, the average measured temperature is 15.9°C, while the predicted temperature is 16.2°C.

In terms of supply airflow rates, the measured and predicted values show similar trend. However, during the occupied hour, the simulated results are much lower. During the unoccupied period, the supply airflow rate is close to the monitored values (Figure 6.14). The supply airflow rate calculated by the EnergyPlus program corresponds to the space cooling/heating loads. The laboratories exhaust airflow rates are not included in the EnergyPlus model, thus the additional airflow rate must be added to the simulated results. By considering the coefficient of simultaneous usage, the airflow required by the hoods is 45.5 m^3/s. A continuous minimum exhaust airflow rate of 17.0 m^3/s has already been included in the input file, thus the additional airflow rate required is the difference between the airflow rates calculated using the diversity factor and the minimum exhaust flow rate. Hence, the airflow rate of 28.5 m^3/s is added to the results obtained using EnergyPlus during the occupied period (Figure 6.15). By including the additional flow for the laboratories exhaust, the difference between the simulated results and the monitored data is reduced.

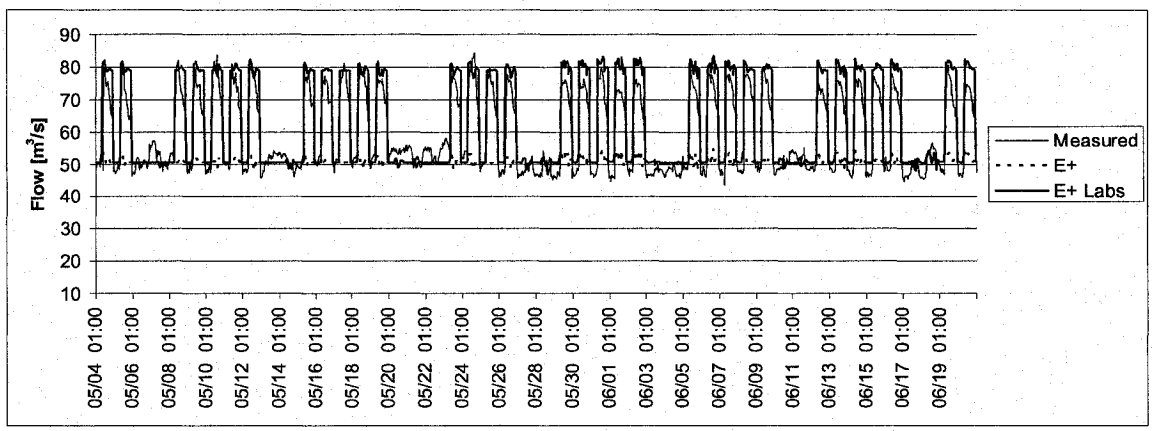

Figure 6.15: Airflow Rate including Laboratories Requirements from May 4th to June 20th; Sector A

The comparison of the sector load is performed for the shown period. Equations (6.1) and (6.2) are used to calculate the sector thermal load from measured data and compared with the estimated thermal load from the EnergyPlus program (Figure 6.16).

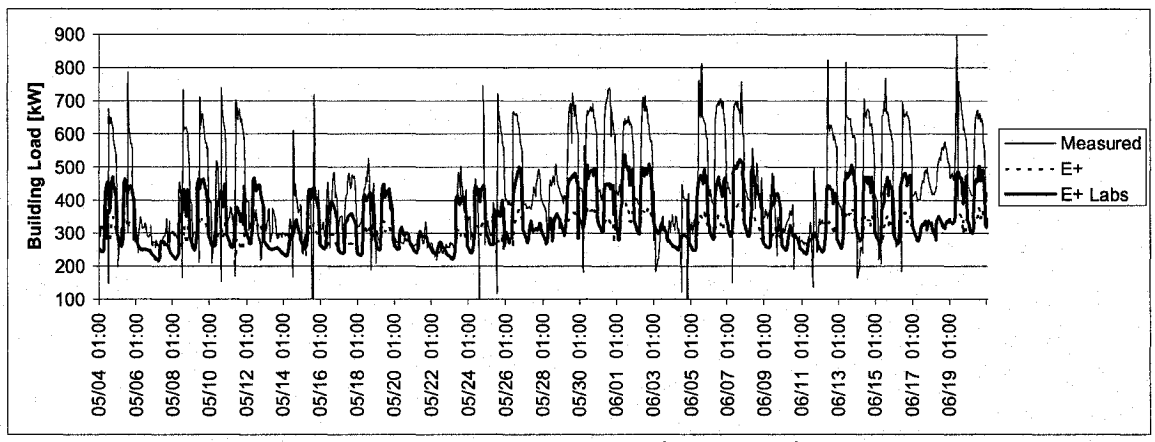

Figure 6.16: Sector Load from May 4th to June 20th; Sector A

For the unoccupied period, the measured and estimated sector loads are similar. However, during occupied hours, the EnergyPlus program underestimates the load. The percentage difference is 19.0% on the average value, which is close to the recommended maximum difference between measured and predicted results presented earlier. For sector A, the measured average load is 421 ± 150 kW, while the average estimated load is 341 ± 83 kW.

The estimated thermal load calculated on the air-side using equations (6.1) and (6.2) is also compared to the summation of all the zone thermal loads and the cooling coil load estimated by EnergyPlus. The calculated sector thermal load varies between 200 and 400 kW (Figure 6.17), while the summation of all the zone thermal loads estimated by EnergyPlus varies between 150 and 400 kW (Figure 6.18). The distribution pattern is similar for both set of data: the load increases with the increase in outdoor air temperature.

The cooling coil load also increases with increase in outdoor air temperature for outdoor air temperatures above 16°C, which is the design supply air temperature for the

system (Figure 6.19). For outdoor air temperatures below 16°C, the cooling coil is not operational. At outdoor air temperatures between 22°C and 24°C, some points are outside the linear pattern noticed for increase in outdoor air temperature. At these temperatures, the system is still working under economizer mode, i.e. the system uses a 100% outside air, and thus the cooling requirements are higher. For temperatures above 24°C, the cooling coil load is around 600 kW, which is close to the maximum sector and zone thermal loads. The closeness between the results for the estimated thermal loads, the summation of the zone thermal loads and the cooling coil load shows that EnergyPlus results are plausible.

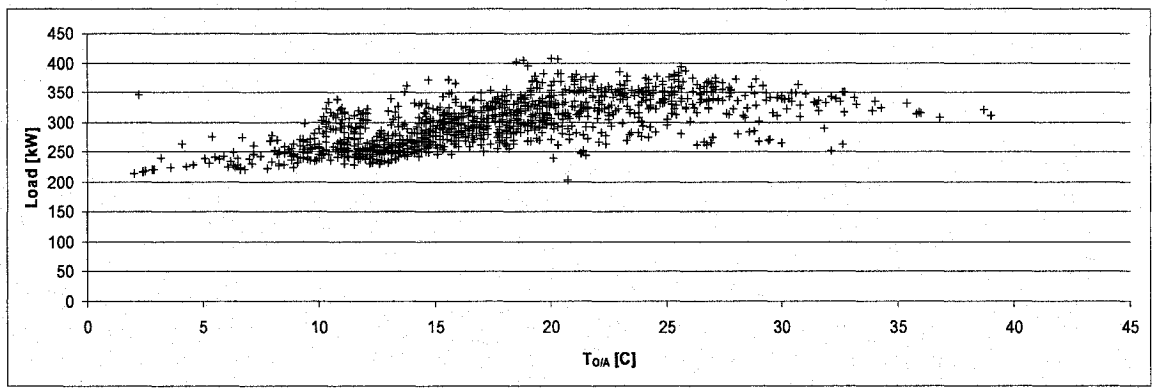

Figure 6.17: Estimated Sector Air-Side Thermal Load versus Outdoor Air Temperature from May 4th to June 20th; Sector A

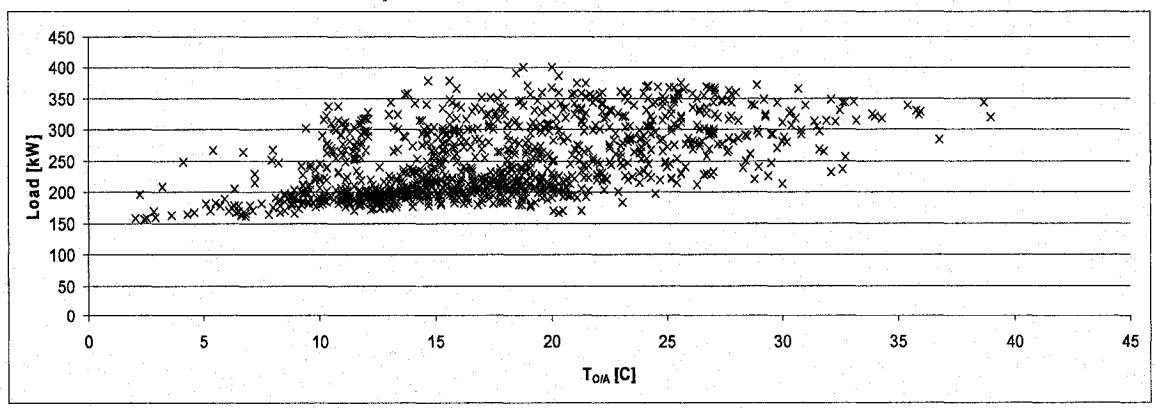

Figure 6.18: Estimated Thermal Load of all Zones versus Outdoor Air Temperature from May 4th to June 20th; Sector A

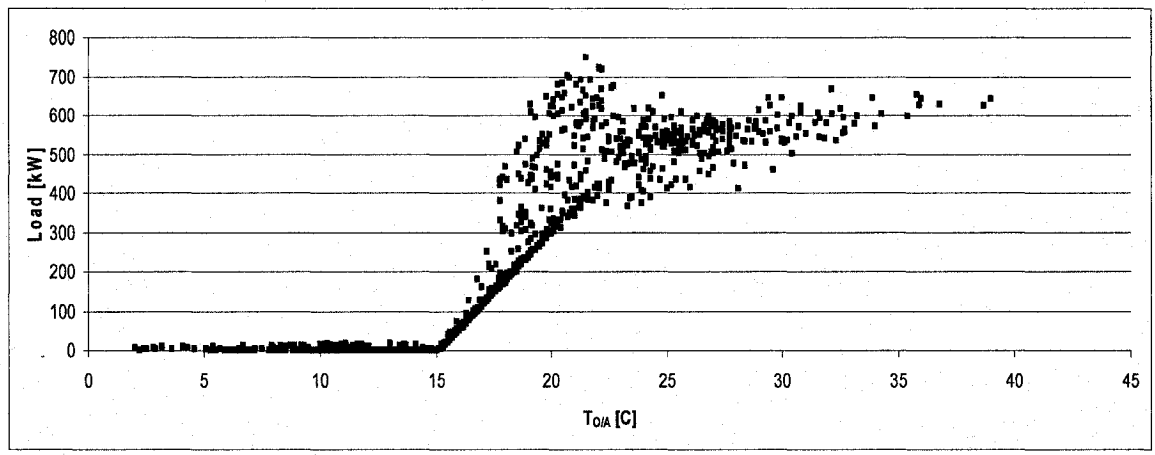

Figure 6.19: Estimated Cooling Coil Load versus Outdoor Air Temperature from May 4th to June 20th; Sector A

Table 6.1 presents an overview of data analyzed over period A, which is from May 4th to June 20th. The relative errors are less than 6% for all variables for sector A and sectors B and C, which shows that the predicted data are in agreement with the measured building data.

Table 6.1: Overview of Period A

	SECTOR A			SECTORS B & C		
ITEM	Measured	EnergyPlus	R.D. (%)	Measured	EnergyPlus	R.D. (%)
Airflow Rate[m^3/s]	59.04	62.20	5.36	20.23	20.94	3.51
$T_{S/A}$ [C]	15.92	16.21	1.84	15.59	15.65	0.42
$T_{R/A}$ [C]	22.00	21.21	3.57	22.12	23.14	4.57

6.1.2 Analysis of Period B

Comparison between simulated and measured data for period B is presented for sectors A, B and C. The approach used for the calibration of period A is also used for the analysis. The analysis period is from March 20th to May 3rd.

6.1.2.1 Sectors B and C

For sectors B and C, the airflow rate variation shows some differences with the measured data (Figure 6.20). The unoccupied airflow rate shows similar trend for both

sets of data, measured and predicted. However, during occupied hours, the airflow rate calculated using EnergyPlus and the exhaust laboratories requirement is greater than the measured value. The cooling coil is not operational for that period, and if the outdoor air temperature is higher than the design supply air temperature, the program might be increasing the airflow rate in order to extract the cooling load to keep the indoor air temperature within acceptable comfort limits. The predicted airflow rate level is compared with the outdoor air temperature to better understand the increase in airflow rates (Figure 6.21). Two different levels of airflow rate are noticed, one for the occupied and another for the unoccupied hours. At outdoor air temperatures above 16°C, the predicted airflow rate is increased during occupied hours. For outdoor air temperatures between 0°C and 10°C, the systems works in heating mode, and the airflow predicted by EnergyPlus is also increased (Figure 6.21).

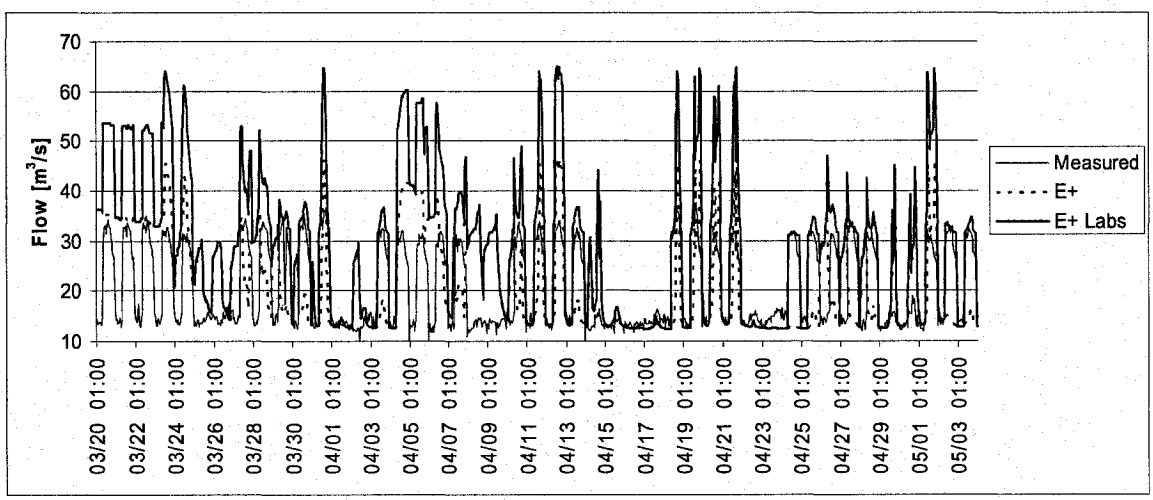

Figure 6.20: Airflow Rate Variation from March 20th to May 3rd; Sectors B & C

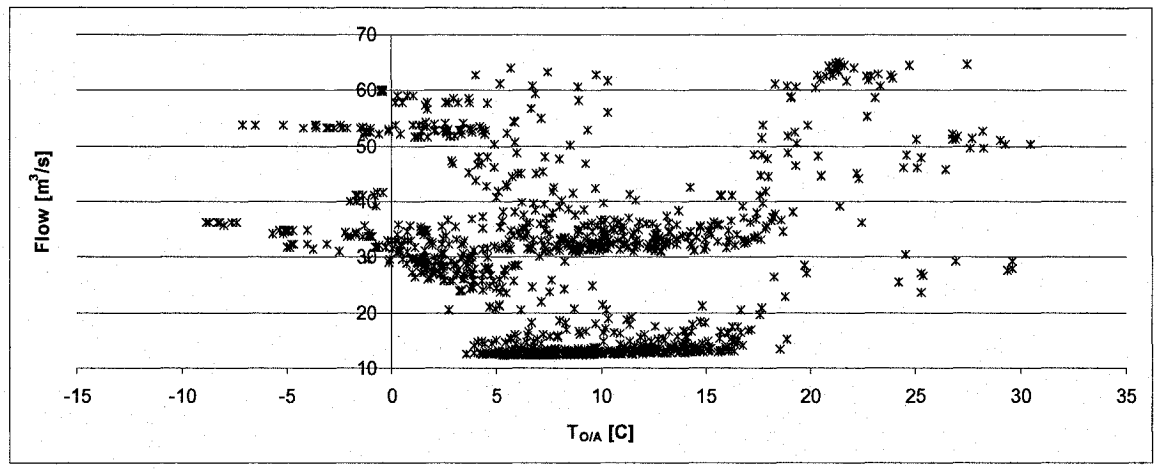

Figure 6.21: Predicted Airflow Rate versus Outdoor Air Temperature from March 20th to May 3rd; Sectors B & C

The supply and return air temperature variations are compared for a better understanding of differences between simulated and measured data (Figure 6.22). On the return side, the temperature variations are similar, while the predicted supply air temperature varies between 16°C and 30°C, rather than being constant around 16°C. For period B, outdoor air is directly introduced to the building, thus explaining the high supply air temperature. For outdoor air temperatures between 4°C and 16°C, the supply air temperature is maintained around the design set point (Figure 6.23). At outdoor air temperatures above 16°C, the supply air temperature proportionally increases with increase in outdoor air temperature. For outdoor air temperatures below 4°C, the supply air temperature is around 25°C, which is higher than the supply air temperature set point.

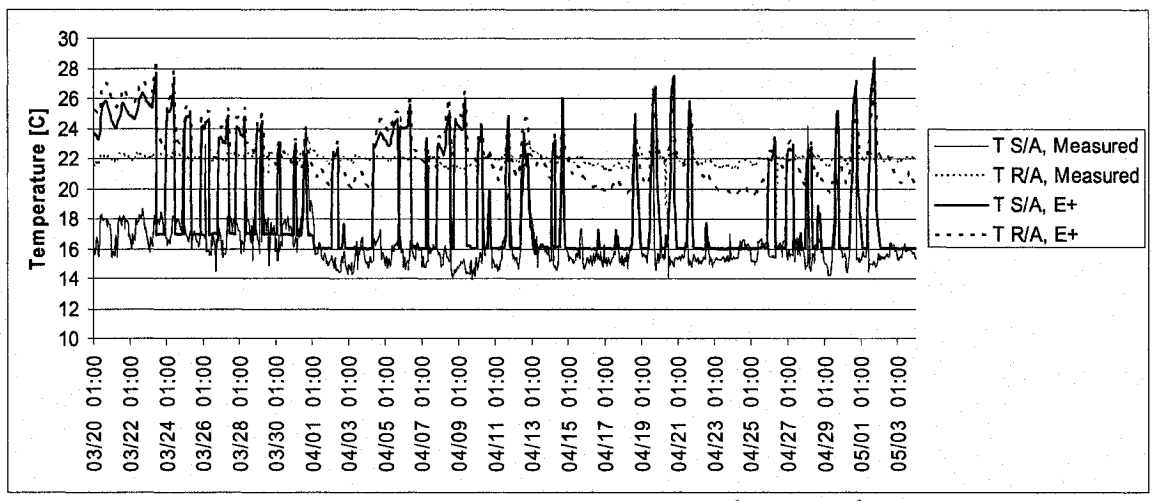

Figure 6.22: Air Temperature Variation from March 20th to May 3rd; Sectors B & C

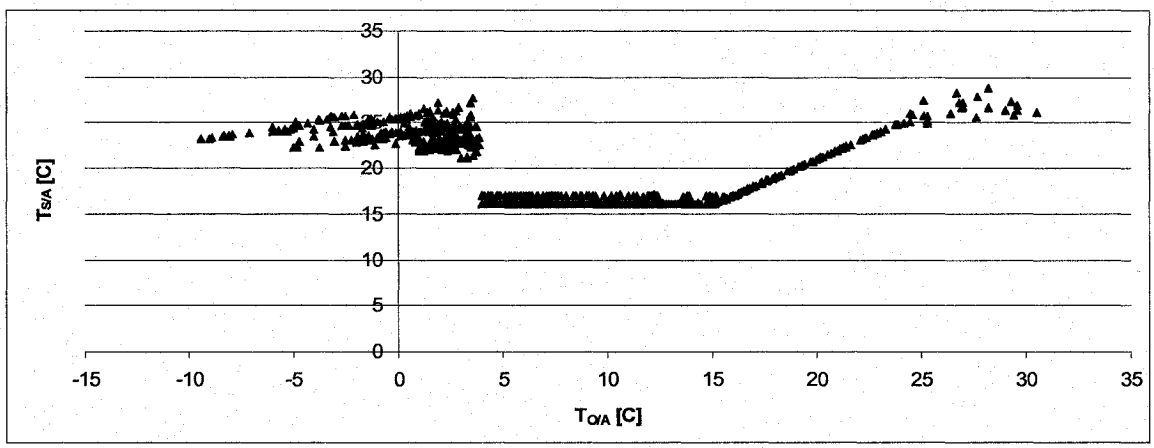

Figure 6.23: Predicted Supply Air Temperature versus Outdoor Air Temperature from March 20th to May 3rd; Sectors B & C

The differences between simulated and predicted supply air temperatures for outdoor air temperatures below 4°C is further investigated by reviewing the input file and outputs generated by the EnergyPlus program. The analysis revealed that the economizer settings are inappropriate. The economizer minimum outdoor air level was originally set to proportional minimum with the minimum outdoor airflow rate set to autosize, which varies the zone outdoor airflow rate in proportion to the total system airflow rate. Also, the economizer lower temperature limit was set to 4°C. Under this set of conditions, the outdoor airflow rate dropped below the calculated minimum coincident outdoor air level

for all zones. In order to eliminate the error, the minimum coincident outdoor air level for all zones is determined by adding the minimum outdoor airflow rate for each zone, which is given by the outdoor airflow rate per occupant multiplied by the number of occupants in the zone during unoccupied hour. For sectors B and C, a minimum outdoor airflow rate of 3.46 m^3/s is required. Thus, the economizer minimum outdoor air level is revised to be set to fixed minimum with a minimum outdoor airflow rate of 3.46 m^3/s. The lower limit is also modified to be -10°C, thus the outdoor air airflow rate decreases linearly until reaching the minimum outdoor air level of 3.46 m^3/s. Revised airflow rates and air temperatures are presented in Figures 6.24 and 6.25.

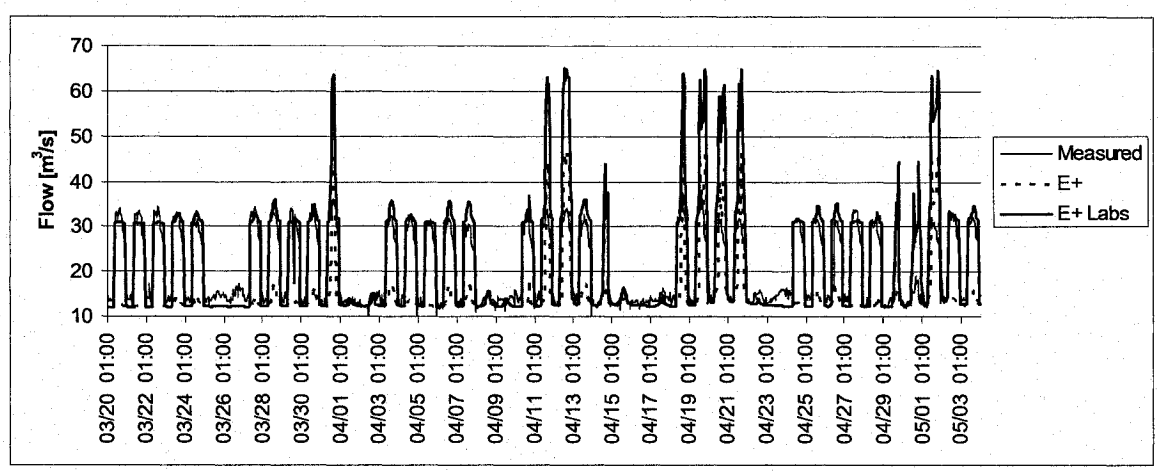

Figure 6.24: Revised Airflow Rate Variation from March 20th to May 3rd; Sectors B & C

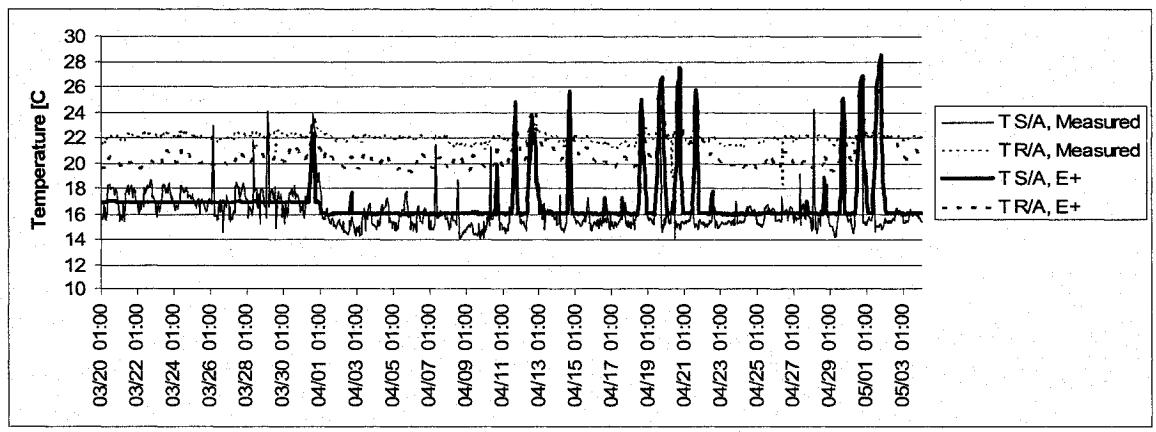

Figure 6.25: Revised Air Temperature Variation from March 20th to May 3rd; Sectors B & C

The revised predicted airflow rates and air temperatures still show some differences with the measured data. This case mostly occurs for outdoor air temperatures above 16°C when the outdoor air is directly introduced to the building and the cooling coil is not in operation, thus the program might be increasing the airflow rate in order to extract the cooling load to keep the indoor air temperature within acceptable comfort limits. For outdoor air temperatures above 16°C, the predicted airflow rate increases with increase in outdoor air temperature (Figure 6.26). Similarly, the predicted supply air temperature increases linearly for increase in outdoor air temperature for outdoor air temperatures above 16°C (Figure 6.27), thus endorsing the assumption stated previously concerning the EnergyPlus program simulation behaviours when the cooling coil is not in operation.

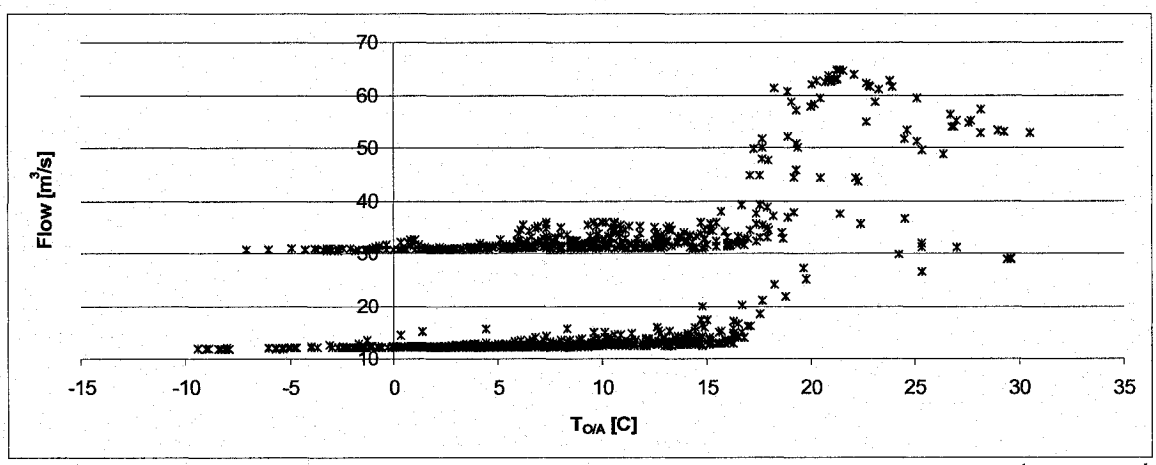

Figure 6.26: Revised Predicted Airflow Rate versus Outdoor Air Temperature from March 20th to May 3rd; Sectors B & C

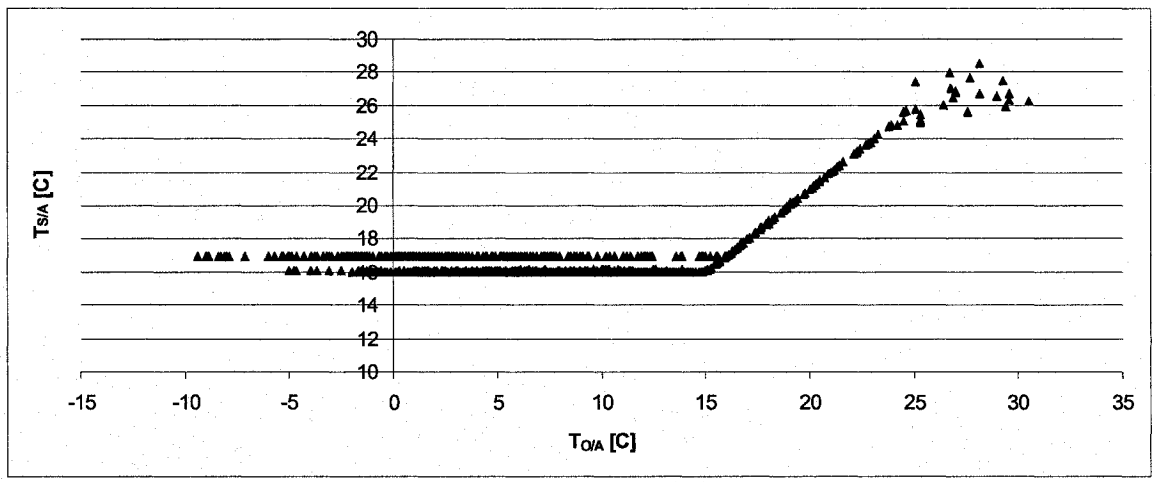

Figure 6.27: Revised Predicted Air Temperature versus Outdoor Air Temperature from March 20th to May 3rd; Sectors B & C

To complete the analysis of period B for sectors B and C, the sector thermal loads are compared for the shown period. Equations (6.1) and (6.2) are used to perform the comparison (Figure 6.28). The measured and estimated sector loads show a similar trend. The percentage difference on the average value is less than 5.0%. For sectors B and C, the average measured load is 129 ± 56 kW, while the average estimated load is 126 ± 54 kW.

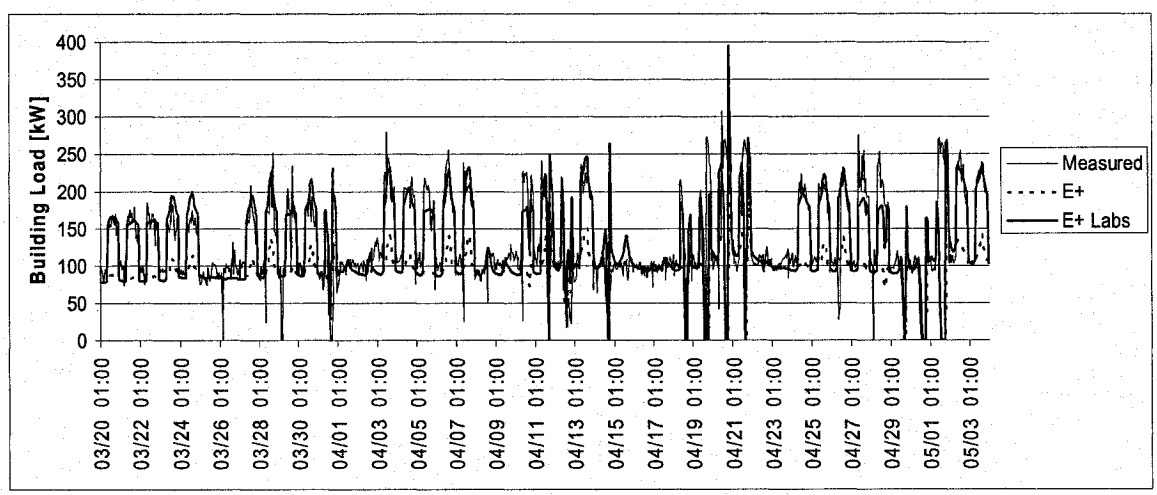

Figure 6.28: Sector Air-Side Thermal Load from March 20th to May 3rd; Sectors B & C

The estimated thermal load calculated on the air-side is compared to the summation of all re-heat and heating coils load estimated by EnergyPlus. The calculated sector thermal load is about 100 kW for unoccupied hours, and between 160kW and 240 kW for occupied hours (Figure 6.29), while the summation of all the coil loads estimated by EnergyPlus decreases with increase in outdoor air temperature (Figure 6.30). For outdoor air temperatures above 16°C, the coils are not in operation and the calculated sector air-side load decreases with the increase in outdoor air temperature.

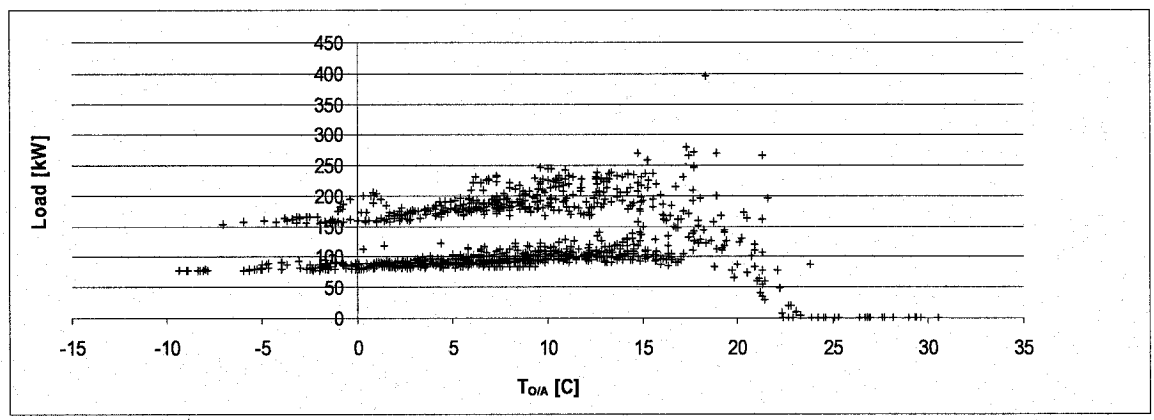

Figure 6.29: Estimated Sector Air-Side Thermal Load versus Outdoor Air Temperature from March 20th to May 3rd; Sectors B & C

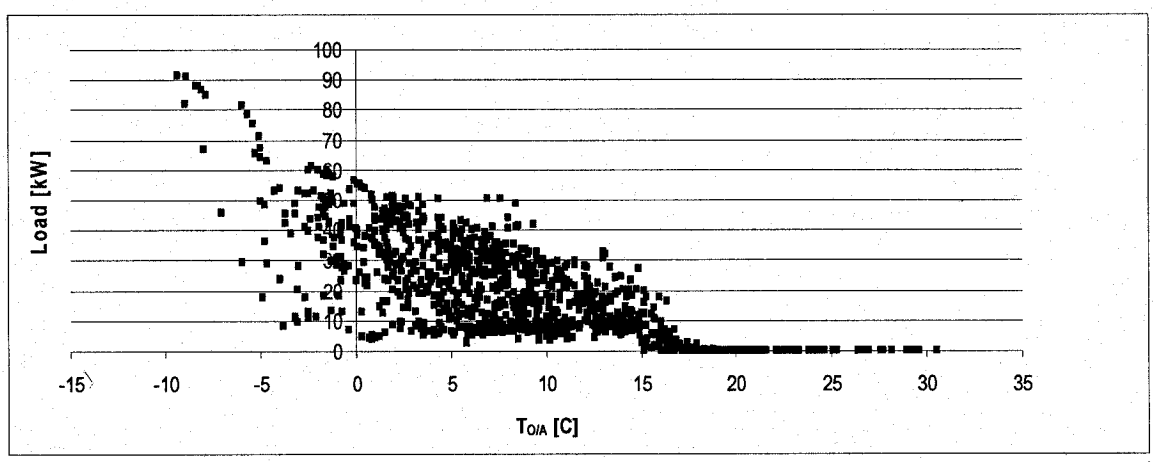

Figure 6.30: Estimated Re-heat and Heating Coils Load versus Outdoor Air Temperature from March 20th to May 3rd; Sectors B & C

6.1.2.2 Sector A

The sector A EnergyPlus input file is modified to reflect the findings made while simulating sectors B and C. Thus, the economizer settings were modified to a fixed minimum outdoor airflow rate of 5.8 m^3/s and a lower cut-off outdoor air temperature limit of -10°C. Consequently, the measured and simulated airflow rate variation show a similar trend over period B of the spring season (Figure 6.31). The occupied airflow rate, which includes the airflow rates predicted by EnergyPlus and the laboratories exhaust rate, is close to the measured airflow rate. During unoccupied period, EnergyPlus slightly underestimates the airflow rates.

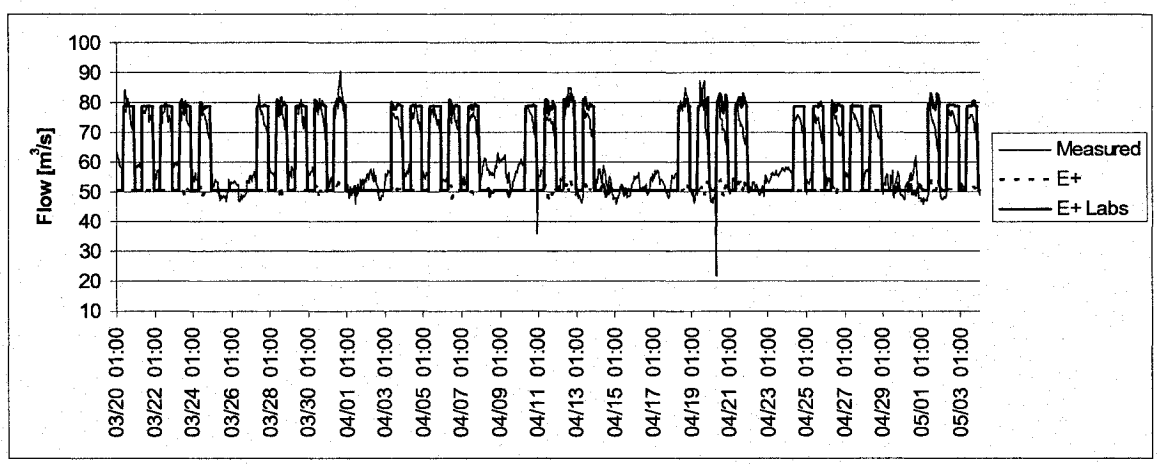

Figure 6.31: Airflow Rate Variation from March 20th to May 3rd; Sector A

The air temperatures are also compared with the measured data (Figure 6.32). On the return side, the temperature variation is similar, while on the supply side the temperature varies between 15°C and 29°C. The increase in supply air temperature occurs for outdoor air temperatures above 16°C (Figure 6.33). For period B, the cooling coils are not operational and outdoor air is directly introduced to the building, thus explaining the increase in supply air temperature.

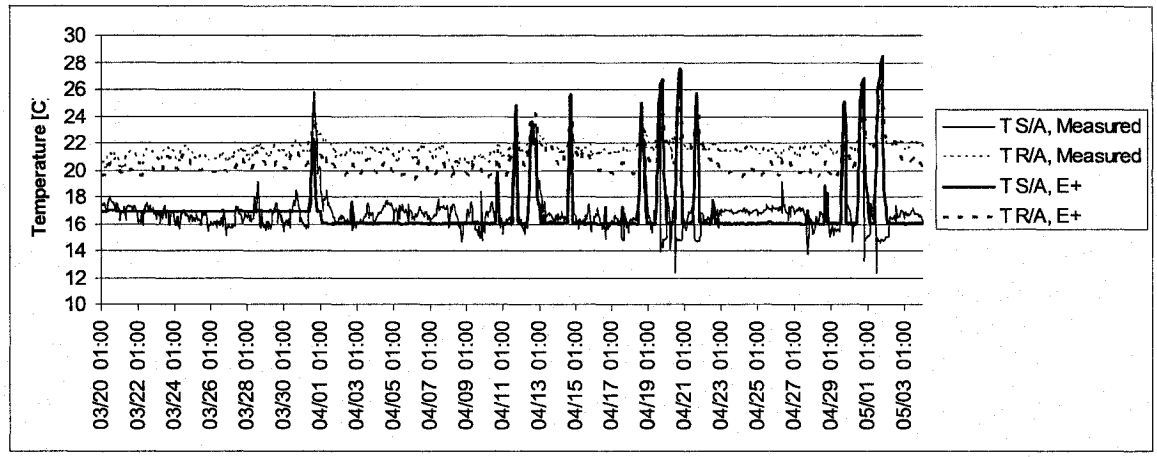

Figure 6.32: Air Temperature Variation from March 20th to May 3rd; Sector A

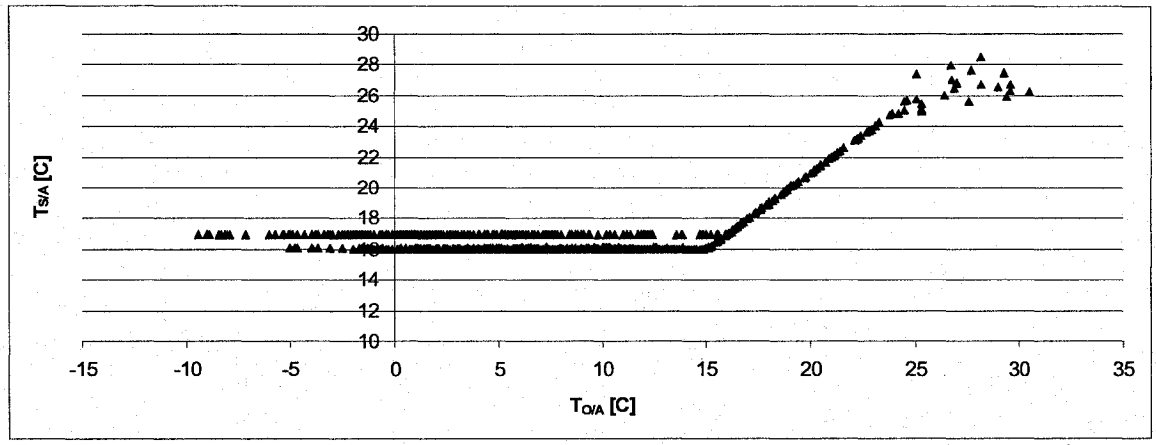

Figure 6.33: Supply Air Temperature versus Outdoor Air Temperature from March 20th to May 3rd; Sector A

To complete the analysis, the sector load is compared for the shown period. Equations (6.1) and (6.2) are used to perform the comparison (Figure 6.34). The measured and estimated sector loads show a similar trend. The predicted load is lower than the measured calculated load. The percentage difference on the average value is less than 25.0%. For sector A, the measured average load is 337 ± 111 kW, while the average estimated load is 256 ± 87 kW.

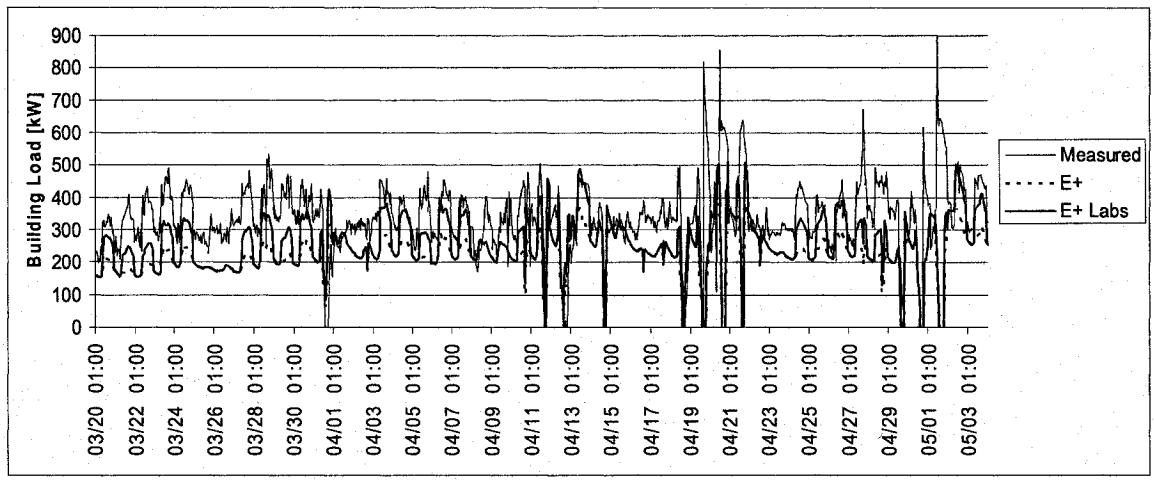

Figure 6.34: Sector Air-Side Thermal Load from March 20th to May 3rd; Sector A

The estimated thermal load calculated on the air-side is compared to the summation of all re-heat and heating coils load estimated by EnergyPlus. The calculated sector thermal load is about 200 kW for unoccupied hours and about 400 kW for occupied hours (Figure 6.35), while the summation of all the coil loads estimated by EnergyPlus decreases with increase in outdoor air temperature (Figure 6.36). For outdoor air temperatures above 16°C, the coils are not in operation and the calculated sector air-side thermal load decreases with the increase in outdoor air temperature. At outdoor air temperatures above 16°C, re-heat is still required for a number of zones, explaining the presence of the heating load for outdoor air temperatures between 16°C and 22°C (Figure 6.36). Both set of EnergyPlus data, estimated sector thermal load and coils load, show similar trend throughout period B.

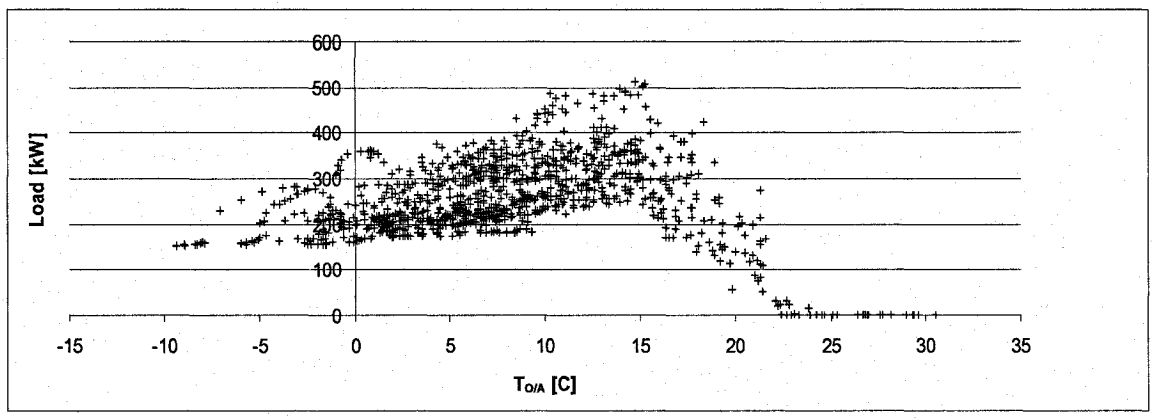

Figure 6.35: Estimated Sector Air-Side Thermal Load versus Outdoor Air Temperature from March 20th to May 3rd; Sector A

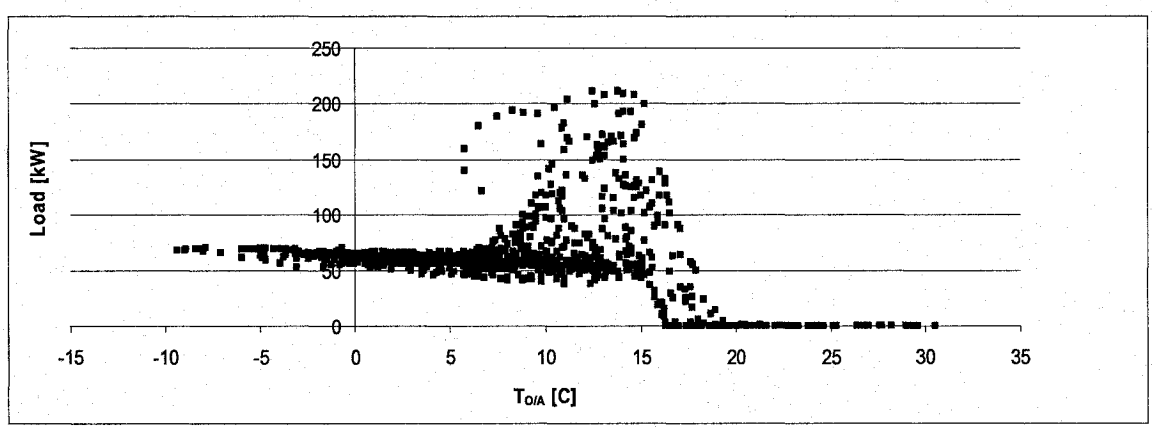

Figure 6.36: Estimated Re-heat and Heating Coils Load versus Outdoor Air Temperature from March 20th to May 3rd; Sector A

For period B, the difference between measured and predicted data is less than 10% (Table 6.2). For sector A, the average measured and predicted values are in agreement with each other, both in terms of airflow rates and air temperatures. For sectors B and C, the difference in airflow rates is slightly higher than the air temperatures difference.

Table 6.2: Overview of Period B

	SECTOR A			SECTORS B & C		
ITEM	Measured	EnergyPlus	R.D. (%)	Measured	EnergyPlus	R.D. (%)
Airflow Rate[m^3/s]	61.92	61.99	0.10	20.36	22.39	9.97
$T_{S/A}$ [C]	16.78	16.86	0.47	16.32	16.85	3.22
$T_{R/A}$ [C]	21.48	20.65	3.89	21.96	22.82	3.90

For the overall spring season, the differences between the predicted and measured variables under comparison (airflow rates and air temperatures) are below the recommended value of 25% [17] for HVAC systems (Table 6.3). The predictions made by the EnergyPlus model over the spring season (from March 20th to June 20th) are in agreement with the measured building data.

Table 6.3: Overview of Spring Season

	SECTOR A			SECTORS B & C		
ITEM	Measured	EnergyPlus	R.D. (%)	Measured	EnergyPlus	R.D. (%)
Airflow Rate[m^3/s]	60.42	62.41	-3.28	20.27	24.92	-22.94
$T_{S/A}$ [°C]	16.34	17.48	-6.96	15.94	18.51	-16.08
$T_{R/A}$ [°C]	21.74	21.79	-0.21	22.05	24.51	-11.18

The comparison between the measured and predicted data during the calibration process has led to a better understanding of the features and capabilities of the EnergyPlus program. First, EnergyPlus estimated the airflow rate and supply/return air temperature for the space cooling/heating loads. The additional airflow rate required for the ventilation hoods were added separately to the predicted results. Also, the economizer settings have a considerable impact on the level of outdoor air introduced to the building and needs to be properly adjusted to reflect the building behaviour. When the cooling coil is not operational and the outdoor air temperature is higher than the design supply air temperature, the program increases the airflow rate in order to extract the cooling load to keep the indoor air temperature within acceptable comfort limits. The heat recovery efficiency on the exhaust stream must be taken into consideration when evaluating the sector thermal load. Properly integrating all components in EnergyPlus has led to the conclusion that the model predictions are in agreement with measured building data.

6.2 Sensitivity Analysis

When developing a computer model, a number of assumptions and approximations are made about the building architectural, mechanical and electrical characteristics. Sensitivity analysis is often used to increase the level of confidence in the developed model. Sensitivity methods study the impacts of input parameters on simulation outputs. In its simplest form the sensitivity analysis uses the influence coefficient (IC_1) that is determined as the output variation over the change in the input value [44].

$$IC_1 = \frac{\Delta OP}{\Delta IP} = \frac{OP_1 - OP_{BC}}{IP_1 - IP_{BC}} \tag{6.3}$$

where,

ΔOP, ΔIP are changes in output and input, respectively;

OP_{BC}, IP_{BC} are base case values of output and input, respectively;

IP_1, OP_1 are values of input and output, respectively.

The influence coefficient IC_1 is similar to the slope of the linear regression line. The current sensitivity analysis uses the slope of the linear regression line, denoted by the symbol IC_1*, to compare changes in output with respect to input variations. The dimensionless sensitivity coefficient (IC_2) can also be calculated using equation (6.4) [20]:

$$IC_2 = \frac{\Delta OP/OP_{BC}}{\Delta IP/IP_{BC}} = \frac{(OP_1 - OP_{BC})/OP_{BC}}{(IP_1 - IP_{BC})/ IP_{BC}} \tag{6.4}$$

So far, most studies performed the sensitivity analysis on the annual basis, hence, by mixing up the cooling and heating seasons. In this study, the sensitivity analysis is performed for only two periods from the calibration period: (1) the week of March 20th to March 26th, in which the mechanical cooling is not in operation (Figure 6.37), and (2) the week of June 12th to June 18th, with mechanical cooling (Figure 6.38). Both weeks are starting on Mondays and ending on Sundays, thus the airflow rates for the last two days of the week are lower than during occupied hours. The air handling units are operating at higher capacity during occupied hours (9:00 to 22:00). The analysis is performed for sectors B and C only for certain parameters.

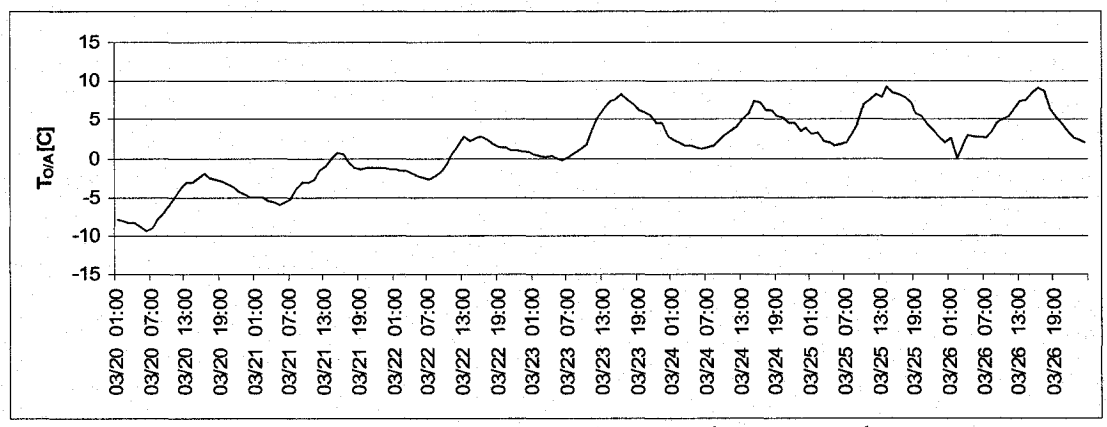

Figure 6.37: Outdoor Air Temperature Variation from March 20th to March 26th; Without Mechanical Cooling

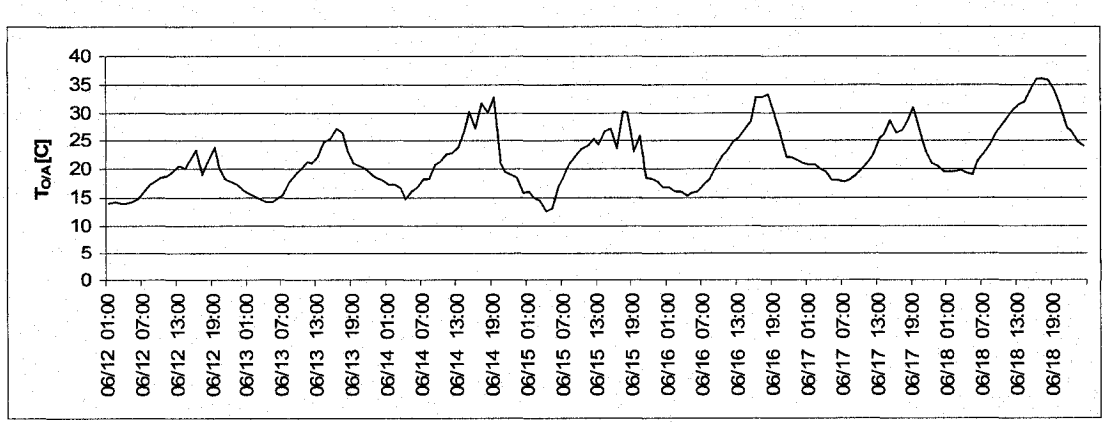

Figure 6.38: Outdoor Air Temperature Variation from June 12th to June 18th; With Mechanical Cooling

Six categories of parameters are usually considered for sensitivity analysis: 1) the envelope loads, 2) the systems schedules, 3) the load schedules, 4) the auxiliary electrical loads, 5) the internal loads, and 6) the systems variables [18]. Several conclusions are drawn from the calibration process and the analysis of collected data for sectors B and C that led to the selection of the parameters to be used for the sensitivity analysis. First, it is noticed that the supply airflow rate does not significantly vary with the variation in outdoor air temperature; hence, one can conclude that the space heating/cooling loads due to heat losses/gains through the exterior envelope are smaller compared to the building internal gains (refer to Chapter 5 for detailed analysis). Thus, parameters influencing the envelope assemblies are not considered in this study. Since the computer model is developed based on monitored data, no modifications are required for the system operating schedule and load schedules. The auxiliary electrical loads, which are non-HVAC electrical loads, are not included in the model; hence this parameter is not considered in the sensitivity analysis.

Therefore, the sensitivity analysis is limited to some variables of the HVAC systems, air infiltration and internal loads. For envelope loads, assumptions are made for the air infiltration level and thus this parameter is included in the sensitivity analysis. Equipment loads and lighting loads, as well as occupancy levels, are defined from data specified for the CBIP incentive program. Schedules of operation and loads are taken from the original DOE-2 file. Only a limited number of rooms have installed equipment and consequently, it is assumed that the equipment loads have a limited impact on the systems; hence no sensitivity analysis is performed for this parameter.

The building under study has been in operation for three years, and thus information related to the installed equipments and operating conditions are available for developing the EnergyPlus input file. However, assumptions are made for the economizer operation and the fan efficiencies; hence these parameters are included in the sensitivity analysis.

6.2.1 Air Infiltration

In the base case, the infiltration is assumed to occur only when the HVAC systems is OFF. When the system is ON, no infiltration occurs due to building pressurization. For this building, the systems are always ON and thus for the base case the air infiltration rate is set to zero in the calibrated model. For the sensitivity analysis, the infiltration rate is changed from zero to 0.15 air changes per hour (ACH) for sectors B and C together. This value is calculated from the recommended value given by MNECB of 0.25 $(l/s)/m^2$ of gross exterior wall area for natural infiltration rate, for above ground perimeter zones only [5].

Since the annual or daily electrical and/or gas consumption information are not available, comparison is performed in terms of average supply airflow rates (Figure 6.39) and the average return air temperature (Figure 6.40).

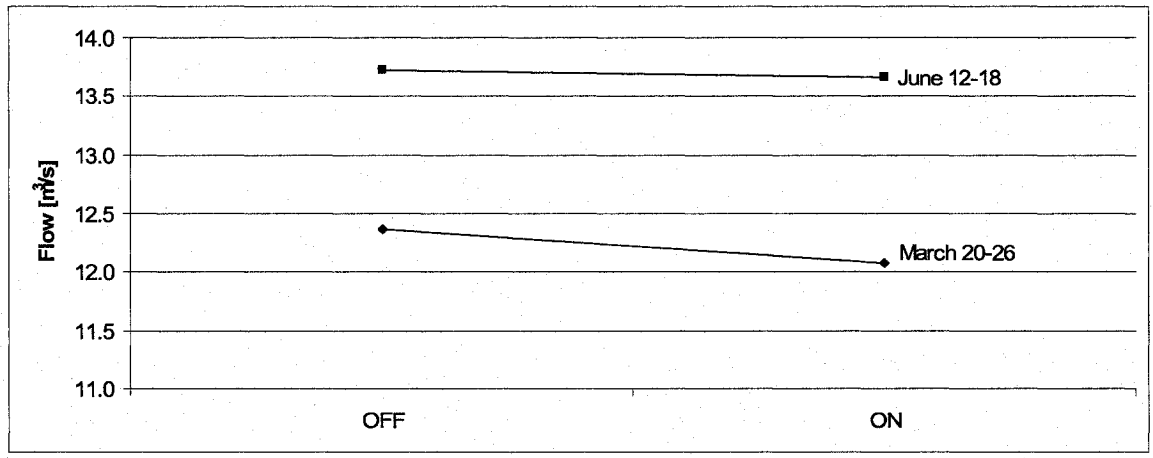

Figure 6.39: Variation of the Supply Airflow Rate without and with Air Infiltration; Sectors B & C

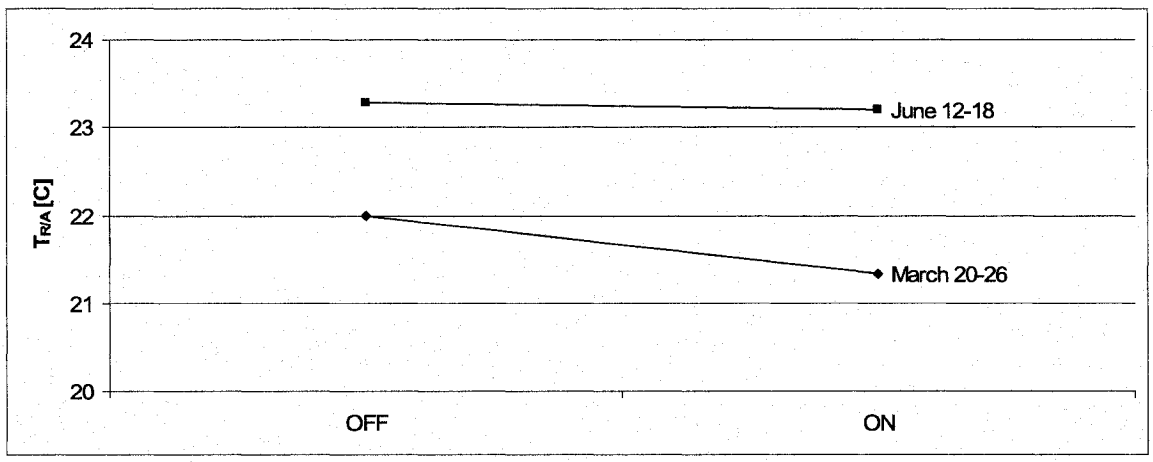

Figure 6.40: Variation of the Return Air Temperature without and with Air Infiltration; Sectors B & C

The impact of infiltration on the airflow rate and return air temperature is limited when the outdoor air temperature is above the design set point of the supply air (~16 °C), which is the case for the week of June 12th to the 18th. The influence coefficient (IC_1*) is less than -3.33 m^3/s/ACH for the supply airflow rate, and -3.33 °C/ACH for the return air temperature.

When the outdoor air temperature is below the supply air design set point, i.e. below 16 °C (week of March 20th to March 26th), the presence of infiltration reduced the airflow rate by 0.3 m^3/s, and the IC_1* is –13.13 m^3/s/ACH. When air infiltration is ON,

the air infiltration is included for the return plenums, and as a consequence the return air temperature is reduced. However, this reduction is less than 1°C, and the IC_1* is -29.5 °C/ACH. The assumption that the infiltration is ON for every hours of the day probably overestimates the actual infiltration rate in the building. However, since it has a limited impact on the simulation results, one can conclude that the level of air infiltration, when evaluated using MNECB guidelines, does not influence the predicted results from the calibrated EnergyPlus model.

6.2.2 Internal Gains

For sectors B and C, the average lighting load is 8.2 W/m^2, and the occupancy density is 0.057 occupant/m^2. These internal loads are modified by ± 20% for the sensitivity analysis.

6.2.2.1 Lighting

For sectors B and C, the average lighting load is 8.2 W/m^2. This load is modified by ± 20%, which leads to a load of 6.5 W/m^2 (- 20%) and of 9.8 W/m^2 (+ 20%). These load densities are much lower than the value of 18 W/m^2 recommended by MNECB for office buildings [5]. As expected, increasing the lighting load has a larger impact on the supply airflow rate when cooling is required, for the week of June 12th - 18th (Figure 6.41). For this period the influence coefficient is 0.35 m^3/s / W/m^2. When heating is required (March 20th - 26th), the IC_1* is 0.19 m^3/s / W/m^2, which is less than the one calculated for the week of June. Hence, the decrease or increase in lighting load mainly impacts the cooling supply airflow rate. The summation of all zone thermal loads is also compared for the three cases (Figure 6.42). The IC_1* is 5.0 kW / W/m^2 for the week of

June, and 4.3 kW / W/m^2 for the week of March. The change in lighting load has a stronger impact on the difference between the IC_1* values calculated for airflow rate (0.35 m^3/s / W/m^2 vs. 0.19 m^3/s / W/m^2), compare with the IC_1* values calculated for the cooling load (5.0 kW / W/m^2 vs. 4.3 kW / W/m^2).

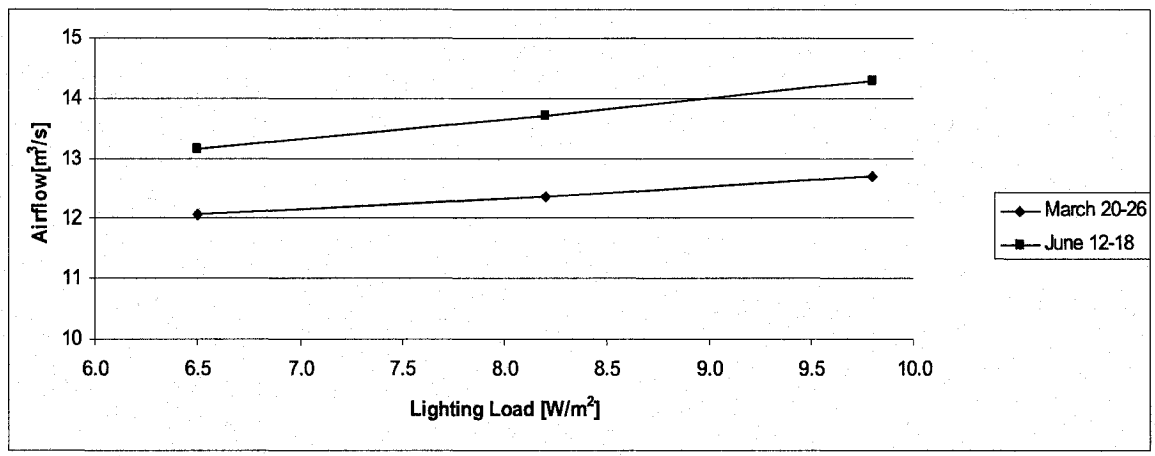

Figure 6.41: Variation of the Supply Airflow Rate with Lighting Load; Sectors B & C

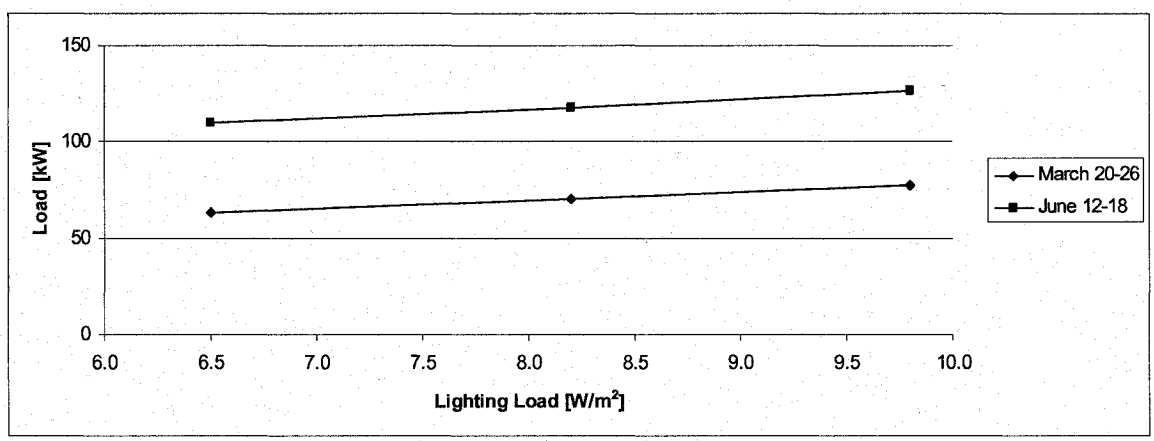

Figure 6.42: Variation of the Cooling Air-Side Thermal Load with Lighting Load; Sectors B & C

To verify that the systems response is appropriate for the change in lighting load, the change in return air temperature is assessed (Figure 6.43). The IC_1* for the week of June 12th – 18th is 0.08 °C / W/m^2 and 0.09 °C / W/m^2 for the week of March 20th – 26th. As expected, the change in return air temperature is minimal, since the HVAC system control the indoor air temperature around the temperature set point.

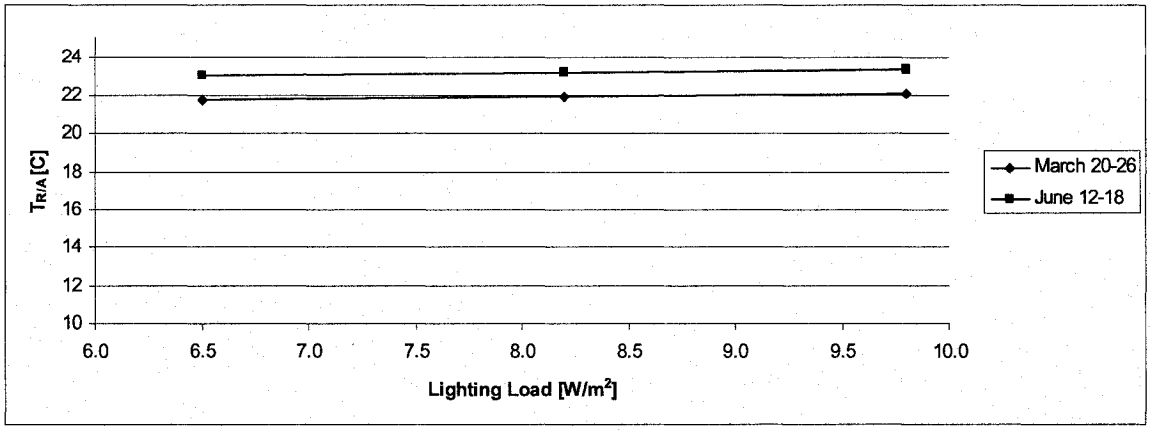

Figure 6.43: Variation of the Return Air Temperature with Lighting Load; Sectors B & C

6.2.2.2 Occupants

The initial occupancy level is estimated at 0.057 occupant/m^2. This level is varied by ± 20%, thus for an occupancy level of 0.045 occupant/m^2 and 0.068 occupant/m^2. In addition, the minimum fresh air level is also modified to include the increase in occupancy level. In terms of total number of occupants for sectors B and C, the base case included approximately 370 persons and a minimum outdoor airflow rate of 3.46 m^3/s. This value is increase to 4.01 m^3/s (+20%) and reduced to 2.90 m^3/s (-20%) for the sensitivity analysis. The airflow rate is barely changed by varying the occupancy level (Figure 6.44). For the June week, the average supply airflow rate of the base case is 13.75 m^3/s, and it is reduced to 13.60 m^3/s when the occupancy is decreased by 20% and increased to 13.94 m^3/s when increased by 20%, with and IC_1* of 0.1735 $m^3/s/m^2$/occupant. For the week of March, the average airflow rate levels are 12.32 m^3/s, 12.40 m^3/s and 12.51 m^3/s respectively, with the IC_1* of 0.095 $m^3/s/m^2$/occupant. Therefore, for sectors B and C, the total number of occupants has minor influence on the supply airflow rate.

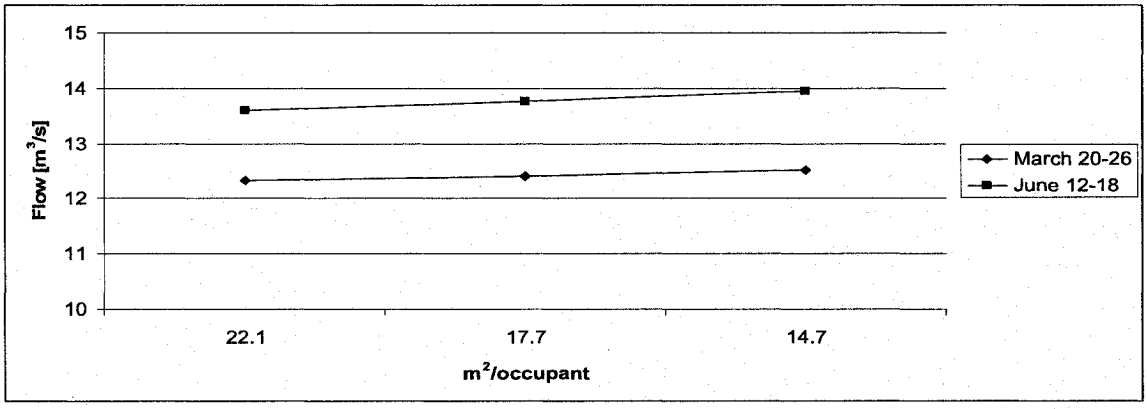

Figure 6.44: Variation of the Supply Airflow Rate with Occupancy Level; Sectors B & C

In terms of return air temperature, the variation in occupancy level has no impact on the values (Figure 6.45). The IC_1* for the week of June is 0.006 °C/m^2/occupant and 0.012 °C/m^2/occupant for the week of March. The airflow rate is increased/decreased to maintain the zone design indoor air temperature set point, hence the absence of variation in return air temperature.

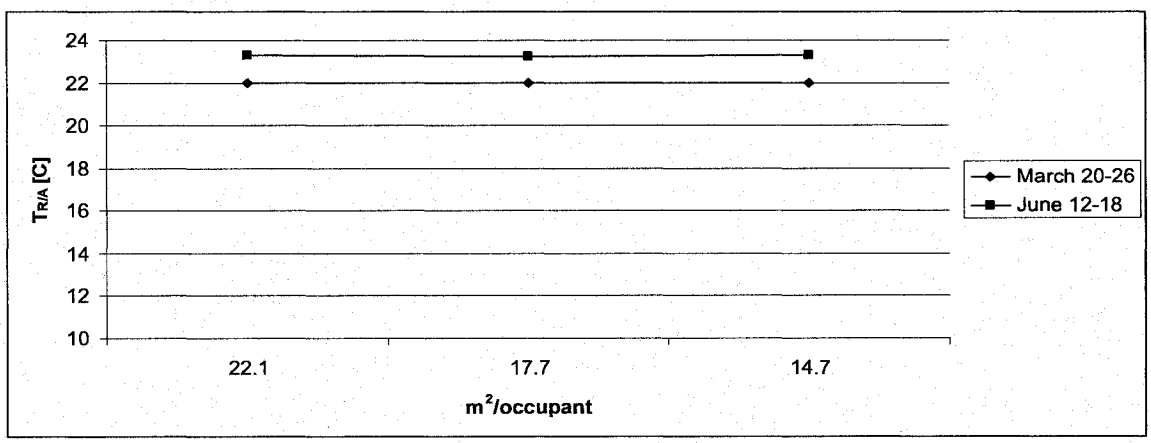

Figure 6.45: Variation of the Return Air Temperature with Occupancy Level; Sectors B & C

The variation in total zones thermal cooling loads for different occupancy level is also analyzed (Figure 6.46). For the June week, the IC_1* is 2.80 kW / m^2/occupant, and for the week of March, the IC_1* is 2.58 kW / m^2/occupant; hence, since the occupancy

level is relatively low for sectors B and C, varying the occupancy level by ± 20% does not significantly influence the overall performance of the system.

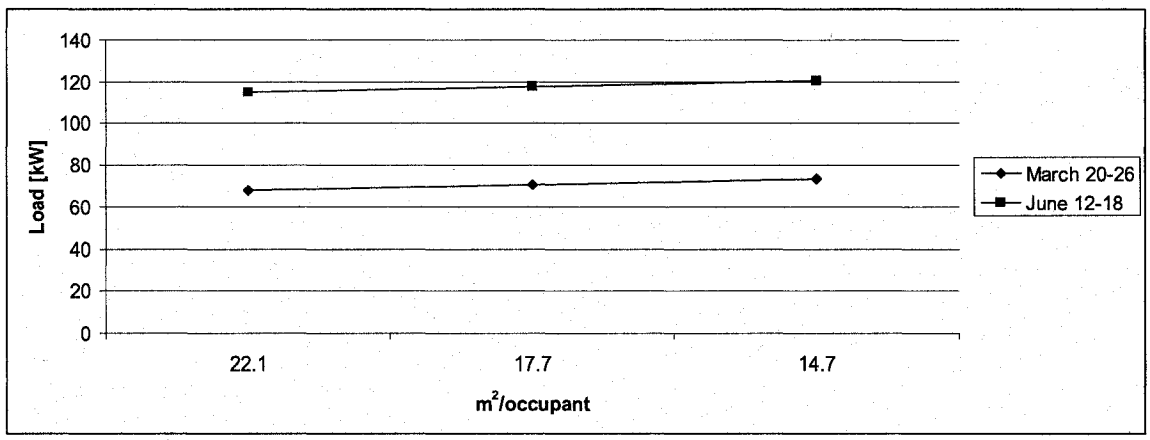

Figure 6.46: Variation of the Cooling Air-Side Thermal Load with Occupancy Level; Sectors B & C

6.2.3 Economizer Settings

During the calibration process, it was noticed that the economizer minimum limits defined in the EnergyPlus input file have to be complete to ensure adequate response from the air system. The minimum outdoor airflow rate was adjusted during the calibration process, but no particular attention was given to the upper cut-off limit of the outdoor air temperature. This is the outdoor air temperature at which the outdoor airflow rate is changed from a 100% of total supply to the minimum required by the ventilation rates. The base case upper outdoor air temperature limit is 24°C. The limit is now modified for different outdoor air temperature and the variation in supply airflow rate and cooling coil load is assessed. Originally this value was changed by ± 1°C and ± 2°C, but no major differences in outputs were noticed. Additional simulations were performed for temperature change of ± 4°C. Thus, the simulations are performed for the week of June 12th to June 18th only, for the cut-off outdoor air temperature between 20°C and 28°C.

Varying the economizer upper outdoor air temperature limit has no impact on the supply airflow rate (Figure 6.47). The IC_1* is 0.009 m^3/s / °C for the average airflow rate for the week of June 12th - 18th; hence one can conclude that the change in the economizer upper temperature limit does not induce a variation in the supply airflow rate.

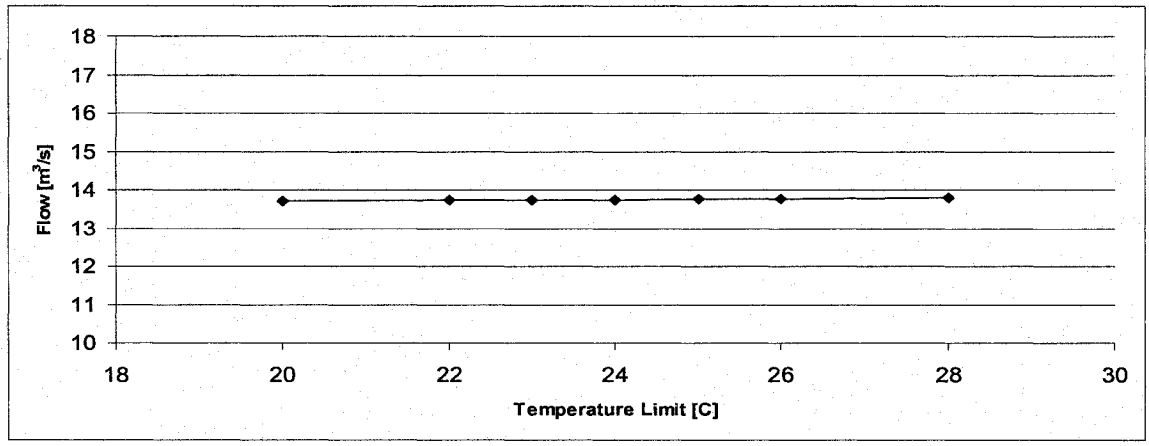

Figure 6.47: Variation of the Supply Airflow Rate with Economizer Cut-Off Temperature; Sectors B & C

The cooling coil load is also compared for all cases (Figure 6.48). The cooling coil load barely varies for economizer outdoor air temperature cut-off limits above 22°C. Therefore, the assumption of 24°C used for the base case is suitable for the climate and building used for the case study. The model is insensitive to varying the cut-off temperature between 22°C and 28°C.

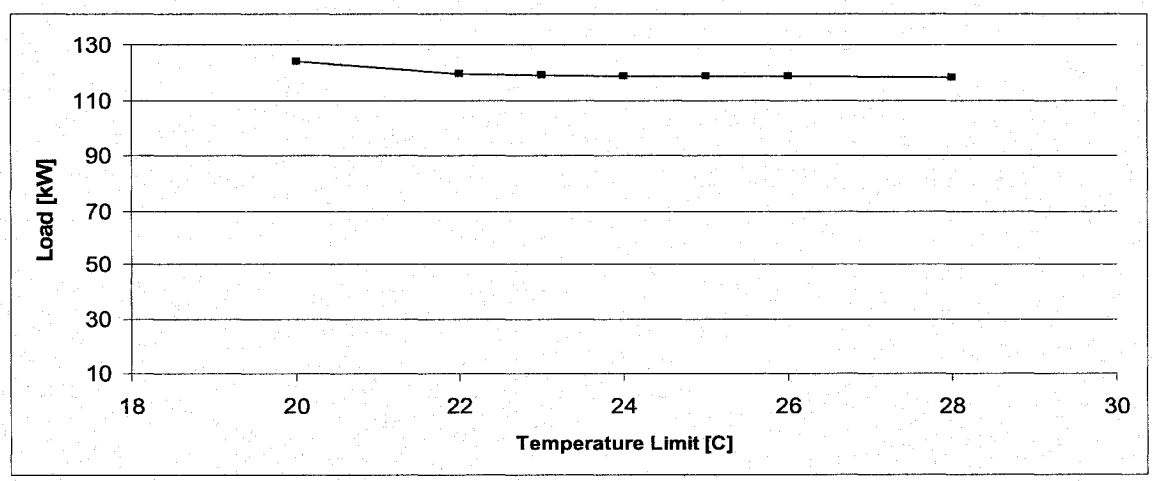

Figure 6.48: Variation of the Cooling Coil Load with Economizer Cut-Off Temperature; Sectors B & C

6.2.4 Fan Efficiency

In EnergyPlus, the supply and return fan efficiencies are inputted based on data specified for the CBIP application. For the base case, the supply fan efficiency is 65% and the return fan efficiency is 58%. These efficiencies are based on design fan capacities and pressure losses. During the analysis of the as-built and as-operated thermal performance of the Sciences building, the measurements for sectors B and C indicate that during the occupied period, the supply fans work on the average at 40% of total capacity, and during the night at 18.5% of capacity (refer to Chapter 5 for detail). Therefore, the fan efficiencies used for the base case might not be representative of the actual system operating conditions. The efficiencies for both supply and return fans are modified by ± 5% and ± 10%, and the impact on fan electric consumption is assessed. For the supply fan, the relation between the fan power and its efficiency is almost linear (Figure 6.49). The IC_1* is - 0.221 kW/% efficiency for the week of June 12th - 18th, and - 0.178 kW/% efficiency for the week of March 20th - 26th.

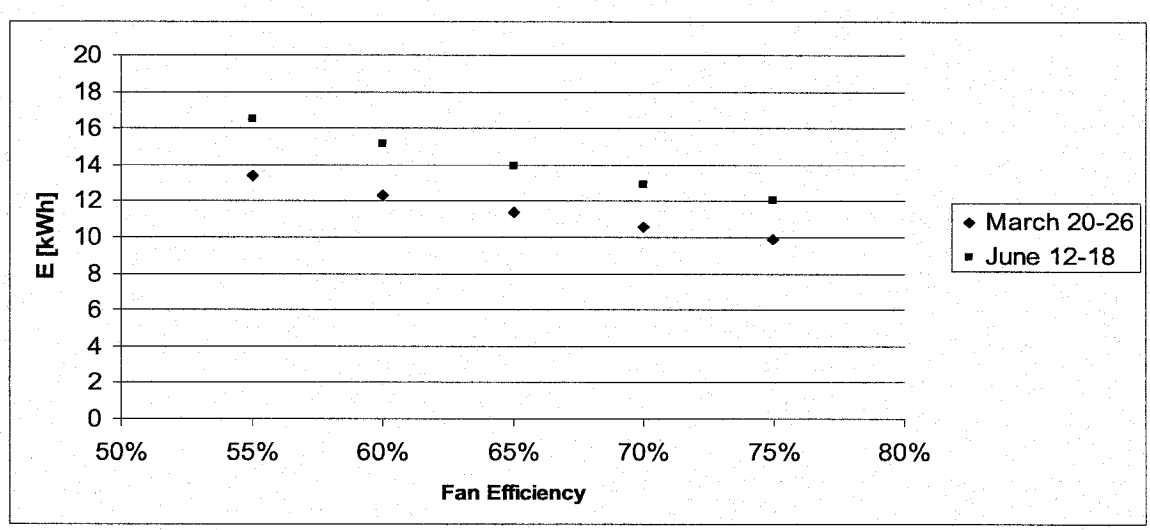

Figure 6.49: Variation of the Supply Fan Electricity Consumption with Fan Efficiency; Sectors B & C

Similarly, for the return fan, the IC_1* is - 0.157 kW/% efficiency for the week of June 12th - 18th, and - 0.127 kW/% efficiency for the week of March 20th - 26th (Figure 6.50). Varying the fans efficiencies does have an impact on the fans electrical consumption, and ideally measuring the efficiencies on-site would probably lead to more accurate simulation results.

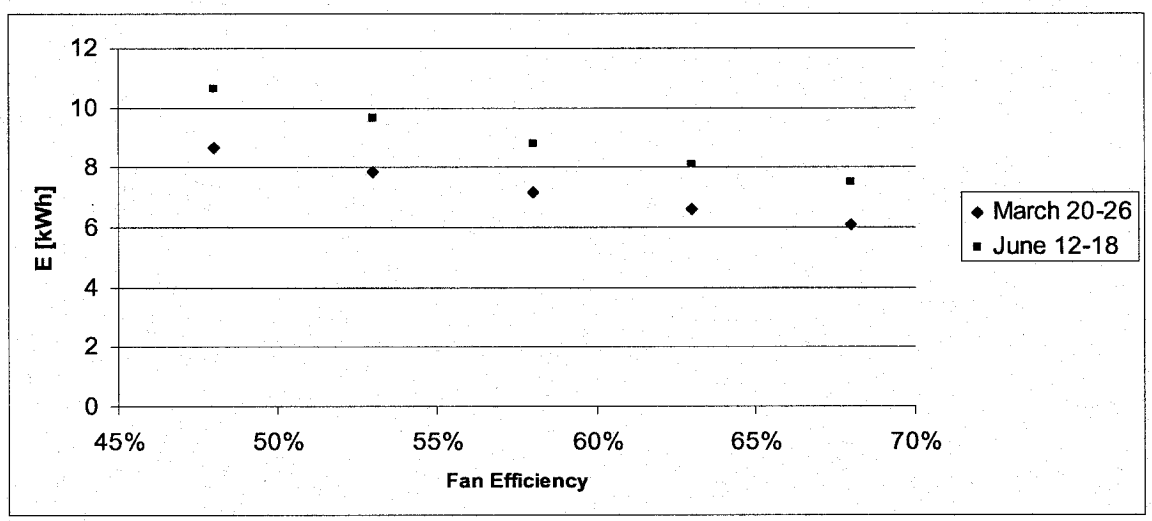

Figure 6.50: Variation of the Return Fan Electricity Consumption with Fan Efficiency; Sectors B & C

Previous sensitivity analyzes, presented in the literature, have been performed for different type of buildings on the annual basis, hence, by mixing up the cooling and heating seasons. Results evaluated for some of the parameters used in this study are presented (Table 6.4). These results can be compared with the sensitivity coefficient calculated for the two periods, March 20th to 26th, and June 12th to 18th.

Table 6.4: Sensitivity Coefficients for Office Buildings [20]

Input Parameter	Annual Electricity (IC_2)	Peak Electricity (IC_2)
Lighting load [W/m^2]	0.418	0.289
Occupancy density [occ./m^2]	0.210	0.328
Fan efficiency	0.145	0.154

An overview of the influence coefficients calculated for internal loads is presented in Table 6.5. For changes in lighting load, the thermal cooling load influence coefficient (IC_2) is similar to the annual value presented in the literature (Table 6.4), thus showing similar impact in terms of percent variations compared with base case values. For occupancy level, since the building under study has a low level of occupancy, the calculated values for influence coefficient IC_2 are lower than values presented in Table 6.4. Additional variation in occupancy level would be required to complete the sensitivity analysis for the building under study.

Table 6.5: Overview of Average Influence Coefficients for Internal Gains; Sectors B & C

	Airflow			$T_{R/A}$			Load		
LIGHTING	IC_1 $\frac{m^3/s}{W/m^2}$	IC_1* $\frac{m^3/s}{W/m^2}$	IC_2 $\frac{\%OP}{\%IP}$	IC_1 $\frac{°C}{W/m^2}$	IC_1* $\frac{°C}{W/m^2}$	IC_2 $\frac{\%OP}{\%IP}$	IC_1 $\frac{kW}{W/m^2}$	IC_1* $\frac{kW}{W/m^2}$	IC_2 $\frac{\%OP}{\%IP}$
March 20th to 26th	0.195	0.194	0.092	0.091	0.034	0.129	4.352	4.342	0.506
June 12th to 18th	0.349	0.349	0.083	0.083	0.029	0.209	5.055	5.048	0.352
OCCUPANT	$\frac{m^3/s}{m^2/occ.}$	$\frac{m^3/s}{m^2/occ.}$	$\frac{\%OP}{\%IP}$	$\frac{°C}{m^2/occ.}$	$\frac{°C}{m^2/occ.}$	$\frac{\%OP}{\%IP}$	$\frac{kW}{m^2/occ.}$	$\frac{kW}{m^2/occ.}$	$\frac{\%OP}{\%IP}$
March 20th to 26th	-0.027	0.095	-0.005	0.012	-0.004	-0.039	-0.728	2.576	-0.183
June 12th to 18th	-0.049	0.174	-0.003	0.006	-0.002	-0.064	-0.792	2.799	-0.119

For the impact of fan efficiency on electricity consumption (Table 6.6), the data are also compared with data presented in the literature. In the literature, data are available for the impact of fan efficiency on the whole building energy consumption, while results presented in this study are limited to the fan electricity consumption. Thus, the IC_2 calculated for sectors B and C is about 10 times higher than values presented in the literature (Table 6.4).

Table 6.6: Overview of Average Influence Coefficients for Fan Electricity Consumption; Sectors B & C

	March 20th to 26th			June 12th to 18th		
	IC_1 [kW/%]	IC_1* [kW/%]	IC_2 [%OP/%IP]	IC_1 [kW/%]	IC_1* [kW/%]	IC_2 [%OP/%IP]
Supply Fan	-0.177	-0.221	-1.050	-0.219984	-0.178	-1.026
Return Fan	-0.124	-0.127	-1.014	-0.156	-0.157	-1.049

For the impact of economizer cut-off temperature, no data is presented in the literature. However, all influence coefficients calculated for values close to the base case show minor variation in outputs (Table 6.7). Consequently, the minor variation in influence coefficients confirms the validity of the initial assumptions.

Table 6.7: Overview of Influence Coefficients for Economizer Cut-Off Temperature; Sectors B & C

	Airflow		Load	
	IC_1	IC_2	IC_1	IC_2
Temp. [C]	[$m^3/s/°C$]	[%OP/%IP]	[kW/°C]	[%OP/%IP]
20	0.008	0.013	-1.335	-0.270
22	0.006	0.011	-0.293	-0.059
23	0.002	0.004	-0.007	-0.033
24	IP_{BC}	IP_{BC}	IP_{BC}	IP_{BC}
25	0.018	0.031	0.009	0.002
26	0.013	0.023	-0.076	-0.015
28	0.010	0.018	-0.130	-0.026

Sensitivity analysis evaluates the magnitude of the assumptions made in the building simulation. The model used for the case study was first tuned up using monitored data collected at the building. The use of monitored data has limited the amount of parameters to be assessed by sensitivity analysis. Since the system is always ON, the building is pressurized, and the air infiltration rate has only a minor impact on the supply airflow rates. Thus, excluding the infiltration rate in the model does not influence the overall performance of the systems. In terms of lighting and occupant loads, varying the load level influences the supply airflow rates and the zone cooling loads. However, it is concluded that the initial assumptions are suitable since the airflow rates comparison, between monitored and estimated values, were in agreement. The sensitivity analysis performed on the economizer settings has shown that the assumption made in the base case are adequate for the climate and building used for the case study. No major variation in supply airflow rate and cooling coil load are noticed around the economizer

outdoor air temperature upper cut-off limit of 24°C. Performing the sensitivity analysis confirms that most assumptions made throughout the modeling process are reasonable and increases the level of confidence in the results estimated by EnergyPlus.

6.3 Annual Energy Performance

To evaluate the overall performance of the EnergyPlus program, annual indices, such as peak kW, kWh and kWh/m^2, are compared with information from the CBIP application and specification cut-sheets. The cooling coil loads are compared to the design coil capacity (Table 6.8). The load needed to accommodate the hood ventilation requirement is evaluated using airflow rate ratio. For sector A, the total cooling coil load is estimated at 1720 kW, while a capacity of 3310 kW is available. For sectors B and C, the estimated cooling coil load is 1090 kW, while the installed capacity is 1640 kW. The estimated and design airflow rates are different, and consequently the cooling coil loads estimated by the EnergyPlus program are lower than the design loads. For the heating coil load, since glycol systems are not available in EnergyPlus, the coil loads are not taken into consideration.

Table 6.8: Cooling Coil Loads; Simulated versus Design

	Sector A		Sectors B & C	
Item	S/A flow rate [m^3/s]	Cooling [kW]	S/A flow rate [m^3/s]	Cooling [kW]
EnergyPlus	50.5	905	13.2	454
Hoods	45. 5	815	18.5	636
Total	**96.0**	**1720**	**31.7**	**1090**
Design	**151.0**	**3280**	**75.5**	**1640**

In the existing central plant, the design of the heating and cooling equipment is complex and it can not directly be simulated by the EnergyPlus program. For instance, there are many heat recovery systems present in the building that are not included in the model. Thus, no attempt is made to estimate the cooling and heating electricity

consumption due to differences between the building and EnergyPlus model operating conditions. The annual electricity consumption is only evaluated for secondary systems, fans, and building components such as lighting and appliances (Table 6.9).

Table 6.9: Annual Electricity Consumption Estimated by the EnergyPlus Program

Item	Floor Area [m^2]	Lighting [kWh]	Appliances [kWh]	Fans [kWh]
Sector A & Animal Labs	18,970	924,043	731,123	851,641
Sectors B & C	9,550	431,543	353,739	191,107
TOTAL	**28,520**	**1,355,586**	**1,084,862**	**1,042,748**

The electrical consumption estimated by EnergyPlus, in terms of kWh/m^2 (Table 6.10), is compared with data extracted for the CBIP application with no ventilation hood and presented by GazMétro [45]. For the lighting electricity consumption, a value of 56.4 kWh/m^2 was estimated from CBIP, while the EnergyPlus estimation is 47.5 kWh/m^2. For appliances, the electricity consumption estimated by EnergyPlus is 38.0 kWh/m^2 compared to 38.8 kWh/m^2 for CBIP. For fans, the estimated values are also in agreement: 36.6 kWh/m^2 for the EnergyPlus program versus 31.0 kWh/m^2 for CBIP. The evaluation of electricity consumptions for the selected items shows that the values estimated by the EnergyPlus program are close to design and CBIP values.

Table 6.10: Annual Electricity Consumption per Floor Area Estimated by EnergyPlus Program

ITEM	Consumption [kWh/m^2]
LIGHTING	47.5
APPLIANCES	38.0
FANS	36.6

6.4 Summary

The identification of differences between building operating conditions and simulation conditions was made possible during the calibration of the EnergyPlus model. The differences were modified to improve the data estimated by the program. For the

overall spring season, the differences between the predicted and measured variables under comparison (airflow rates and air temperatures) are below the recommended value of 25% for HVAC systems. The comparison between the measured and predicted data during the calibration process has led to a better understanding of the features and capabilities of the EnergyPlus program.

The sensitivity analysis confirmed the validity of the assumptions made and increased the confidence in the developed model. Influence coefficients calculated for infiltration rate and economizer cut-off temperatures are low, thus demonstrating that the assumption made in the base case are adequate for the climate and building used for the case study. In terms, of lighting and occupant loads, it was concluded that the initial assumptions are suitable since the airflow rates comparison, between monitored and estimated values, were in agreement. Performing the sensitivity analysis has confirmed that most assumptions made throughout the modeling process were reasonable and increased the level of confidence in the results estimated by EnergyPlus.

The calibrated model was then used to assess annual indices and evaluate the whole performance of the EnergyPlus program. Peak cooling coil loads and electricity consumptions for lighting, appliances and fans are compared with design and CBIP data. The values estimated by EnergyPlus are in agreement with design and CBIP data, demonstrating that properly integrating all components in EnergyPlus leads to good model predictions.

7. CONCLUSIONS

Different approaches are available to evaluate building energy performance. In most cases, detailed modeling of the systems allows the building manager to determine the overall energy consumption of the building. The energy analysis program EnergyPlus was first released in 2001. No detailed evaluation of the program for large buildings with complex electro-mechanical systems has been performed so far.

7.1 Discussion of Results

Modeling the Concordia Sciences building using the EnergyPlus program was a challenge in many ways. The large number of zones and surfaces has made the definition of the architectural systems a long and labour intensive process. Recent developments of graphical user interfaces (GUI) for the EnergyPlus program should accelerate and simplify the overall data entry process for architectural features. In terms of HVAC systems, the use of compact HVAC objects has quite simplified the process. By getting the loops, branches and nodes to be automatically defined by the program, it was possible to properly interconnect all of the components of the HVAC systems without compromising the complexity of the secondary systems. For primary systems, many components used for the heating of large buildings for cold climates, such as glycol heating coils and water-to-water heat exchanger, are not yet available within EnergyPlus. Thus, due to these limitations, the central plant was simulated as two separate entities, one for sectors B and C and one for sector A. Overall, the EnergyPlus program offers a wide range of system configurations. However, GUI and new mechanical components

need to be made available with the program to simplify the development of virtual models for large and complex buildings for cold climates.

The performance of the Sciences building was analyzed using monitored data. The analysis has led to a number of conclusions regarding the performance of the building:

1. For sector A, the average airflow rate during the occupied period is 73.5 m^3/s and the average airflow rate during the unoccupied period is 52.0 m^3/s. For sectors B and C, the average airflow rate during the occupied period is 30.0 m^3/s and 14.0 m^3/s during the unoccupied period.
2. For all sectors, the supply air temperature is maintained constant at around 16°C, while the airflow rate varies depending on the level of occupancy in the building. The supply airflow rate does not vary significantly with variation in outdoor air temperature; hence, one can conclude that the heating/cooling load due to heat losses/gains through the exterior envelope are smaller compared to the building internal gains.
3. For all sectors, the return air temperature is around 22°C for all hours of the day. Constant return air temperature implies no setback or setup on the room temperature set point.

The model was calibrated over the spring season, from March 20th to June 20th. Since the annual or daily electrical and gas consumption are not available, comparison is performed in terms of supply airflow rates, and supply and return air temperatures. For the spring season, the differences between the predicted and measured variables under

comparison (airflow rates and air temperatures) are below the recommended value of 25% for HVAC systems [17]. Properly integrating all components in EnergyPlus has led to the conclusion that the model predictions are in agreement with measured building data.

A sensitivity analysis was also performed to assess the impact of some selected parameters and the validity of certain assumptions for the calibrated model. Influence coefficients calculated for air infiltration rate and economizer cut-off temperatures are low, thus demonstrating that the assumptions made in the base case are adequate for the climate and building used for the case study. In terms of lighting and occupant loads, it was concluded that the initial assumptions are adequate since the comparison between monitored and estimated airflow rates was in agreement. Performing the sensitivity analysis has confirmed that most assumptions made throughout the modeling process were reasonable and increased the level of confidence in the results estimated by EnergyPlus.

Finally, the annual demand and consumption were evaluated using the calibrated model. Peak cooling coil loads and electricity consumptions for lighting, appliances and fans were compared with design and CBIP data. The values estimated by EnergyPlus are in agreement with design and CBIP data, demonstrating that properly integrating all components in EnergyPlus has led to good model predictions.

Therefore, the final result is a virtual model of the Concordia Sciences building that the building operators could use to evaluate the impact of certain modifications made to the HVAC systems and the overall building. It could allow the introduction of different scenarios to improve the performance of the building in comparison with the current design.

This research project has given me the opportunity to acquire knowledge about building simulation in general and more specifically about the EnergyPlus program. This knowledge could be used to train colleagues about the best approach to develop virtual models using EnergyPlus. My understanding of the program could also be used to describe the best features and capabilities of the program. The development of the computer model has led to the detection of missing equipments and limitations related to performing a detailed simulation of the building under study. My overall experience could be used to enhance the characteristics and the capabilities of the EnergyPlus program.

7.2 Recommendations for Future Work

The development of a virtual model for the Concordia Sciences building has led to the identification of some missing components in the EnergyPlus program required to evaluate the energy performance of large buildings with complex electro-mechanical systems for cold climates. The following are recommendations for future work:

- Complete the central plant simulation;
- Include utility rooms and fan coil units to adequately incorporate the heat recovery loop into the virtual model;

- Develop a model for water-to-water and steam-to-water heat exchangers to be included in the EnergyPlus program;
- Include a glycol water loop that can be used for heating purposes to simulate air handling unit heating coils;
- Develop a module to simulate ventilation hoods for laboratories that would include total required capacity and diversity factors to determine the energy requirements of the system;
- Perform a complete sensitivity analysis that would include the identification analysis, numerical optimization and uncertainty analysis.

REFERENCES

1. http://www.statcan.ca/Daily/English/050323/d050323c.htm (latest access 28/10/2006)
2. *ASHRAE Handbook - Fundamentals*, Atlanta: American Society of Heating, Refrigeration and Air-Conditioning Engineers, Inc., 2001.
3. Clarke, J. A., *Energy Simulation in Building Design*, 2nd edition, Oxford, Butterworth- Heinemann, 2001.
4. Crawley, D. B., Hand, J. W., Kummert, M. and Griffith, B. T., *Contrasting the Capabilities of Building Energy Performance Simulation Programs*, v.1, 2005, http://www.eere.energy.gov/buildings/tools_directory/pdfs/contrasting_the_capabilities_of_building_energy_performance_simulation_programs_v1.0.pdf (latest access 28/10/2006).
5. http://oee.nrcan.gc.ca/newbuildings/mnecb-cmneb/index_e.cfm?Text=N&PrintView=N (latest access 28/10/2006).
6. Zmeureanu, R., *Defining the Methodology for the Next-Generation HOT2000 Simulator – Task 1*, Centre for Building Studies, Concordia University, Montreal, 1997.
7. Fels, M. F., Reynolds, C. L. and Stram, D. O., *Documentation for Heating-only or Cooling-only Estimation Program: Version 4.0*, The Center for Energy and Environmental Studies, Princeton University, New Jersey, October 1986.
8. http://www.osti.gov/energycitations/product.biblio.jsp?osti_id=6402903&query_id=0 (latest access 28/10/2006).

9. Witte, M. J., Pederson, C.O. and Spitler, J. D., *Techniques for Simultaneous Simulation of Buildings and Mechanical Systems in Heat Balance Based Energy Analysis Programs*, IBSPA Conference, Vancouver, British Colombia, 1989.
10. Brandemuehi, M. J., Gabel, S. and Andresen, I., *HVAC 2 Toolkit*, Atlanta: American Society of Heating, Refrigeration and Air-Conditioning Engineers, Inc., 1993.
11. Lebrun, J., Bourdouxhe, J.-P. and Grodent, J., *HVAC 1 Toolkit*, Liege: American Society of Heating, Refrigeration and Air-Conditioning Engineers, Inc., 1994.
12. *ASHRAE Handbook – Applications*, Atlanta: American Society of Heating, Refrigeration and Air-Conditioning Engineers, Inc., 2003.
13. Neymark, J., Judkoof, R., Knabe, G., Le, H.-T., Dürig, M., Glass, A. and Zweifel, G., *HVAC BESTEST: A procedure for testing the ability of whole building energy simulation programs to model space conditioning equipment*, Seventh International IBPSA Conference, Rio de Janeiro, 2001.
14. Hayer, S., Dalibart, C., Guyon, G. and Feburie, J, *HVAC BESTEST: Clim2000 and CA-SIS Results*, Seventh International IBPSA Conference, Rio de Janeiro, 2001.
15. Witte, M. J., Henninger, R. H. and Glazer, J., *Testing and Validation of a New Building Energy Simulation Program*, Seventh International IBPSA Conference, Rio de Janeiro, 2001.
16. Zmeureanu, R., Pasqualetto, L. and Bilas, F., *Comparison of Cost and Energy Savings in an Existing Large Building as Predicted by Three Simulation Programs,* IBSPA Conference, Madison, Wisconsin, 1995.

17. Kaplan, M. and Canner, P., *Guidelines for Energy Simulation of Commercial Buildings*, Portland, 1992.

18. Sun, J. and Reddy, T. A., *Calibration of Building Energy Simulation Programs Using the Analytic Optimization Approach (RP-1051)*, HVAC&R Research, Vol.12, No.1, pp.177-196, January 2006.

19. Reddy, T. A., *Literature Review on Calibration of Building Energy Simulation Programs: Uses, Problems, Procedures, Uncertainty, and Tools*, AHSRAE Transactions: Research, Vol. 112, Part 1, pp. 226-240, 2006.

20. Lam, J. C. and Hui, S. C. M., *Sensitivity Analysis of Energy Performance of Office Buildings*, Building and Environment, Vol. 31, No. 1, pp. 27-39, Elsevier Science, Great Britain, 1996.

21. Carroll, W. L. and Hitchcock, R. J., *Tuning Simulated Building Descriptions to Match Actual Utility Data: Methods and Implementation*, ASHRAE Transactions, Vol. 99, Part 2, 1993 ASHRAE Annual Meeting, Denver, Colorado, 1993.

22. Pasqualetto, L., Zmeureanu, R., and Fazio, P., *A Case Study of Validation of an Energy Analysis Program : MICRO-DOE2.1E*, Pergamon, 1997.

23. Crawley, D.B., Pederson, C. O., Strand, R. K., Liesen, R. J., Witte, M. J., Henninger, R. J., Glazer, J., Lawrie, L. K., Winkelmann, F. C., Buhl, W. F., Huang, Y. J., Fisher, D. E., and Shirey, D., *EnergyPlus: New, Capable and Linked,* http://www.esim.ca/2002/documents/Proceedings/Session%205-2.pdf (latest access 28/10/2006).

24. Crawley, D. B., Lawrie, L. K., Winkelmann, F. C., Buhl, W. F., Huang, Y. J., Pederson, C. O., Strand, R. K., Liesen, R. J., Fisher, D. E., Witte, M. J. and Glazer, J., *EnergyPlus: creating a new-generation building energy simulation*, http://www.p2pays.org/ref/18/17924.pdf (latest access 28/10/2006).

25. Crawley, D. B., Lawrie, L. K., Pederson, C. O., Winkelmann, F. C., Witte, M. J., Strand, R. K., Liesen, R. J., Buhl, W. F., Huang, Y. J., Henninger, R. J., Glazer, J., Fisher, D. E., Shirey, D.B., Griffith, B. T., Ellis, P. G., and Gu, L., *EnergyPlus: An Update,* Boulder: US Department of Energy, 2004, http://ceae.colorado.edu/ibpsa/ocs/viewpaper.php?id=75&cf=1 (latest access 28/10/2006).

26. Bazjanac, V., *IFC HVAC Interface to EnergyPlus – A Case of Expended Interoperability for Energy Simulation*, University of California, Berkeley, August 2004.

27. Strand, R. K., Pedersen, C. O. & Crawley, D.B., *Modularization and Simulation Techniques for Heat Balance Based Energy and Load Calculation Programs: The Experience of the ASHRAE Loads Toolkit and EnergyPlus*, 7th IBPSA Conference, Rio de Janeiro, 2001.

28. Strand, R., Winkelmann, F., Buhl, F., Huang, J., Liesen, R., Pedersen, C., Fisher, D., Taylor, R., Crawley, D. and Lawrie, L., *Enhancing and Extending the Capabilities of the Building Heat Balance Simulation Technique for Use in EnergyPlus*, 6th IBPSA Conference, Kyoto, 1999.

29. *EnergyPlus Engineering Manual*, http://www.eere.energy.gov/buildings/energyplus/pdfs/engineeringreference.pdf (latest access 28/10/2006).

30. Fisher, D. E., Taylor, R. D., Buhl, F., Liesen, R. J. and Stand, R. K., *A Modular, Loop-Based Approach to HVAC Energy Simulation and its Implementation in EnergyPlus*, 6th IBPSA Conference, Kyoto, 1999.

31. Wikelmann, F.C., *Modeling Windows in EnergyPlus*, 7th IBPSA Conference, Rio de Janeiro, p.457 – 464, 2001.

32. Mehta, M., *Natural Ventilation Analysis of an Office Building with Open Atrium*, 9th IBPSA Conference, Montreal, p.741 – 746, 2005.

33. Fisher, D.E. and Rees, S.J., *Modeling Ground Source Heat Pump Systems in a Building Energy Simulation Program (EnergyPlus)*, 9th IBPSA Conference, Montreal, p.311 – 318, 2005.

34. Zhou, G., Ihm, P., Krarti , M., Liu, S. and Henze, G.P., *Integration of an Internal Optimization Module within EnergyPlus*, 8th IBPSA Conference, Eindhoven, 2003.

35. Mithraratne, K. and Vale, B., *Thermal Characteristics of High Thermal Mass Passive Solar Buildings*, School of Architecture, The University of Auckland, Auckland, New Zealand, http://nzsses.auckland.ac.nz/conference/2004/Session5/34%20kumar_mithraratne.pdf (latest access 28/10/2006).

36. Bellemare, R., Kajl, S. and Roberge, M.-A., *Modélisation de systèmes CVCA à l'aide du logiciel EnergyPlus*, e-Sim Conference, Montreal, 2002.

37. Ellis, P.G. and Torcellini, P.A., *Simulating Tall Buildings using EnergyPlus*, 9th IBPSA Conference, Montreal, p.279 – 286, 2005.

38. Witte, M. J., Henninger, R.H. and Glazer, J., *Testing and Validation of a New Building Energy Simulation Program*, 7th IBPSA Conference, Rio de Janeiro, 2001.

39. Pageau, Morel & Associés, *Soumission PEBI - Simulation EE4, Université Concordia, Pavillons des Sciences*, Montréal, Québec, 2003.

40. Lemire, N. and Charneux, R., *Energy-Efficient Laboratory Design*, ASHRAE Journal – School HVAC, American Society of Heating, Refrigeration and Air-Conditioning Engineers, Inc., Atlanta, Ga., May 2005.

41. *ASHRAE Pocket Guide*, Atlanta: American Society of Heating, Refrigeration and Air-Conditioning Engineers, Inc., 1997.

42. York, D. A. and Cappiello, C. C., *DOE-2 Engineers Manual V. 2.1A*, Energy and Environment Division, Building Energy Simulation Group, Lawrence Berkeley Laboratory, Berkeley, California, 1981.

43. http://www.pennbarry.com/ecatalog/GetFile.aspx?FileID=5795 (latest access 28/10/2006).

44. Spitler J., Fisher, D. and Zietlow, D. C., *A Primer on the Use of Influence Coefficients in Building Simulation*, Building Simulation '89, Vancouver, British Colombia, 1989.

45. Groupe DATECH, *informa-TECH*, GazMétro, Vol. 20, No. 1, June 2006.